University of Strathclyde

Biomedical Engineering Department

Biomechanical Comparison of a Rigid and Dynamic Seating System for Children with Special Needs

By

Katika Samaneein (BSc, MEng)

This thesis is submitted in partial fulfilment of the requirements for the degree of PhD in Biomedical Engineering

2014

Declaration of Author's Rights

This thesis is the result of the author's original research. It has been composed by the author and has not been previously submitted for examination which has led to the award of a degree.

The copyright of this thesis belongs to the author under the terms of the United Kingdom Copyright Acts as qualified by University of Strathclyde Regulation 3.50. Due acknowledgement must always be made of the use of any material contained in, or derived from, this thesis.

Signed: ....

Date: ....

Acknowledgements

First of all, I would like to thank my fantastic supervisor, Dr Philip Riches, for his encouragement, enthusiasm and all support.

Special thanks go to Mr Stephan Solomonidis, for his kindness to educate me about mechanics for wheelchair, and brilliant suggestion for a various source of knowledge.

I would like also to thank Mr John Maclean for technical assistance in the preparation of the experimental devices. Without him, this research would have been a nightmare.

Thank you to Mr Stephen Murray, John Wilson, Anne Marie Baran, Ashley Urie and all the people in the Biomedical Engineering Department for direct and indirect ways in which you have all contributed to this study.

Thank you for all collaborations: WestMARC, John, Karl, Peter, Neil, Alison, Owen, Sido and everyone who provided the opportunity to carry out clinical training and allowed me to be a part of their services for a number of days. Thank Noel McQuaid and Laura Finney from James Leckey Design Ltd., who provided experimental equipment and financial support for conferences.

Thank my colleagues in this department who helped me in various ways. I wish them all the best on their work.

Finally, I would like to thank my parents for their encouragement and unconditional support.

A big thank you to all of you,

```
T | K O N S T A T N O S L M O N I A N N E
H | O A H T B R U C E L I N P O T N I C O N
A | B O O E E R N O E I N E E B S T A N Y
N | J O H N N I E C H O L E P O P H O N Y
K | O E S I D O N R K I T E E D T O R O Y
S | H E T E A W L A K A N Y T N O N I K E
A   N N E L L I R G S H I N E I L Y C A T
R   J O P H I L I S A H E B R R I C H E S
I   O E H E S A S H E L L E I S S E A N N
C   H L A N O U T L Y S T E V E T H A N Y
H   N Y N R N P H I L I P Y L O N O P E
A   M O N I C A A R Y A N A U U G B O L U
R   O W E C A T H Y A R O T E N K R I A G
D   N E I A L I Z A R J K A T H I Y I N G
O   W N A N C Y A N O A A N A N T A I C H
H   E L E N H B R I A N T L P H I L L N Y
A   N G L E R E A N O T I M I N P E N N Y
H   U D S O I N B J Y O K A E T H Y T O A
I   T O E N S Y I A N N A P O L O O S H S
M   T G A S C O N W A Y S H I C L A I R Y
```

Abstract

In wheelchair users who experience strong extensor spasms, high muscular forces exerted during the episode may lead to high contact forces between the child and the wheelchair. The forces may be physically powerful enough to cause pain and injury to the child, and can damage or break components of the wheelchair. Dynamic seating systems have been used in an attempt to reduce these contact forces. Such systems permit forward and backward movements as the occupant extends and retracts their body, consequently they are assumed to be beneficial to patients with strong extensor spasms. Questions about the magnitude and direction of the loads which these children can exert through a seating system have been raised. Additionally, the effectiveness of using dynamic components and the advantages of prolonged use remain unclear.

The aim of this study was to quantify and compare the imparted forces on equivalent rigid and dynamic seating systems throughout activities of daily living. To achieve this, a mobile strain gauged seating system was developed which allowed the strain generated in the back and footrest components to be measured. At a certain instant of exerted force, the strain data was converted into force and moments acting on the backrest and footrests in three dimensions, assuming static equilibrium. The position of the resultant force on the backrest, termed the centre of pressure (COP), was also calculated.

This project shows that the development of a fully mobile data acquisition system is achievable and practical. Results obtained from twelve children during their community based activity of daily living showed no significant differences in the mean and peak interface forces on the backrest between the rigid and dynamic systems. However, when using the dynamic backrest system, a significant decrease in force and bending moments were observed on the right footrest, the dominant side of most participants. Conversely, for the left footrest only the average bending moment about the transverse axis through the ankle showed a statistically significant

decrease, with no significant difference demonstrated between the other variables for the two backrest systems.

This work included a long-term case study using the dynamic backrest seating system. The data did not elicit any observable differences of changing in movement, probably due to the relative inactivity of the recruited volunteer. Further work and recruitment should focus on users who exhibit strong extensor spasms, as this work suggest that these are the population who may benefit the most from dynamic seating.

Publications Arising from This Work

Katika S, Peter G, Philip R (2011): Development of a fully mobile, strain gauged seating system for the assessment of forces imparted on the Mygo™ seating system by children with special needs through daily activity. *Proceeding of the National Training Event, Posture and Mobility Group (PMG)*, University of Warwick, UK, April, 2011

Katika S, Karl L, Peter G, Philip R (2011): A Strain-gauged Mygo™ Seating System for Use by Children with Special Needs: From Lab to Communal Testing. *Proceeding of the European Seating Symposium Incorporating Assistive Technology (ESS)*, the Convention Centre, Dublin, November 2011, *pp 137-139*

Katika S, Karl L, Peter G, Philip R (2012): Assessment of Seating Forces Imparted Through Daily Activity by Children with Special Needs. *Proceeding of the 28th International Seating Symposium (ISS)*, the Westin Bayshore, Vancouver, BC Canada, March 2012

Katika S, Karl L, Peter G, Philip R (2012): Assessment of Forces Imparted on Seating Systems by Children with Special Needs During Daily Living Activities. *Proceeding of 2012 IEEE EMBS International Conference on Biomedical Engineering and Sciences (IECBES 2012),* Holiday Villa Beach Resort and Spa, Langkawi, Malaysia, December 2012, *pp 475-478, (http://ieeexplore.ieee.org)*

Katika S, Karl L, Peter G, Philip R, Stephanos S (2013): Effect of Dynamic Components on Interface Forces in Special Seating for Children with Cerebral Palsy. *Poster presentation at the National Training Event, Posture and Mobility Group (PMG)*, University Of The West Of England, Bristol, UK, July 2013

Katika S, Karl L, Peter G, Philip R (2013): Comparison of Imparted Forces between Rigid and Dynamic Seating Systems during Activities of Daily Living by Children with Cerebral Palsy. *Proceeding of XXIV congress of the International Society of Biomechanics (ISB 2013),* The Convention Centre of Natal, Rio Grande do Norte, Brazil, August 2013

Katika S, Karl L, Peter G, Philip R (2013): A Comparison of Force Exerted on Rigid and Dynamic Backrest Systems by Children with Cerebral Palsy. *Proceeding of the European Seating Symposium Incorporating Assistive Technology (ESS)*, the Burlington Hotel, Dublin, November 2013

Katika S, Karl L, Peter G, Philip R, Stephanos S (2013): Mechanical Analysis of Rigid and Dynamic Seating Systems during Activities of Daily Living by Children with Cerebral Palsy. *Journal of Engineering in Medicine*, (in preparation)

Katika S, Karl L, Peter G, Philip R, Stephanos S: Benefits of Dynamic Seating Systems for Children with Special Needs in their Activities of Daily Living. *Achieves of Physical Medicine and Rehabilitation*, (in preparation)

Contents

List of figures

List of tables

CHAPTER 1
INTRODUCTION

1.1   BACKGROUND

Extensor spasms commonly occur in children with cerebral palsy, affecting them mainly in the seated position. The contact force of the seat on the child, as a consequence of the extensor spasm, can make the child uncomfortable and unstable. Furthermore, the force may be physically powerful enough to either injure the child or break the components of the wheelchair. Hence, children who have hyperactive stretch reflexes or whole body extension need carefully prescribed seating requirements. To reduce these contact forces, dynamic seating systems have been proposed and used. Since such systems permit forward and backward movement as the occupants extend and flex their joints, dynamic seating systems are assumed to be beneficial to patients with extensors spasms.

Controversy exists regarding the scientific evidence for the quantitative effectiveness of using dynamic seating systems over rigid systems. The first systematic study of extensor loads generated on the seating system was reported by Brown et al. (2001), however it was laboratory-based and focused on stimulated extensor spasms. Another study (Wook et al., 2006) established a model to predict the forces generated by extensor spasms. Yet, to the author's knowledge, no research has been undertaken to measure these forces as they occur naturally.

Several attempts have been made to incorporate a dynamic component into the special seating system and the users, who were children with extensor spasms, decreased in extensor tone after using the dynamic backrest systems for a few months (Orpwood, 1996, Ault et al., 1997).

In addition, regarding the long term use of the dynamic seating system, the Gross Motor Function Measure has been used to evaluate the performance of motor skills in children with CP. Hahn analysed the data from 12 children and concluded that there was no significant difference of improvement between using the rigid and dynamic backrest systems (Hahn et al., 2009).

1.2   AIMS OF THE RESEARCH

This study aims to provide quantitative force data on both rigid and dynamic seating systems. By collecting component force data during community-based activities of daily living and, in particular, during an extensor spasm, two different seating are compared: a rigid system and a dynamic system. Another aim was to assess the interaction of the seating system with a child in terms of quality of movement over a 6 month period. It was hoped that the data acquired would provide evidence for the appropriateness and indications for prescribing dynamic systems for children with CP. Finally, the quantification of chassis stresses should, hopefully, help designers improve wheelchair design for the benefit of the child, and to reduce chassis failures.

1.3   COLLABORATIONS

The collaborative partners of this research project were the NHSGGC West of Scotland Mobility and Rehabilitation Service (WestMARC) and James Leckey Design Ltd. specialising in postural care products.

WestMARC, at the Southern General Hospital, Glasgow, provides rehabilitation technology services to people in Greater Glasgow and Clyde. The Wheelchair Service section provides wheelchairs to people of all ages who have a long term disability and special wheelchairs for people with special needs. Accordingly, the potential pool of volunteers for this study was filtered by Clinical Scientists at WestMARC, and those who fulfilled the inclusion criteria were invited to participate.

The project was part-funded by James Leckey Design Ltd., manufacturers of the Mygo wheelchair which was used in this study.

1.4   THESIS OUTLINE

This thesis consists of 8 chapters. Initially, the literature review describes the relevant patho-physiology of CP and spasticity in children. Following this there will be a brief description of different special seating systems for children, focusing on dynamic seating systems, and a discussion of the differences between them. The chapter then continues with a review of research studies conducted up to the present date concerning or contributing to the analysis of forces on seating systems for children with limited mobility.

One aspect of this study was the necessary development of a methodology to collect force data on a wheelchair during a child's daily living activities. To achieve this, a fully mobile data acquisition system on the Mygo seating system was developed and chapter 3 presents a full description of the experimental requirements and the utilised measurement method used in this work.

Chapters 4 and 5 comprise details of the calibration of the force transducers and gas springs. The results from these chapters were used to calculate component forces presented in the subsequent chapters.

Chapter 6 provides details of the experimental test protocols and results of the force analysis of the rigid and dynamic seating systems. A case study of a child, who experienced strong extensor spasms during the investigation of rigid and dynamic backrest seating systems, is also included in this chapter.

The last experimental chapter describes a longitudinal case study of the effect of a dynamic backrest system. .

Chapter 8 concludes the thesis by bringing together and discussing the different findings of each study. The most promising aspects of the work are highlighted together with recommendations for areas that justify further study.

CHAPTER 2
LITERATURE REVIEW

2.1 INTRODUCTION

The first section of this chapter is intended to provide an overview of children with cerebral palsy (CP). Among children with special needs, children with CP are the ones who make use of special seating systems most widely. Those with severe extensor muscle tone are expected to obtain benefits from dynamic seating. Consequently, the next section reviews currently available seating systems and the expected effect of dynamic components on the child.

The past decade has seen the development of dynamic systems by many wheelchair providers. One major question that has dominated this field for many years is whether the capability to adopt an open posture with a dynamic system eliminates or reduces pathological muscle activity, such as extensor spasm. This capability was believed to result in an improvement in functional ability (Cooper and Antoniuk, 2007, Orpwood, 1996, Ault et al., 1997). However, in recent years, scant evidence has demonstrated that the users would gain any advantage from such a design. Furthermore, questions about the effects of prolonged use of dynamic seating systems have also been raised. Several attempts have been made to quantify the benefits but there is still insufficient data to clarify their effectiveness in the long term. This review aims to discuss the pertinent literature regarding these issues.

2.2   CEREBRAL PALSY

2.2.1 Aetiology and description

Cerebral palsy encompasses a set of congenital disorders which affect the development of the brain and its ability to control movement and posture (Rosenbaum et al., 2007, Ashwal et al., 2004). The rate of incidence is about 2 to 3 per 1000 live births (Pharoah, 1998, Sciberras C, 1999, Bonellie, 2007, SCPE, 2000, Hagberg et al., 2001). The causes of damage, or why there is failed development of brain, are unclear. Damage can occur during fetal development or shortly after birth and during infancy (Hagberg et al., 2001, Salihu, 2008, Kulak and Sobaniec, 2003, Jacobsson and Hagberg, 2004). These lesions do not damage the child's muscle and the connected nerves but only injure the brain's ability to control the muscle, impair the body movement and muscle coordination and these are the most common cause of disability in children (Rosenbaum, 2006, Cans et al., 2008). Motor neuron dysfunction can affect a child's functional ability with either low muscle tone (hypotonia) or high muscle tone (hypertonia) or a combination of the two (fluctuating tone). Symptoms range from mild to severe conditions and depend on the location and severity of the lesion in the brain (Geralis, 1991).

The physiology of the body is such that the motor neuron in the spinal cord or brainstem (lower motor neuron, LMN) sends the signal to muscle cells, whilst the upper motor neuron (UMN) sends inhibitory impulses to restrain LMN signal. These two processes allow muscle cells have a relatively constant amount of minor contraction, known as 'muscle tone'. Since a lesion of the LMN affects the nerve impulse delivery to muscle cells, the muscles lose their normal tone resulting in low muscle tone or hypotonia, which can lead to muscle atrophy in later stages. Since there is a reduction in overall muscle tone, children are "floppy" and can have significant delays in motor milestones with weak facial and oral muscles. Another lesion of the motor neuron is the lack of inhibitory impulse in the UMN, affecting the inhibition of the increasing LMN impulse, creating excessive muscle tension. This condition is known as high muscle tone or hypertonia.

Some children with CP also have visual, speech impairments and/or mental retardation (Sharma et al., 1999). In the Surveillance of Cerebral Palsy in Europe (SCPE) study, 23.5% of children had severe mental retardation (intelligence quotient <50) and 35.2% of children with spastic CP were unable to walk. One-third of children with CP have severe CP (Krägeloh-Mann and Cans, 2009), with some completely disabled and requiring lifelong care.

2.2.2 Classifications

The classification of CP has been a source of a number of discussions over the years. Although differences of opinion still exist, there appears to be some agreement that the classification of CP refers to the dominance symptoms or clinical signs (Jacobsson and Hagberg, 2004) including the type of symptoms in terms of severity: mild, moderate, or severe (Panteliadis and Strassburg, 2004, Scherzer, 2001). The classification of CP severity is categorised by motor impairment level, and does not include other impairments which children experience such as vision, speech, sensation, and cognition.

- *Spastic CP*

Spasticity is the most common type of CP (Shevell et al., 2003). It includes involuntary muscle contraction and stiff limbs related to the muscle tone. Figure 2.1 shows the stiffness of whole body which occurs more commonly in children with spasticity when lying on the back and sitting on the chair Spasticity can affect many areas of the body and not only mobility but it also makes difficulties with body positioning (Geralis, 1991).

Figure 2.1 Stiffness in children with spasticity (Werner, 2009)

Spastic CP may be anatomically distributed into five types as can be seen in Figure 2.2. The most common movement pattern in spastic hemiplegia are arm flexion and foot extension, in diplegia flexion or extension of the lower extremities and in tetraplegia or quadriplegia flexion or extension of all four limbs (Lieber, 1990).

Monoplegia
Only one limb is affected, usually an arm.

Diplegia
All four limbs are affected. Both legs are more affected than the arms.

Triplegia
Three limbs are involved, usually both arms and a leg.

Quadriplegia
All four limbs are involved.

Hemiplegia
One side of the body is affected. The arm is usually more involved than the leg
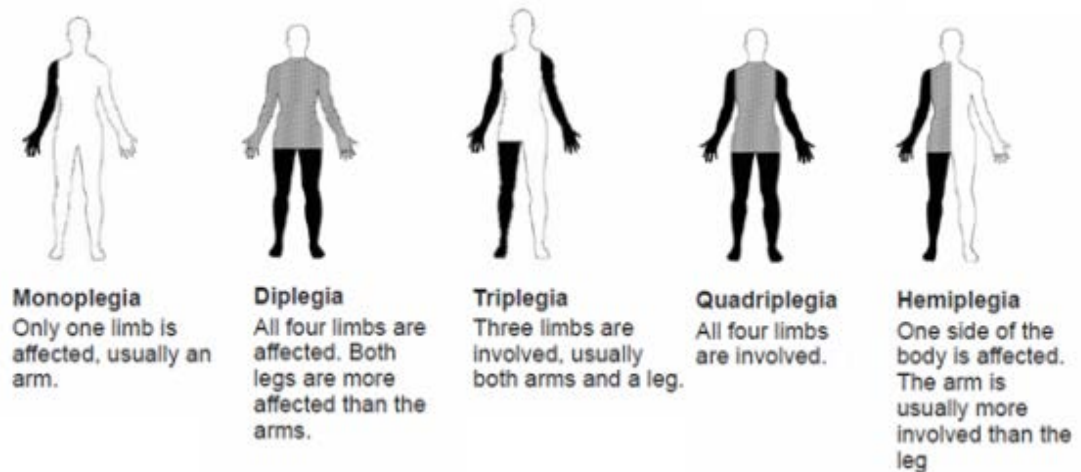
Figure 2.2 Location of movement problems in spastic CP (http://www.ofcp.ca)

- *Dyskinetic CP*

Dyskinetic CP is present in about 12% of people with CP (Hagberg et al., 2001). Dyskinetic refers to uncoordinated and uncontrolled movements. Patients experience difficulty in maintaining an upright position and have uncoordinated movement of the head, arms, hands or feet (Figure 2.3). These involuntary movements often interfere with speaking, feeding, and other important functional skills.
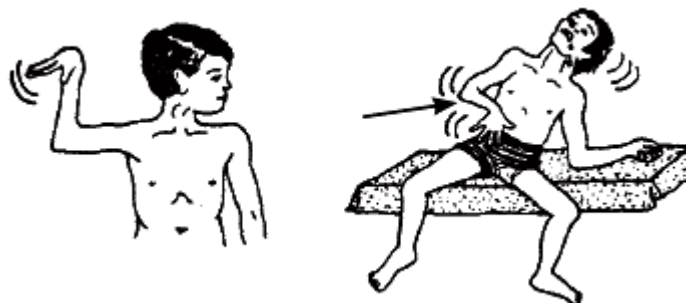
Figure 2.3 Suddenly uncoordinated movement (Werner, 2009)

- *Ataxic CP*

Ataxic CP is found about 4% of people with CP (Hagberg et al., 2001). Ataxic CP affects the sense of balance and depth perception; to the symptoms of which are unsteady and shaky muscles during moving (Figure 2.4).

Figure 2.4 Balance problems often appear in children with ataxia (Werner, 2009)

- *Mixed CP*

It is both possible and common to have a combination of two or more types in one person. Most have spastic CP in combination with another type. CP has a lifelong effect and the symptoms can present till adulthood. However, the condition may change over time. Accordingly those who was diagnosed as one category of CP may be diagnosed as another type in the future (Laughton, 2004).

The Gross Motor Function Classification System (GMFC system) is used to classify children with CP by dividing them into 5 levels (I-V) of functional movement as shown in Table 2.1

Table 2.1 GMFC system of cerebral palsy and approximate percentage prevalence in each group (Agarwal and Verma, 2012)

Level	Function	Prevalence
I	Has nearly normal gross motor function	35%
II	Walks independently, but has limitations with running and jumping	16%
III	Uses assistive devices to walk and wheel chair for long distances	14%
IV	Has ability to stand for transfers, but minimal walking ability; depends on wheel chair for mobility	16%
V	Lacks head control, cannot sit independently, is dependent for all aspects of care	18%

2.3   SPASTICITY AND MUSCLE SPASMS

The nature of spasticity remains controversial. A widely accepted definition of spasticity, which is classically defined by Lance (1980), is "a motor disorder characterised by a velocity-dependent increase in tonic stretch reflexes with exaggerated tendon jerks, resulting from hyper-excitability of the stretch reflex" (Lance, 1980). In other words, spasticity leads to a fast stretch reflex in the muscle which is result of uncoordinated agonist and antagonist muscle activity due to dysfunction of the electrical signal from the motor neuron system (Neilson and McCaughey, 1982).

There are several pathological conditions which can produce spasticity. The most common conditions are: CP 70 – 90 percent of case, multiple sclerosis (MS) 65 – 90 percent, stroke 35 –51 percent, spinal cord injury (SCI) 12 – 37 percent and multiple system atrophy (MSA) 10 percent (MedicalAdvisorySecretariat, 2005, Simpson et al., 2008).

Spasticity can occur with any type of UMN injury including stroke, spinal lesions and other forms of brain injury, but there are some differences between them. Spinal spasticity develops flexion and adduction tone, and extensor tone becomes the main form in the lower extremities (Preston and Hecht, 1999). Spasticity with spastic CP tends to be less severe and more often involve the extensors with a posture of lower limb extension. Spasticity is different from rigidity, although both include involuntary increase in muscle tone, spasticity is velocity-dependent, generally occurs only during muscle stretch and it usually accompanied by increase tendon reflexes (Gelber and Jeffery, 2002).

Painful spasms are frequently seen in both flexor and extensor spasms. In a sample group of 60 patients with spasticity, age range 3-91 years, almost half of the sample were stroke patients, 15 percent were CP, 8 percent were spinal injury, the magnitude and frequency of the extensor thrust varied between individuals and was different from day to day (Wissel et al., 2000). The degree of these involuntary contractions of muscle can vary throughout the day and can be encouraged by many causes including body's positioning, the onset of sleep, pain, discomfort, noise and infection (Bowker, 1993). Some patients find that their spasms are worse in certain

positions than other positions (Gelber and Jeffery, 2002, Preston and Hecht, 1999). Furthermore these conditions have to be taken into account to efficiently decide the type of physical management provided to them.

2.3.1 Treatments and Therapies

The aims of treatment are to relieve the effects of CP and to enhance the development of children performing more independent activities of daily living (Papavasiliou, 2009). There is no specific treatment for CP; in many cases the patients may not require any special treatment, while for those who have severe conditions, they may need more than one treatment at the same time. Some treatments seem beneficial for some patients but not for others.

- *Medication*

Many CP children have medication for spasticity to reduce the impact of the condition. It is complex treatment because various muscles are involved and respective therapeutic purposes vary widely between patients.

There are several medications such as Baclofen, Benzodiazepines, and Tizanidine which act at the level of the central nervous system, and Dentrolene sodium which acts directly on the muscle. It is to be noted that most of these treatments are in the form of centrally, peripherally or locally acting muscle relaxants. The prognosis of the medication for those with spasticity depends on the severity of the spasticity and the associated disorders.

- *Surgery*

Surgical treatment is needed for some patients to correct the posture of the body as a result of deformity. Surgery is sometimes indicated in the treatment of spasticity when a permanent reduction in muscle tone is necessary. This treatment involves both a neurosurgical and orthopaedic aspect to the operation. Some patients' treatments may also include both surgery and medications. Also the physical therapy programme may be needed to maximize the benefits from the operation.

- *Physical therapy*

For the everyday management of patients with spasms, a balanced programme of stretching and strengthening exercises must always be implemented to relieve spasticity. The role of these exercises: stretching or attempting to move the parts of the body through the full range of motion, can help to improve flexibility. Each stretch should be performed slowly, with no sudden jerking or bouncing (Fink, 2009). Strengthening exercises decrease muscle tone and improve the quality of muscles and also prevent contractures.

- *Specialised support*

The use of specialized orthotics for limbs is one methods employed to support the patient depending on their movements. These serve to improve gait and minimise the risk of joint deformity. Many patients, especially children who have CP, lack the ability to sit unsupported, unable to keep their balance and their posture. They require special supports to maintain their body posture, termed orthotic devices, such as special seating, and standing and walking aids. These devices have been individually created based on the specific needs of each patient's orthotic management.

2.4   SEATING FOR SPECIAL NEEDS

Special seating systems for children have been continually developed for many decades. They have been designed by considering requirements such as stage of development, disability and other special needs of children. The objectives of designs are to achieve a better body position, improve functional ability and increase independence in activities of daily living (ADL) (Santangelo and O'Reilly, 1999, Green and Nelham, 1991, Wright C, 2010, Clark et al., 2004).

Approximately 10% of wheelchair users are children under the age of 20 (Barnaby, 1994) and children with cerebral palsy often make use of special seating systems (Simpson et al., 2008). Other people with neurological conditions such as multiple sclerosis, multiple system atrophy or spinal cord could also potentially find benefits in special seating technology to optimize comfort and performance in their ADLs depending on their individual requirements and health condition.

2.4.1 Seating Considerations

Sitting is asymmetrical and dynamic (Aissaoui et al., 2001). It is easy for non-disabled people to find a suitable sitting position when they feel uncomfortable; they can adjust and stabilize themselves and always have movement at least every 5-10 minutes (Yang et al., 1996). On the other hand, for those who suffer from a loss of movement control, it is not as easy or, indeed, may be impossible to change their position by themselves. Therefore special seating must be provided to support the right position based on biomechanical principles. Moreover, the technique to decrease the pressure on the contact points and to avoid severe pressing on any part of the body which may cause injury, should also be considered.

The body is subjected to external forces and moments in all the three orthogonal directions. Ideally the suitable sitting position balances forces and moments in all planes (Bowker, 1993, Letts, 1991). For children who have severe difficulties in maintaining stability, unstable and unbalanced sitting positions significantly increase the curvature of spine and lead to poor control of their upper body. Therefore the supports on seating systems play the major role to organise external forces and moments acting across the body in order to restore more normal functions. The optimum positioning of the pelvis, trunk, head, leg and foot, facilitates the user's daily activities and also prevents the deformity leading to muscle spasm (Trefler and Schmeler, 2001, Cogher et al., 1992).

The centre of mass (COM) is involved in the assessment of seating stability. In order to balance the body over a stable sitting base the COM must be directly over the sitting base. Therefore, stability of the sitting posture is improved when the area of contact between the body and the support surface is increased (Ham et al., 1998). For some postural deformities, the area of contact on the seat is limited and , accordingly, sitting stability is improved by increasing the support on other areas of the body such as the chest and trunk.

Sitting balance can be also described by measuring the centre of pressure (COP). It can be used to describe body sway which is useful for positioning management. The COM is a point equivalent to the total body mass while the COP corresponds to the point of application of the resultant force under the area of contact with the seat

surface. Therefore in a balanced upright position, the weight vector, which passes through the COM, passes through the COP within the base of support (Lacoste et al., 2006). Geffen et al. pointed to the relationship between sagittal positions on the chair and COP. They mentioned that during the change of back angle in reclining, COP had not been significantly affected, but the largest effect on COP was observed during pelvis rotations when tilting the seat (van Geffen et al., 2008).

If positioning devices are provided, many new interface areas are also created and they may possibly generate pressure and shear forces at their respective contact points. High interface and shear forces on wheelchairs could cause wheelchair users uncomfortable and physical pain (Hahn et al., 2009, Dawley and Julian, 2003). Such risks will be higher when users have more severe postural control issues (Hobson, 1992). Consequently, the aim of comfort management on seating is to lessen the risk of pressure and forces. This will result in the encouragement of users' functions and participation in their ADL (Green and Nelham, 1991, Carlson et al., 1986, Barnes, 1998).

- *Minimum pressure*

Pressure sores are one problem that often occur for wheelchair users (Hobson, 1992). The most likely areas of sores that occur are spaces which are compressed between a bone in the patient's body and a hard surface either on the bed or chair. Pressure sores can be exacerbated in wheelchair users with advanced diseases or severe injuries such as paralysis, diabetes and auto immune diseases. These make them have high skin sensitivity. Other risk factors such as shear forces, skin temperature and anatomic structure also add to the possibility of pressure sores or pressure ulcers (Polliack and Scheinberg, 2006).

Support surfaces or cushions are the main part of the chair which is considered to be the most important for pressure distribution. Recently, support surfaces available include gel, foams, air or a combination of these. They are used to reduce or relieve interface pressures on the seat (Stockton and Rithalia, 2009). The suitable types of support surfaces are different depending on the various needs of the users. For example, a fluid material is suggested to users who have unbalanced interface

pressure on the seat because the flow character of the liquid can balance and absorb the pressure of their sitting (Bar, 1991).

Another method to manage the pressure problem on the wheelchair is to physically adjust the user. Care givers should change the position of wheelchair clients at least every two hours to redistribute pressure onto other areas (Stall, 2013). Alternatively, wheelchairs could provide dynamic (moveable) components to allow occupants to regularly change their own sitting position.

- *Minimum shear force*

The force of the chair on the user at each interface consists of both normal (pressure) and shear forces (Clark, 2006). Shear forces can be generated on the wheelchair depending on the movement of body, the type of cushion and the motion of the wheelchair.

The performance or movement of users on their chairs, either voluntary or involuntary, can make them slide off the chair, generate shear force and possibly induce injury or discomfort. Especially for those patients who have extensor spasms, involuntary extension can create high shear forces and high contact forces on the chair. The range of forces applied to seating components needs to be understood, otherwise the seating structure will not only provide ineffective support but also may potentially be deleterious for the user.

2.4.2 Assessment of Seating Force

Whilst minimising the pressure and/or interface force on the chair is a major concern in special seating design, quantifying the force exerted on the wheelchair is a difficult and challenging problem. The magnitude and direction of force imparted on the seating systems depend individually on a variety of factors, including stability of posture, time spent on the chair and the characteristics of the user's impairments.

With these conditions in mind, many studies have been conducted to investigate optimal seating designs. This section reviews the various methods which have been applied to measure the force imparted to such seating systems, and clarifies the advantages and limitations of each.

- *Pressure Mat*

Pressure mats have been commonly used for the investigation of pressure distribution on the seating systems. A significant number of studies have been published which compare results of various cushions in which the pressure mat was placed between the seat surface and user in a fixed position or for use in various body positions and activities (Aissaoui et al., 2001, Gil-Agudo et al., 2009, Brienza and Karg, 1998, Bar, 1991) (Henderson et al., 1994, Tam et al., 2003, Crawford et al., 2005, Anne Fenety et al., 2000, Parkinson et al., 2002).

Using an ultra-light force sensing array mat, forces on a rigid seating system have been gathered during extensor spasms of 18 children. The 30 minute test required participants to perform three extensor spasms when they heard a sound produced at 5, 10 and 15 minutes. The mean force on the seat was 410.74 ± 273.70 N with the peak force up to 1050 N (Brown et al., 2001).

The first drawback of using a pressure mat is the interface of the sensor, which in the case of seating investigations can lead to distortions of the transducer. Thus inaccuracies may arise by the potential folding or wrinkling of the sensor (Grieve et al., 1975). Furthermore, because the mat has to be in direct contact with the user's body, this might disturb the natural position of sitting causing discomfort for applicants particularly when they participated in the prolonged investigation. The sensitivity of the sensor is another limitation of this methodology. For example, it has been shown that if a participant sways a little in a specific direction on the seat, the data read from the mat will still be constant (Lacoste et al., 2006).

However, the main limitation of pressure mats is related to its ability to determine the direction of the applied forces. Pressure mats can only measure the normal force, and are unable to determine the acting shear force, which is one of the major issues for a patient with extensor spasms.

- *Force Platforms*

Several studies have investigated the force on seating systems by modifying a force platform and assembling it under the seat as shown in Figure 2.5 (Aissaoui et al., 2001). However, the use of a force platform under the wheelchair seat is limited

by the size and weight of the force platform. The force platform cannot be integrated into most wheelchairs and cannot be used in a clinical setting (Lacoste et al., 2006).
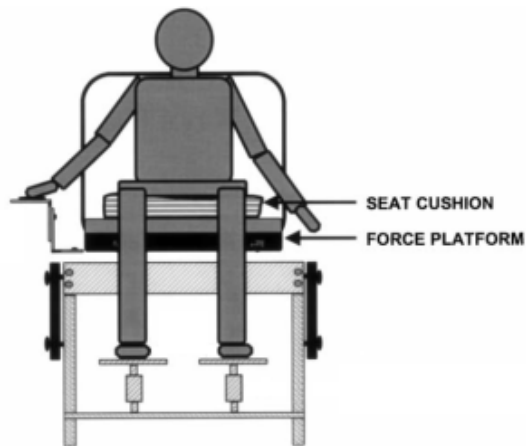
Figure 2.5 The test on effects of seat cushion by using the force platform
(Aissaoui et al., 2001)

Strain gauges have been used to measure forces on wheelchairs by putting them on some parts of the chair such as head support, backrest or lateral supports. In 2003, Holmes et al. published a paper in which they investigated the effects of special seating for wheelchair users with scoliosis. They redesigned a modular seating system, the backrest was replaced with clear plastic piece which is the same size as the original one and the strain gauged transducers were attached on the mounting bars for the lateral pads for measuring all three dimensions of forces and moments acting on the pads from the participant (Holmes et al., 2003).

Another quantitative study by Hirose and team measured the force on the special seating by installing loads measurements on wheelchair. The participant in this study was a young man with CP and strong extension who spent 8 hours a day in the wheelchair fitted with a force data acquisition system. The results showed that on the head support the peak load was 98 N, lateral support was 78 N for inward and 98-96 N for downward and at anterior support belts was 294–392 N (Hirose et al., 2008).

Using load cells connected to a data logger is a practical method for communal testing. However, the design of the data acquisition system must not create any inconvenience to the user and not hinder their mobility when data collection is performed over a long period of time, potentially outdoors.

- *Motion Analysis*

A number of researchers have investigated load measurements combined with motion analysis (Piccinini et al., 2009, Wook et al., 2006, Simon and Foulds, 2004). These have been achieved by using the force platform to collect kinetic data in company with an Infrared (IR) camera system to collect kinematic data. The analysis software evaluated the time varying output of sensors and computed the change in each body position. This method requires IR reflective markers to be placed on the participants' bodies (Figure 2.6), so that the IR cameras can capture the dimensions and coordinates of the model. Then kinematic data were analysed using the software to differentiate the different markers from each other and calculate with the external applied forces.

There are some possible inaccuracies produced by this method. For example, the reflective markers are assumed to be located in a constant position, but if the arrangement of markers had slipped due to dynamic movements during testing their trajectories will be incorrect (Zahedi et al., 1987).

Another problem is that this investigation needs to be done in a laboratory with the appropriate equipment, including enough IR cameras. This prevents this approach being used for the analysis of forces during ADL.
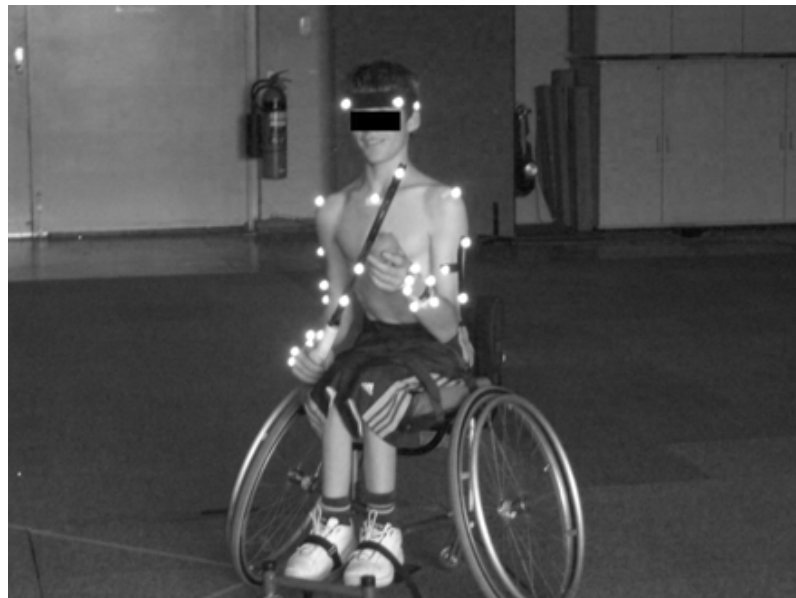
Figure 2.6 Motion analysis of wheelchair user (Reid et al., 2007)

2.5   RIGID AND DYNAMIC SEATING SYSTEMS

Special seating systems may be classified on the basis of positioning control into two types, namely rigid systems and dynamic systems.

2.5.1 Rigid Seating System

A rigid seating system has a seat with a fixed backrest position during use. This provides the user with the correct posture at all times removing undesired seat motion during ADLs which may interfere and change the occupant's position. However, the angle of the seat and backrest can be manually adjusted to optimise the arrangement for users and release some pressure in their sitting position.

A study about the effects of body orientation of children with CP on a rigid chair suggested that the upright position may have more advantages than a reclined position (Nwaobi, 1986). This paper compared EMG when patients were sitting in the upright position, 0 degree (90 degree of seat and backrest) and reclined at 30 degrees. The results showed that EMG signals and muscle tone were increased when the back angle was reclined at 30 degrees. It was suggested that the muscle tone increases because the participants' centre of mass (COM) is changed in this position, which resulted in an increase in abnormal tone, which could lead to extensor spasm. The upright position supported the movement of the upper body and participant eye contact in a better manner. Participants were asked to do the same functional tasks at different seat angles and children spent lowest task time when they were sitting at 0 degrees of posterior inclination. The time spent on each task was longer when the position was changed to 15 degrees and the longest performance time was when sitting at 30 degrees (Nwaobi, 1987, Nwaobi, 1986).

It has further been postulated that to maintain a good posture for most children who use special seating, users should sit with their hips, knees, and ankles at right angles (Werner, 2009). These positions can be achieved by using the postural guides to balance body segments on the chair. Defects in postural stability and structural asymmetries on the chair can also have a negative impact on the user leading to orthopaedic deformities, discomfort, decreased physiologic functions, self-image, and quality of life (Trefler et al., 1993).

Since users have diverse individual problems of motor control or muscle tone, such as muscle weakness, muscle imbalance, spasm or poor sensation, seating supports have to be varied as well based on requirements. The simplest modification is the angle of the backrest, which is is adjustable. This is of particular use for those who tend to fall forward on the seat, because the body can be leaned back, whilst other chair adjustments can maintain the hip, knees and ankles, at their preferred angle.

A recent study corroborates the findings of the previous work in patients with spinal cord injury. The angle of tilt-in-space should be at least 35° when combined with a recline of 100° and at least 25° with a recline of 120° for enhancing skin perfusion over the ischial tuberosity. But wheelchair with tilt-in-space less than 25° and recline less than 100° may not be sufficient for effective pressure reduction (Jan et al., 2010).

Despite rigid seating systems meeting the requirements of position management, there has been anecdotal evidence of a few problems with injuries on the chair or with the backrest breaking when used with children with strong extensor spasms. Therefore some wheelchair providers have incorporated a dynamic component on the chair to those users. The ultimate goal of such systems is to reduce the contact forces compared with a rigid seating system.

2.5.2 Dynamic Seating System

Dynamic seating systems have been available for some time by including active components such as spring loaded, elastic components or powered devices (Cooper et al., 2001). It is necessary here to clarify exactly what is meant by a dynamic seating system. The term "dynamic system" is generally understood to allow relative movement of the seat's components initiated by muscular action of the user. It is different from the adjustable systems that the components will be changed by caregivers. Typically the dynamic components can be incorporated into the headrest, backrest, footrest or any combination of these.

Dynamic systems have been designed to absorb and lessen the extensor force from the user. Cooper and Antoniuk reviewed the literature from the period and found little evidence for dynamic components lessening the contact pressure between the chair and the body compared with a rigid seating system (Cooper and Antoniuk, 2007). Research to date has tended to focus on a holistic outcome which would identify how the dynamic seating systems interact with users.

2.6 EVIDENCE OF BENEFITS OF DYNAMIC SYSTEMS

Whilst dynamic seating has been available for some time, and the beneficial effects of long term use of dynamic seating systems have been reported, research evidence is unclear on this topic.

2.6.1 Increased Range of Motion

The evidence for an increase in range of motion (ROM) of the dynamic component can be clearly seen in the study carried out by Cimolin et al. (2009). Using a pressure mat along with 3D motion camera capture, it was shown that the dynamic backrest system provided an increased ROM when users presented their extensor thrusts, which were artificially stimulated. Then the dynamic component was able to move the backrest back to the original position when users retracted their body. In the anterior–posterior direction, ROM at the head was 7.62 mm in the rigid system increasing to 43.75 mm in dynamic system. The trunk movement was 3.36 mm and 23.23 mm in rigid and dynamic systems respectively (Cimolin et al., 2009).

Whilst a dynamic system provides a greater flexibility in backrest movement increasing the angle between seat and backrest, assisting in mobility and possibly lessening the pressure of the sitting position which often leads to skin disruption and breakdown, it has been suggested that the range of movement should be limited and, importantly, the chair should guide the user back into a neutral posture, otherwise it probably could alter the muscle tone leading to unnecessary spasms (Cooper and Antoniuk, 2007). However, precise quantification of the limits to movement has yet to be determined.

The ROM of users' joints was investigated by Hahn et al. They evaluated the joint ROM after 6 months using two seating systems of the Rock Active™ (Kids Up Inc, Belgrade, MT 59714, United States). Participants with CP were separated into two groups: one was a control group who used a rigid system and another experimental group used the dynamic system. After long term use, joint ROM of both groups was increased, and particularly in the experimental group, where the ROM of the hip and knee were greatly increased. However, this increase was not significantly different between these two groups (Hahn et al., 2009), probably due to the large variability in individuals in these samples.

2.6.2 Reduced Extensor Tone

Only a small number of case studies have been published with regards to reduced extensor tone. These have shown that patients decrease in extensor tone after using the dynamic backrest systems for a while. One case was a client with mixed CP who used a dynamic wheelchair with a 200 N gas spring under the seat. The chair was adjusted to 140 degree of seat-back angle when he had full extension and returned to the original position at 85 degree when he relaxed (Figure 2.7). Over a few months the researcher found that his fluctuating tone and the duration of the full body extensions were decreased (Evans and Nelson, 1996).

A second case is a child with severe extensor spasm. He used the dynamic wheelchair which contained a spring to hold the backrest. After a few weeks his severe spasms were reduced (Orpwood, 1996).
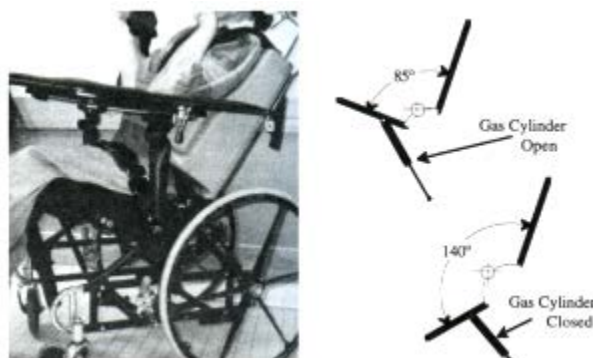
Figure 2.7 Dynamic seatback with gas cylinder (Evans and Nelson, 1996)
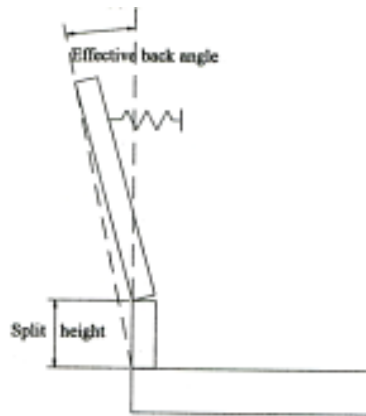
Figure 2.8 Dynamic seatback with spring (Ault et al., 1997).

Further evidence to confirm the benefits of using a dynamic backrest system was provided by Ault et al. (1997). They designed a dynamic backrest as a biangular back by dividing eht seatback into two sections; shoulder and pelvis. When the participant extended his back, the seatback was moved backward while pelvic support was fixed. The height of the pivot point was investigated in order to determine where the spring should go. After using the biangular dynamic chair for a few days, the results showed that the muscle tone was decreased (Ault et al., 1997).

Cooper et al. (2001) provided a dynamic backrest system to 14 adolescent clients with strong extensor spasms for use over 3 years. The qualitative results supported the idea that the use of dynamic backrest systems could decrease the strength and duration of the spasms. However, many of their participants were also undergoing other treatments for their spastic activity and this might have contributed to the reduction of the spasm episodes.

Cooper et al. (2001) also discussed the limited features of dynamic systems. For example: a lockout mechanism of the dynamic component should be provided for when the wheelchair had been driven on rough ground, otherwise the back angle varies during motion; another point was the key identification of the optimum return force which could return the backrest to the original position (Cooper et al., 2001).

2.6.3 Reduced Force and Pressure

Cimolin et al. (2009) found that when a user experienced extensor spasms on a dynamic backrest system the force and pressure were less than the rigid system. They investigated the differential interface force and pressure distributions between rigid and dynamic seating systems with ten children with CP. Participants were seated on a dynamic chair and spasms were stimulated by a loud noise. Kinematic acquisition and pressure distribution were collected whilst participants sat on the chair, during extensors and when the extension spasm was finished. Then the testing process was repeated on the rigid backrest system. Interface forces on the backrest were significantly different between the two systems; the mean force for dynamic backrest system was 33.85 N and the rigid one was 78.73 N. But forces on the headrest were not different between rigid and dynamic systems (Cimolin et al., 2009). However, the pressure mats used in this study can only measure normal forces, and as such may neglect all shear forces. Therefore since the relative position of the components in the dynamic chair changed, it is conceivable that higher shear forces were created, but not measured.

However, if load is reduced with dynamic components, then there are some possible reasons which could explain this benefit. The first possible explanation is the length-tension relationship of the muscle. The load generating capability of muscle changes with its length and muscle has a minimum contraction force when it is fully contracted. Therefore, as the dynamic backrest was reclined backward by the user's extension force, the seating system provided more space as the hip extensors shortened. Consequently, the force could have been lower when compared with the isometric restricted position on the rigid seating system.

A second, and probably more important mechanism, is the force-velocity relationship of muscle. A higher velocity of muscle contraction results in the decrease of the amount of force which a muscle can exert. Therefore on the backrest when the child had extensor spasms, the easier/faster the seat dynamically deforms, the less the force that is exerted on the chair.

The quantitative result from Cimolin et al. (2009) obviously showed that the dynamic configuration could reduce the normal interface force during extensor spasms. However, the study was a laboratory based testing with only 30 minutes of data collection. Moreover, children who participated in this test were activated into extensor spasms by the bursts of sound. Ethically dubious, this method negates the effects of real-life stimuli such as the body's positioning, the onset of sleep, pain, discomfort and environment. The most important of these criticisms is that they failed to note that it is not known how such stimulated spasms compare to those that occur during ADL.

2.6.4 Increase Functional Ability

Some of the case studies using dynamic seating support the view that users used their upper limbs more effectively. In addition, the caregivers also suggested the benefits of the dynamic seating system, for example, the children had more participation with family members. Their children looked more comfortable and the dynamic system aided the caregivers in easier transfer of these patients (Hahn et al., 2009, Orpwood, 1996).

In 2009, Hahn et al. used the GMFC, a reliable method to evaluate the performance of motor skills for children with CP, to compare with the performance of 12 children with CP over 6 months of using the dynamic and rigid backrest system. They mentioned that all children improved their clinical performances of 5 motor functions over the time changes, including:

1) Lying and rolling,

2) Crawling and kneeling,

3) Sitting,

4) Standing

5) Walking, running and jumping.

However, these improvements showed no significant differences between rigid and dynamic backrest systems (Hahn et al., 2009).

2.7   CONCLUSION

CP affects a child's ability to control movement and posture. Children with severe CP require special seating systems to aid their mobility, support their ADL, and lessen the physical workload for their carers. In the case of users who have extensor spasms, the high contact forces generated during spasm are physically powerful enough to injure the client or break the components of the wheelchair. An understanding of the range of forces applied to the seating components is absolutely essential for the design and implementation of appropriate postural support in specialised seating.

To date, various wheelchair providers have developed and introduced a dynamic feature on their wheelchairs. Usually such seating systems incorporate a dynamic component into the backrest, the idea being that it will dissipate the large forces generated by the children and reduce the loads on the product. However, whislt some benefits of dynamic seating have been shown, the effects of the dynamic seating system have to be further studied in order to clearly determine whether interface forces are reduced in dynamic systems.

There has been much interest in the magnitude and direction of the actual forces imparted by patients during extensor spasms. Several studies have been carried out which were concerned with measuring the imparted forces on rigid and dynamic seating systems (Brown et al., 2001, Cimolin et al., 2009, Hirose et al., 2008). In most studies, children were exposed to an external perturbation to elicit an extensor spasm. Moreover, only the short acquisitions of imparted forces measurement were reported whereas the forces applied to the seating system during activities of daily living remain unsolved.

Questions have also been raised about the advantages of prolonged use of dynamic seating systems which have been designed to accommodate a substantial amount of movement and lessen contact forces. Beneficial effects of dynamic seating systems have been reported, but research evidence documented in the literature is affected by significant limitations. Most of the studies rely on one user and consequently may not be representative of the user group as a whole (Orpwood, 1996, Ault et al., 1997). Bias cannot be ruled out as the results were likely to reflect

the authors' favourability towards using dynamic seating systems more than the scientific evidence on the effects of their use (Cooper et al., 2001). Furthermore the outcomes were rather controversial, with no general agreement reached over the long term improvement when compared to use of a rigid seating system. However it should be noted that long term use of a dynamic system did not have any adverse effects (Hahn et al., 2009).

In summary, to establish whether dynamic seating system designs have fulfilled their seating management aims, various measurement methods from the literature review have been developed and implemented, each of which has advantages and drawbacks as mentioned in the previous section. A number of the positive aspects of the measurement methods were utilised in this project, and attempts were made to improve upon the methodological limitations identified previously. In conclusion it was decided that the aims of our research were as follows:

- To design a fully mobile seating system capable of determining the force exerted on specific components by a child with CP over a prolonged period of use during ADL.
- To incorporate in the design the ability to determine any difference between a rigid and dynamic backrest component on chassis forces.
- To recruit and test multiple participants representative of children with CP.
- To use the designed system to collect data on the forces imposed on seating systems by children with CP during ADL and especially during extensor spasms. Spasms would not be artificially simulated.
- To assess any kinematic differences in a participant with an extended use of a dynamic component.

The remainder of this thesis describes the approach taken and the results obtained by addressing these challenges.

CHAPTER 3
DESIGN AND DEVELOPMENT
OF THE DATA ACQUISITION
SYSTEM

3.1   INTRODUCTION

The main aim of this study requires the load, which is applied to a seating system by a child with CP during their community based activity, to be determined. Participant monitoring is therefore required to be recorded throughout daily activity and especially during an extensor spasm. Consequently, the data collection instrument needs to be a robust, fully independent data acquisition system (DAQ). The data collection system must not provoke any physical or emotional reaction of the participant whilst sitting on the chair i.e. it should be completely unobtrusive. It should also be designed for minimal size and weight to minimise the burden on those pushing the chair. In addition, the DAQ system requires a power source which would power the equipment for prolonged periods on a testing day.

In response to these requirements, components on the Mygo™ seating system were fitted with strain gauges designed to capture the load data. One hundred strain gauges were arranged on certain components in such a way that each strain gauge bridge was sensitive to a particular direction or plane. Each bridge produced an output signal that was collected in one of 20 channels of an amplifier module. A fully independent data acquisition system included two amplifiers, an ultra mobile PC and a lithium-ion power source, was located in the base of the wheelchair, facilitating independence and mobility.

Each strain-gauged component had been appropriately calibrated using a linear-torsion materials testing machine (E10000, Instron, U.K.). Calibration matrices for each component were determined to convert measured strain into component stresses and bending moments. These calibration processes will be detailed in chapter 4.

3.2   THE MYGO™ SEATING SYSTEM

The Mygo™ Seating System (Figure 3.1) used in this study, is designed by James Leckey Design Ltd, Linfield Industrial Estate Belfast, UK. The Mygo is an activity chair which is designed specifically for the needs of children from the age of 4-10. Its purpose is to support the child in a safe, stable and secure position with appropriate supports at the pelvis, trunk, head, legs and feet. Depending on the required position, users are comfortable and able to carry out their daily activities. The Mygo seating system conforms to the requirements of the 93/42/EEC Guidelines, Medical Device Regulations 2002 and EN12182 Technical aids for disabled persons and test methods.

Figure 3.1 Mygo seating with Kimba base (Leckey, 2010)

The Mygo seat was attached to a wheeled base unit, the Kimba Spring Stroller, Otto Bock, Germany enabling the seat to be tilted anterior or posterior in space wheelchair (Figure 3.1). The original Mygo design is a rigid backrest system, however, the backrest angle can be adjusted in depth and angle (prone 10° or 80° from seat cushion to recline 25° or 115° from seat cushion) to accommodate posture, growth and angle positioning. The dynamic backrest system is a modified design by James Leckey Design Ltd. which offers a dynamic mechanism on the backrest. A gas spring is incorporated into the back supporting tube to enable the backrest to move forward and backward as the occupant extends and retracts their body.

3.3   EXPERIMENTAL CRITERIA

Previous studies of force measurements on wheelchairs have been detailed in the literature review. The strengths and weaknesses of this prior research has been utilised to achieve the design of the DAQ for this study's objectives. The challenges of the DAQ design included the methodology of collecting valid force data during a period of a participant's typical day and the integration of all the equipment on the wheelchair.

3.3.1 Community Based Testing

The aim of the study was to measure forces and moments applied on the seating of children with CP during daily living activities. The possible imparted forces on the chair are shown in Figure 3.2. The force measurement system should work under all conditions both indoors and outdoors, not only in a laboratory, but, for example, getting in and out of cars, and during school activities. Thus the DAQ system was required to be a fully mobile system which had a rapid response to a quick change of participant's actions.

3.3.2 Power Requirement

The trial period was intended to be a continuous session throughout a typical morning or afternoon in the participant's community. The DAQ system therefire needed sufficient power to supply it continually throughout the entire investigation period.
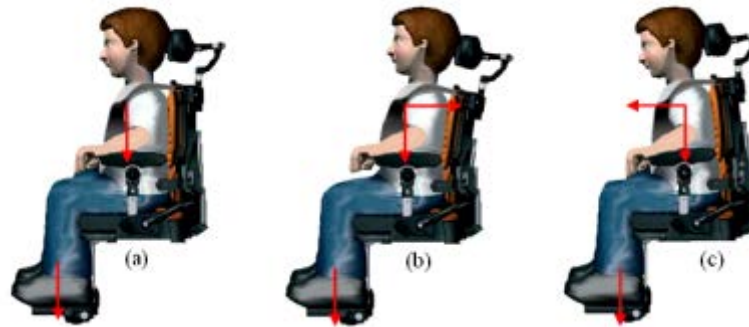
Figure 3.2 Different positions of sitting create forces and moments on the chair
(a) quiet sitting, (b) extending backward and (c) bending forward

Two 12V 8Ahr lithium polymer batteries (BP2544, Tracer Lithium-Ion Polymer Battery, Deben Group Industries, UK), connected in series, were used to power the amplifiers and ultra-mobile PC. Batteries were rechargeable and had capacity of 8Ahr which was enough to supply the DAQ for up to 6 hours.

3.3.3 Monitor Housing

All DAQ devices and connections had been designed to avoid any contact with the participant. The wires of the acquisition system were housed such that they cannot be touched. All strain gauges on the wheelchair components were covered by a couple layers of silicone coating. Cabling and DAQ devices were housed in the basket on an adapted tray underneath the seat without trailing wires. The basket had a cover which provided protection for the DAQ from light rain when testing outdoors. The cover could also keep the appliances hidden from other children who may be interested to grab them in the classroom monitoring period (Figure 3.3).

Figure 3.3 DAQ in basket

3.3.4 Participant Friendly

The investigation was expected to be done without restricting the normal activities of the participant. Therefore the modified wheelchair was required to be user friendly, providing exactly the same feeling as their own chair and to be promptly adjusted to fit a participant's needs. The modified wheelchair should not hinder mobility. The modified chair was slightly heavier than a normal wheelchair, with an increase in weight of 2.5 kg due to the mobile DAQ system, and therefore was a slight increased burden on those pushing the chair. Thus, small and lightweight materials and devices were used in designing the mobile equipment wherever possible.

3.4   DEVELOPMENT OF THE DATA ACQUISITION SYSTEM

3.4.1 Strain Gauge Technology

Strain gauge transducers have been widely used in measurement and accepted in different areas for many years (Beckwith et al., 1993). That is because they have high accuracy, reliability, at a reasonable price (Marioli et al., 1992).

The metallic foil-type strain gauge was the most suitable for this study because it has a low cross-sensitivity and easy to bonded on the specimen even in highly contoured positions (Pratt et al., 1979). For maximum performance, the circuit connection used was a Wheatstone bridge circuit with four strain gauges (full bridge circuit, Figure 3.4) to ensure the utmost sensitivity and to compensate for the effect of temperature. Linearity of this type of bridge circuit is the best (Hoffmann, 2010), and a very small force change can cause the change in bridge's resistance. When the bridge is loaded, two gauges will be in tension and the other two will be in compression. As the electrical resistance is proportional to the force, the resistance will be increased by the tensile force and decreased by the compression force.

After considerable discussion and contemplation, it was decided that strain gauges should be bonded to the framework of a wheelchair and to subsequently calibrate each component. The alternative was to cut the components and insert calibrated load cells into the structure. There are advantages and disadvantages of each approach.
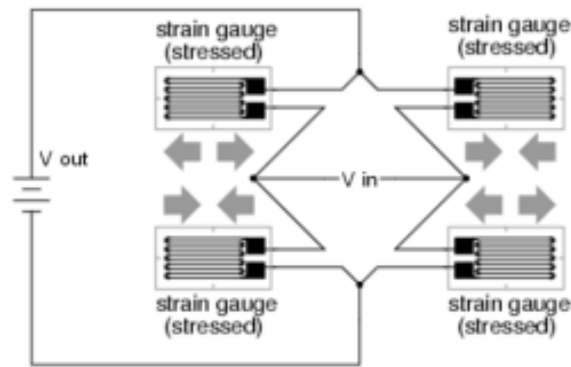
Figure 3.4 Strain gauges in full bridge circuit (http://sensorland.com)
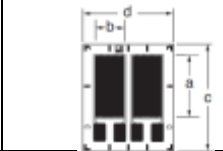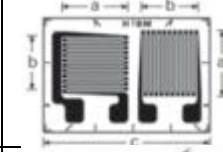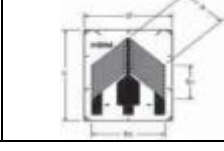
Whilst using pre-calibrated load cells may result in more accurate forces being determined on the chassis, the overriding consideration must be the safety of the child user. Therefore strain gauging individual components was chosen over using load cells because of the insertion of load cells into to the wheelchair's components may have affected the chair's worthiness in a crash scenario. Furthermore, it would have dramatically deviated the chair from the design which was CE marked. Finally, the cost of multiple commercial load cells was also prohibitive.

After considerable discussion and contemplation, it was decided that strain gauges should be bonded to the framework of a wheelchair and to subsequently calibrate each component. The alternative was to cut the components and insert calibrated load cells into the structure. There are advantages and disadvantages of each approach. Whilst using pre-calibrated load cells may result in more accurate forces being determined on the chassis, the overriding consideration must be the safety of the child user. Therefore strain gauging individual components was chosen over using load cells because of the insertion of load cells into to the wheelchair's components may have affected the chair's worthiness in a crash scenario. Furthermore, it would have dramatically deviated the chair from the design which was CE marked. Finally, the cost of multiple commercial load cells was also prohibitive.

3.4.2 Strain gauge methodology

Three types of strain gauges were used in this study (Y Series Strain Gauges, HBM, Germany (Table 3.1)) Strain gauge locations were identified based on the areas of contact between user and the seating (Figure 3.2). Also, James Leckey Design Ltd. suggested that forces be determined on the component which had been broken by a strong extensor thrust.

Table 3.1 Characteristics of strain gauges (Y Series Strain Gauges Catalogue HBM, Germany)

Strain gauge type	Resistance (Ω)	Grid size (mm)					
				a	b	c	d
1-DY41-3	350			3	2.5	8.2	8
1-XY31-3	350			3	2.9	10.9	7.6
1-XY41-3	350			3	4.1,5.6	11	8

Strain gauges were attached to specific components of the seating system in order to determine the complete mechanical environment of each component wherever possible. Size issues in some components reduced the ability to measure the full 3D stress environment, and in these cases, the predominant loading directions were presumed to measure. In general, however, the mechanical analyses in this study concerned the axial force (tension or compression), shear force, bending moment and torsion moment in different chair components: backrest and footrests as shown in Table 3.2

Table 3.2 Details of force measurement on wheelchair components

Component	Force Measurement	Number of strain gauges[1]
Backrest Angle Tube Assembly (BA)	Axial and shear force, bending and torsion moment	56
Backrest Angle Tube (BT)	Axial force, torsion moment	12
Foot Calf Support Lower Assembly (FA)	Axial force, bending moment	32
Gas spring base (GB)	Axial force	8

[1]*Total numbers of strain gauges on the rigid and dynamic backrest systems are 100 and 96 gauges, respectively.*
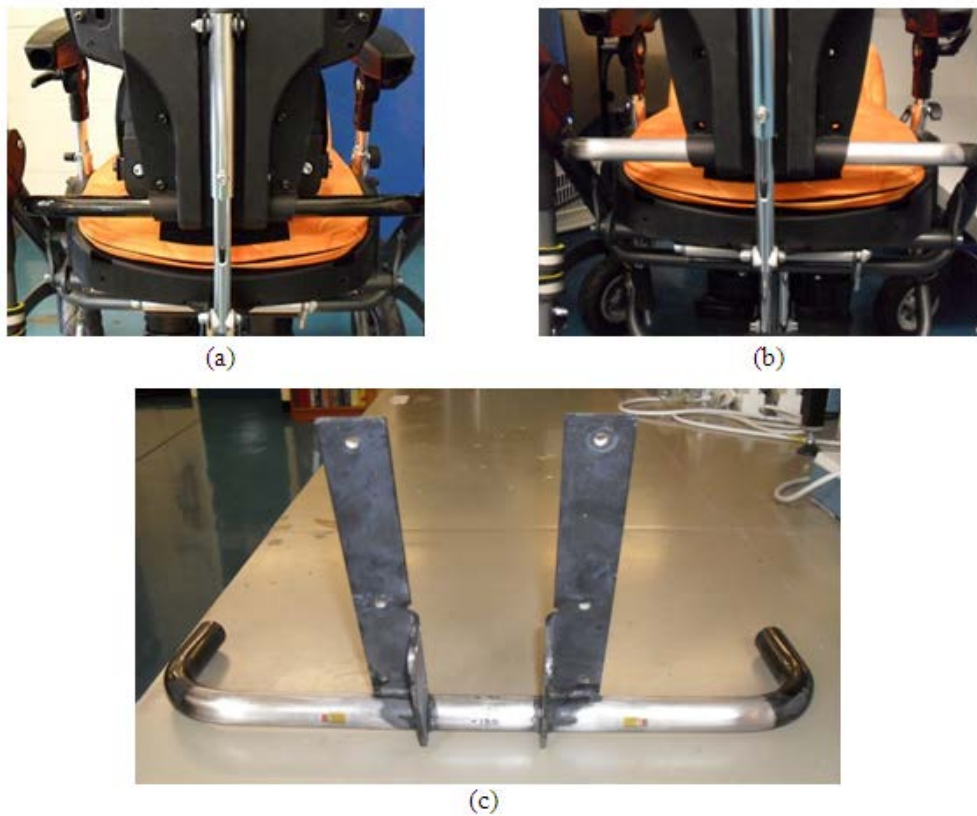
Figure 3.5 Process of strain gauge attachment
(a) BA before, (b) BA after removed the colour coating and (c) BA was marked position
for the strain gauge arrangement

James Leckey Design Ltd. provided the Mygo seating system. It was disassembled and the parts for force analysis were prepared for the strain gauge installation (Figure 3.5). Initially, the coating on the components was removed by high temperature and then the uncoated surface was polished by high grit sandpaper. The parts were then accurately scribed to identify the positions for all the strain gauges. Then strain gauges were bonded to the surface by using an adhesive and bonding material. These were done on 4 components namely, backrest angle tube assembly (BA), backrest angle tube (BT) in the rigid backrest system or gas spring base (GB) in the dynamic backrest system, and left and right foot supports (FA) as shown in Figure 3.6. The strain gauge installations were done by an experienced electronics technician, John Maclean, of the Department of Biomedical Engineering, University of Strathclyde.
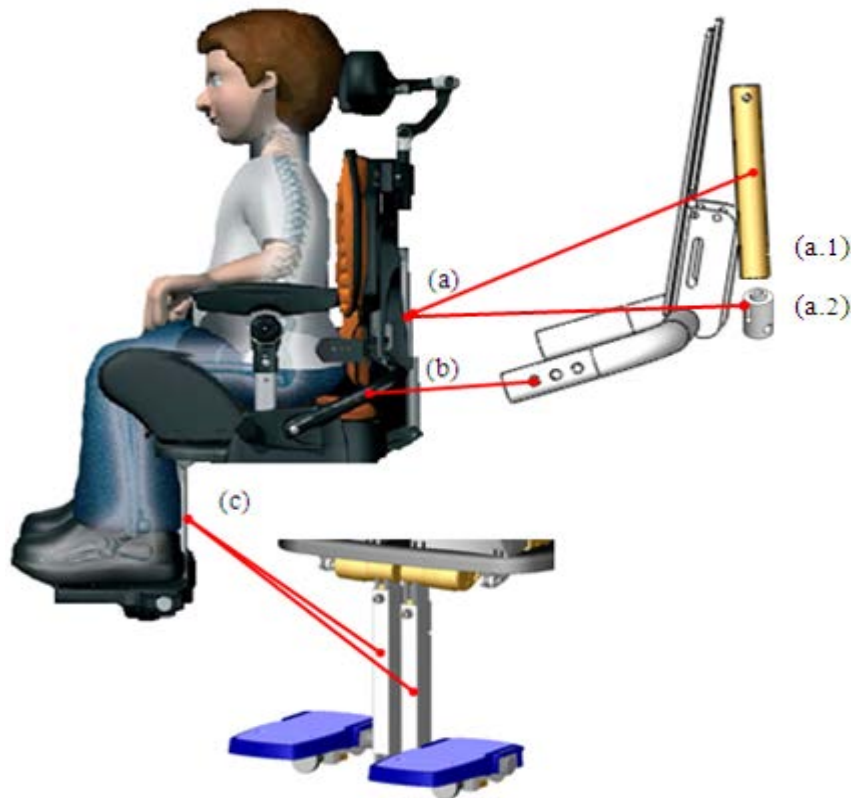
Figure 3.6 Measured components on the backrest and the footrest
(a.1) BT of the rigid system, (a.2) GB of the dynamic system, (b) BA and (c) both

sides of FA

- *Backrest Angle Tube Assembly*

The backrest angle tube assembly (BA) is made of mild steel ERW grade 1 BSEN 10305/3, 420 mm in length, with an outer diameter of 22.2 mm and an inner diameter of 18.2 mm. The BA is one of the main supports for the backrest and as such it was desirable to fully characterise its stress environment. Therefore, in this component it was desired that the axial force, bending moment and torsion moment were determined. The geometrical properties of cross sections of this tube were used in the strain gauge positioning and calibration process. The cross sectional properties of tubes were calculated as detailed in Appendix A (Meriam and Kraige, 1997).

Fifty six strain gauges were used and connected to create twelve full Wheatstone bridge circuits. Six circuits were on the left side of the BA and another six circuits were on the right side. This design of the strain gauging circuit was based on the knowledge of a six-channel force transducer by (Frossard et al., 2003, Zahedi et al., 1987, Magnissalis, 1992a). Each bridge was responsible for measuring one of the directions of general load acting upon the back area. Figure 3.7 shows the position of strain gauges and the wire grid alignment on the BA. The details of strain gauge types were shown in Table 3.3.

Table 3.3 Position of the strain gauges on the BA

Position	Forces	Strain gauge type*
0°	bending and shear	1-DY41-3/350, 1-XY41-3/350
60°	axial and torque	1-XY31-3/350, 1-XY41-3/350
90°	bending and shear	1-DY41-3/350, 1-XY41-3/350
150°	axial	1-XY31-3/350
180°	bending and shear	1-DY41-3/350, 1-XY41-3/350
240°	axial and torque	1-XY31-3/350, 1-XY41-3/350
270°	bending and shear	1-DY41-3/350, 1-XY41-3/350
330°	axial	1-XY31-3/350

Y Series Strain Gauges, HBM
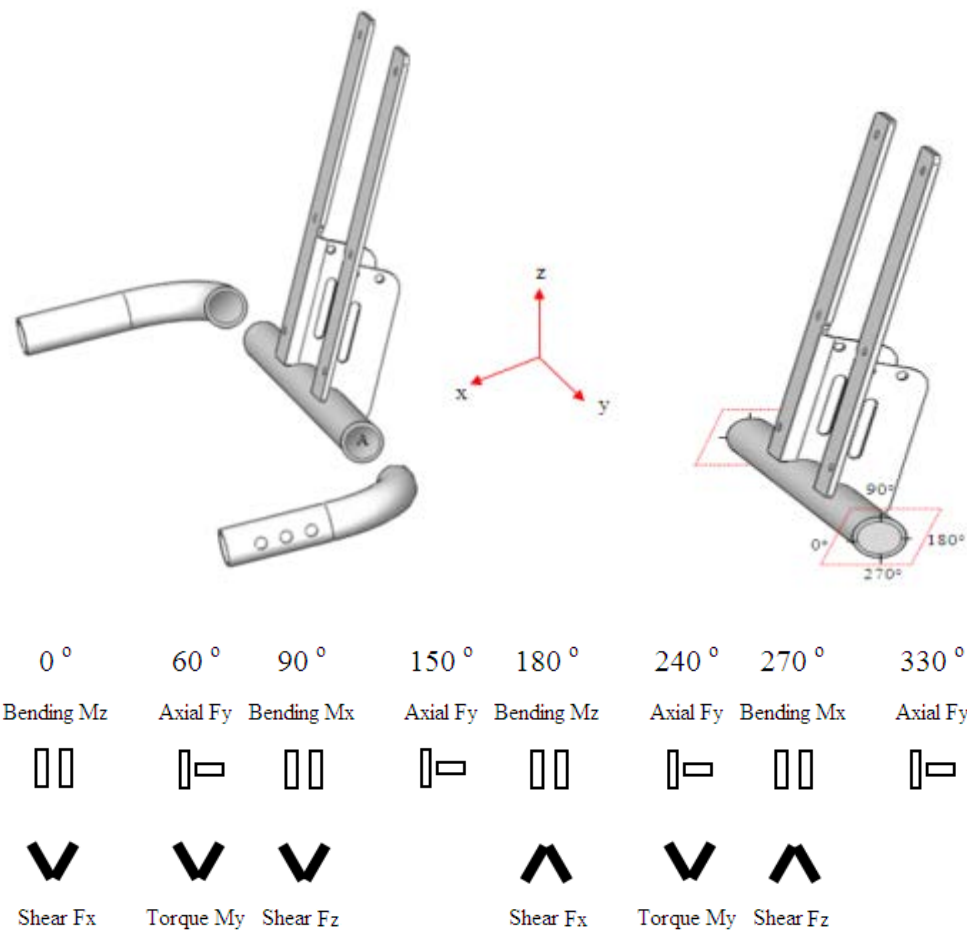
Figure 3.7 Strain gauge bonding diagram of six circuits on each side of the BA
to measure forces in six degrees of freedom (Magnissalis, 1992)

- *Backrest Angle Tube*

The backrest angle tube (BT) is made of Aluminium 6061-T6, with an outer
diameter 22.2 mm and an inner diameter 19.2 mm.

Two full Wheatstone bridge strain gauges were put on backrest angle tube (BT),
one channel measured the axial load and another channel measured torsion about the
long axis. Strain gauges were put on in such a position that the BT that would not be
damaged when the tube was moved for back angle adjustment. Consequently, this
left little room for additional strain gauges to measure forces in the other directions.
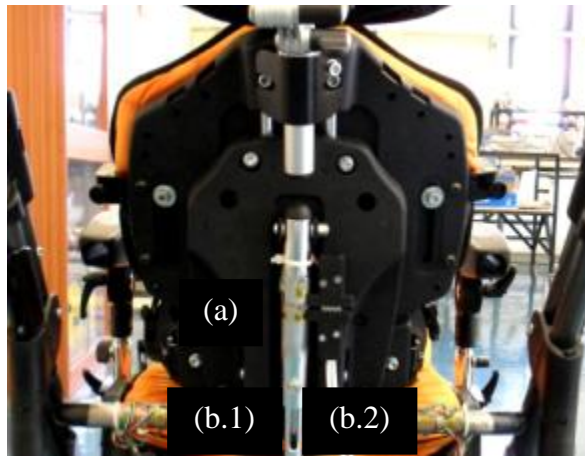
Figure 3.8 Strain gauges location on (a) the backrest angle tube (BT)
and (b.1), (b.2) both sides of the backrest angle tube assembly (BA)

- *Foot Calf Support Lower Assembly*

The footrest consists of left and right calf support assemblies (FA-L and FA-R).
Each footrest collected the axial load and bending moments as shown in Figure 3.9
and Figure 3.10.
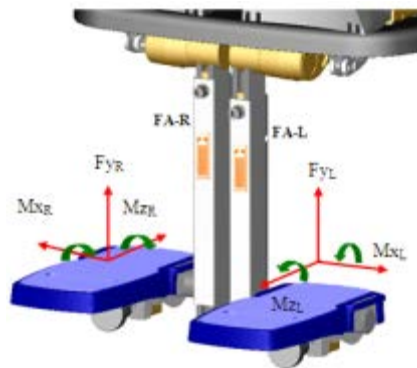
Figure 3.9 Strain gauges location on both sides of FA
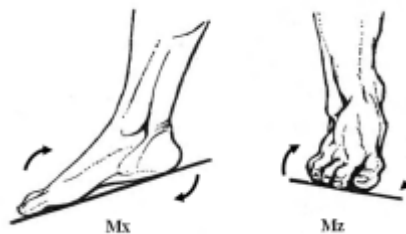
Figure 3.10 Bending moments on the footrest
Mx: moment about transverse axis through ankle,
Mz: moment anterior posterior axis

- *Gas spring*

For the dynamic backrest system, the back angle adjustment shaft of the Mygo seating system included a passive gas spring mechanism. As a replacement for the back angle inner extrusion, both ends of a gas spring were fitted in the backrest and seat connections. The size of the gas spring used depends on the load and extensor force of each user. Three sizes of gas spring, classified by the extension forces of 50, 100 and 150 N and stroke at 150 mm, were provided for each child.

To enable the dynamic backrest system, a gas spring was assembled on the back tube by attaching it to a gas spring base (GB) together with the lever and knobs which facilitate adjustment of the gas spring, as shown in Figure 3.11. The GB was coincident with the axial force from the gas spring. For this investigation, the GB required to be modified because the original one had not enough space to put any strain gauge circuitry. Consequently, strain gauges were attached on a modified GB to measure the axial force only on the back strut for the dynamic backrest system (Figure 3.12).
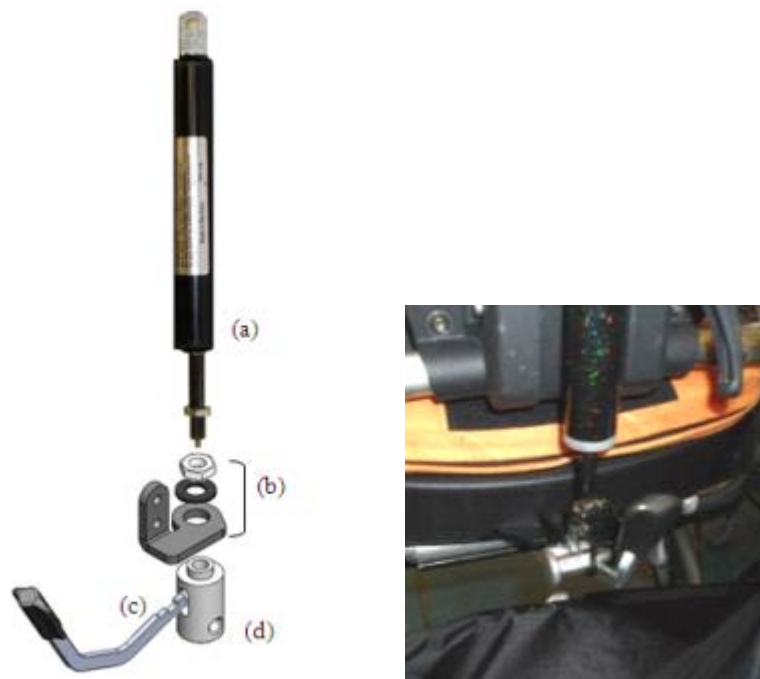
Figure 3.11 Gas spring assembled
(a) gas spring, (b) knobs, (c) lever and (d) GB
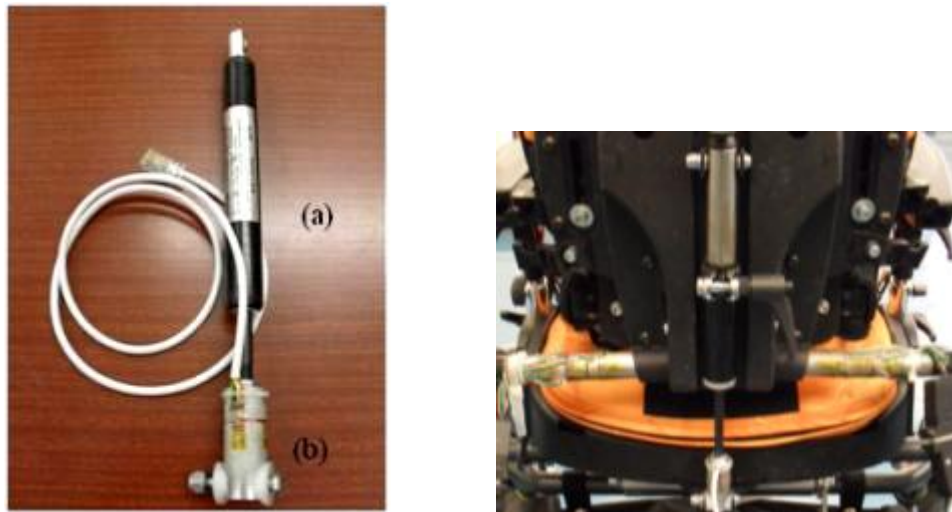
Figure 3.12 Strain gauges on the dynamic backrest component
(a) the 50N Bansbach gas spring, Germany, (b) the modified GB with transducers

3.4.3 Data Processing

The experimental design required a way to perform strain gauge measurements during ADL of participants and not in the laboratory. This was achieved by the installation of a fully independent data acquisition system (DAQ) integrated with a mobile power source located in the base of the wheelchair.

The equipment consisted of four key components including strain gauges, amplifiers, a data logging PC and power supply (Figure 3.13).

Figure 3.13 Distributed measurement acquisition diagram

Approximately one hundred strain gauges were arranged on the chair's components in such a way that each gauge was sensitive to load applied in a certain plane. The strain data were transmitted from the strain gauges through a 20 channel data acquisition system that collected the data and streamed it to an amplifier system.

The amplifier module consisted of 2 distributed amplifier modules (CA1030) for strain gauge full bridge configurations were embedded within 2 base units (CB1010, HBM, Germany). Each unit was approximately 500 grams. Each module had 10 measurement channels and they were connected by RJ45 shielded sockets. The 8 pin RJ45 connectors were plugged into each channel of amplifier.

The distributed amplifier module was the core of the system that collected the data and streamed it to a computer through the communication module (CANHEAD direct HBM, Germany) via a USB port, for storage, viewing and later analysis.

3.4.4 Software and Data Storage

By connecting with a USB port, data from each sensor was transmitted to a ultra-mobile PC (Viliv X70 processor USA 1.33 GHz, screen size 7 inch, dimensions 210 x 117 x 23 mm, 660g). This ultra mobile PC used the software package, CatmanEasy® (HBM, Germany). The elements of the data acquisition system are shown in Figure 3.14: (a) 10 measuring channel sockets connected by RJ45 plug, (b) measuring channel amplifier module, (c) communication module connects amplifier and (d) ultra mobile computer via USB port, (e) batteries connect with communication module via external supply socket.
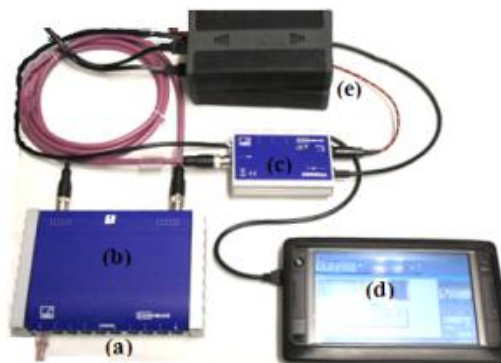
Figure 3.14 Hardware connection for a channel of strain signal to computer

In this investigation, strain gauge data were collected at 10 Hz. This provided sufficient resolution for extensor spasms (suggested by physiotherapists from WestMARC) and some knocks and bumps, whilst minimised data storage requirement. The strain data were transmitted from the strain gauges through 20 channels of the amplifier system when testing on the rigid backrest system and 19 channels when testing on the dynamic backrest system (Table 3.4).

Table 3.4 Detail of the force measured via 20 channels of the amplifier module

Catman strain channel	Component	Force/Moment
1		Shear Force (Fx1)
2		Axial Force (Fy1)
3	BA	Shear Force (Fz1)
4	(left side)	Bending Moment (Mx1)
5		Torsion Moment (My1)
6		Bending Moment (Mz1)
7		Shear Force (Fx2)
8		Axial Force (Fy2)
9	BA	Shear Force (Fz2)
10	(right side)	Bending Moment (Mx2)
11		Torsion Moment (My2)
12		Bending Moment (Mz2)
13	FA-L	Bending A (Mxl)
14	(left side)	Bending B (Mzl)
15		Axial foot (Fyl)
16		
	FA-R	Bending A (Mxr)
17	(right side)	Bending B (Mzr)
18		Axial foot (Fyr)
19	BT/GB	Axial (Fy)
20		Torsion (My)

Since the research was community based, the DAQ always be used through a day for a long period, and thus it needed a mobile power supply unit. Two 12V 8Ah lithium batteries (BP2544, Tracer Lithium-Ion Polymer Battery, UK) were connected in series to provide the power to the DAQ system. Each battery was 600g which was one third of the weight of a sealed lead acid equivalent.

Ideally each gauge will only produce an output signal when its corresponding load is applied. However, crosstalk signals were expected due to some activation of the non-corresponding gauges. The crosstalk or interference between measuring components is an important factor which can threaten the validity of a measurement system. Therefore it is necessary to know how the output from the device is related to the input values applied to the measurement system and eliminate the crosstalk between measuring. The calibration process of the force transducers on the Mygo seating will be explained in the next chapter.

3.5   FORCE IDENTIFICATION

The raw strain data was converted into force and moments by using a full calibration matrix determined by mechanical stress testing for each of the components. A static equilibrium scenario was assumed to determine the force being applied by the child on the components.

Strain data from CatmanEasy$^®$ were exported to MATLAB (version 7.12.0.635 R2011a) within which the calculations were performed. The forces and moments were then calculated using a full calibration matrix and summary statistics determined allowing a representative picture of the maximum and average forces applied to the wheelchair to be determined.

- *Force on the backrest*

The rigid backrest consisted of 14 channels of forces and moments on BA and BT/GB as shown in Figure 3.15. Forces and moments on BA at position (1) were added to the forces and moments at position (2) to represent the total load exerted on the BA.
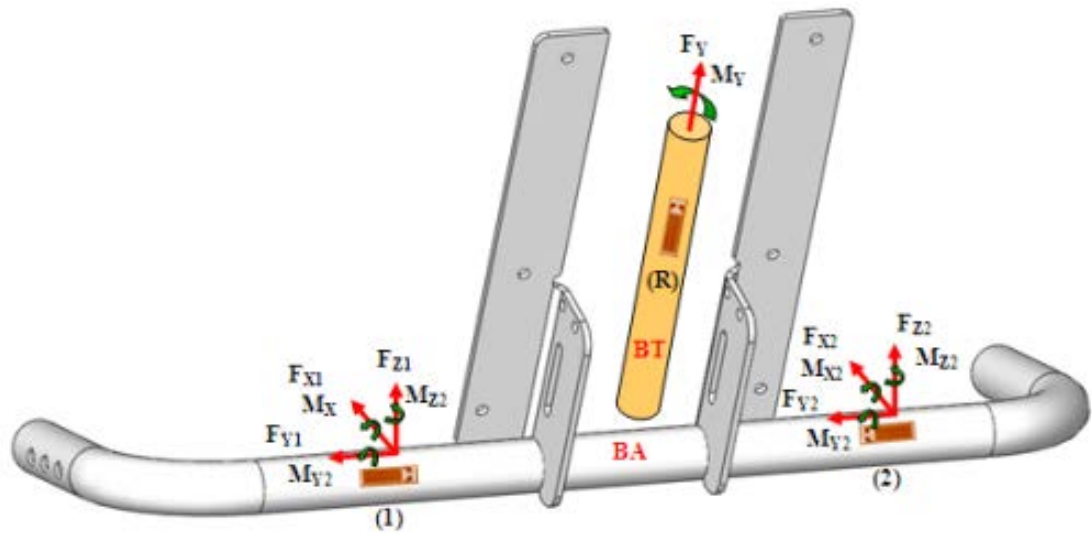
Figure 3.15 Schematic diagram of the backrest (BA)
strain gauges were placed on both sides of BA (1) and BA (2) and on BT (R)

Using translational and rotational equilibrium, the magnitude and direction of the resultant force acting upon the backrest (FB) was calculated (Figure 3.16).
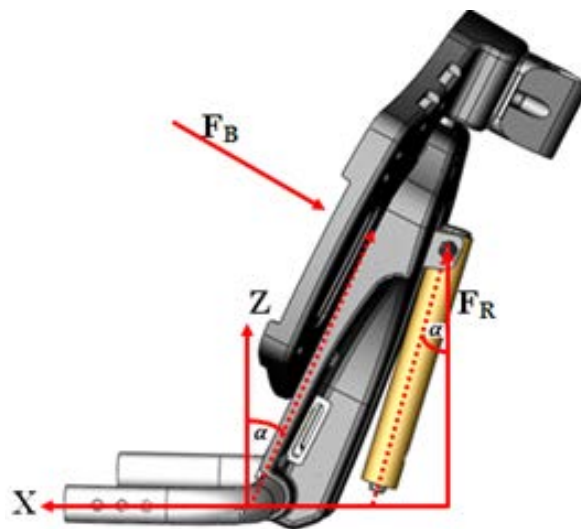
Figure 3.16 Schematic diagram of the backrest (sagittal view from left side)

Magnitude of force on the backrest in sagittal plane can be calculated by these vector equations:

$$\sum F: \quad F_1 + F_2 + F_R + F_B = 0$$

$$\sum Fx: \quad Fx_1 + Fx_2 + F_R \sin\alpha + F_{Bx} = 0$$

$$F_{Bx} = -Fx_1 - Fx_2 - F_R \sin\alpha \qquad \text{Equation (3.1)}$$

$$\sum Fz: \quad Fz_1 + Fz_2 + F_R \cos\alpha + F_{Bz} = 0$$

$$F_{Bz} = -Fz_1 - Fz_2 - F_R \cos\alpha \qquad \text{Equation (3.2)}$$

From which the resultant force on the backrest can be found:

$$F_B = \sqrt{F_{Bx}{}^2 + F_{Bz}{}^2} \qquad \text{Equation (3.3)}$$

- *Centre of Pressure*

In addition to the force of the child on the chair, the centre of pressure (the locus of the intersection of the resultant force with the plane of the backrest) was also determined.
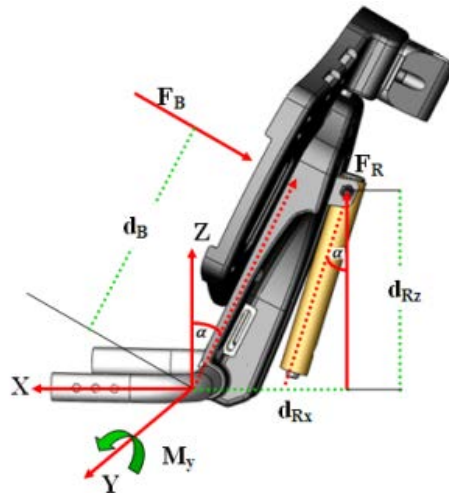
Figure 3.17 Schematic diagram of the backrest

$$\sum My = 0; \quad My_1 + My_2 + d_{Rz}.R_x + d_{Rx}.R_z - d_B.F_B = 0$$

$$My_1 + My_2 + d_{Rz}.\,F_R \sin\alpha + d_{Rx}.F_R \cos\alpha = d_B.F_B$$

$$d_B = \frac{My_1 + My_2 + d_{Rz}.\,F_R \sin\alpha + d_{Rx}.F_R \cos\alpha}{F_B} \qquad \text{Equation (3.4)}$$

The x and z position of the COP was measured with respect to the global coordinate system, which had its origin at the middle of the BA.
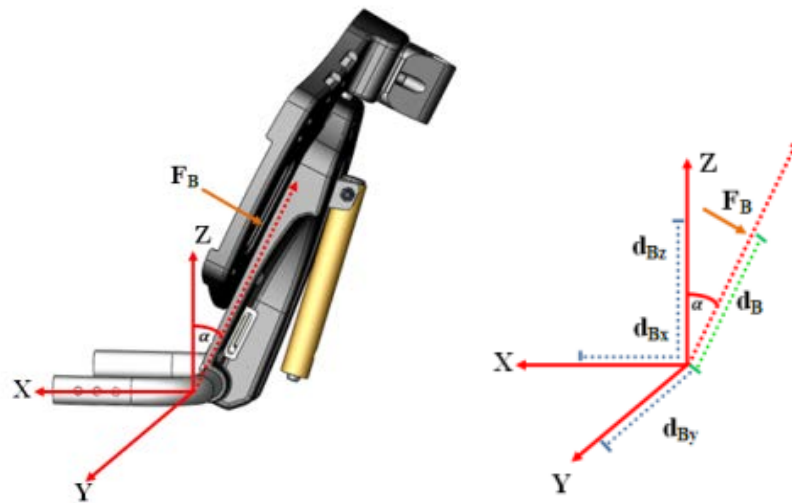
Figure 3.18 Sagittal plane of the backrest and direction of force and point of application

$$d_{Bx} = d_B \sin \alpha \qquad \text{Equation (3.5)}$$

$$d_{Bz} = d_B \cos \alpha \qquad \text{Equation (3.6)}$$
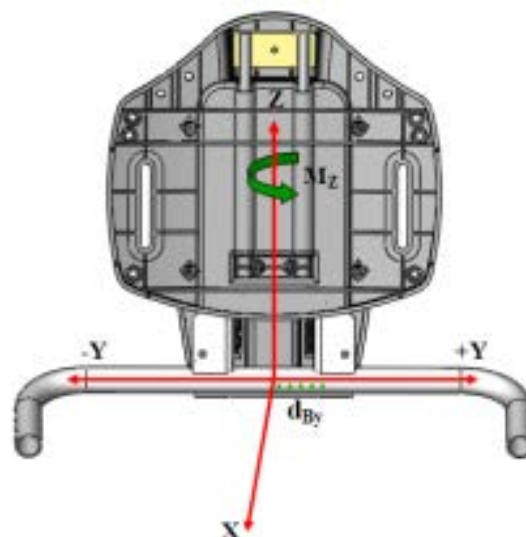
Figure 3.19 Frontal plane of the backrest

The lateral position of the COP, d_{By}, was found by considering the sum of the moments about the Z axis, $\sum Mz = 0$

$$Mz_1 + Mz_2 + F_{By}. \ d_{Bx} + F_{Bx}. \ d_{By} = 0$$

$$d_{By} = \frac{Mz_1 + Mz_2 + F_{By}. \ d_{Bx}}{-F_{Bx}} \qquad \text{Equation (3.7)}$$
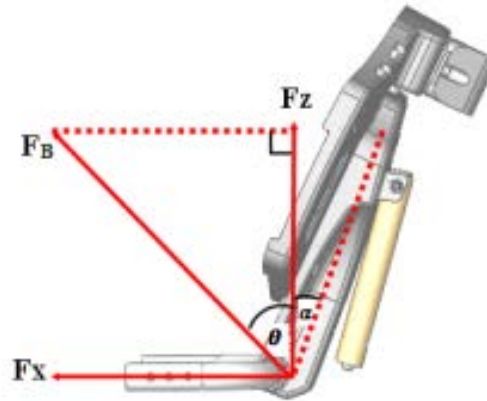
Figure 3.20 Angle of contact point on the backrest

The angle of the contact force on the backrest in sagittal plane can be determined by the forces Fx and Fz as shown in Equation (3.8). Then include the angle of BA, α which was a constant at 26 degrees.

$$\tan \theta = \frac{Fx}{Fz} \qquad \text{Equation (3.8)}$$

3.6 STRESS ANALYSIS

To avoid the possibility of yielding under complex stress situations and to cause a component breakage, results of the applied forces on the wheelchair need to be analysed to find the stress (σ) in the material. This was to ensure that these determined stresses did not exceed the yield strength of material (σ_y).

3.6.1 Backrest Angle Tube Assembly

The two primary transducer circuits, BA1 and BA2, were positioned on the BA to determine the user-applied loads. The BA was deemed the critical component which gained complex applied forces by the child as a result of full body extension. Stresses can be in different directions and the direction and magnitude of stresses change from position to position as shown in Figure 3.21. Even if the principal stresses did not exceed the yield stress, the combination of stresses possibly could result in yielding of the material. Therefore the von Mises equivalent stress was determined and compared to the yield criterion at positions A, B and C on BA1 and BA2.
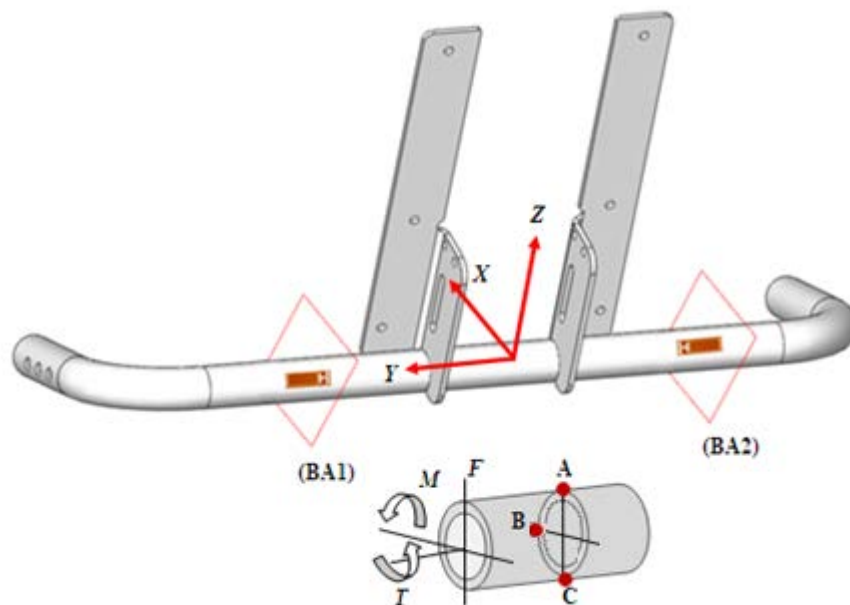
Figure 3.21 Point A, B and C on the BA1 and BA2
subjected to combined axial tensile (*F*), bending (*M*) and torsion (*T)*

The von Mises equivalent stress (σ_e) is based on a combination of principle stresses which is then compared to the yield stress of material. To understand the stress state at point A, B and C both the normal and shear stress at that point should first be determined. Normal stresses are primarily induced from bending and shear stresses from applied torques and shear loads. As the bending moments at the different points A, B and C can induce both positive and negative material stress the direction of the moments should be considered (Benham and Crawford, 1996).

The stress at point A, B and C was determined using the three following Equation (3.9) - Equation (3.11).

$$\frac{M}{I} = \frac{\sigma}{y} = \frac{E}{R}$$ Equation (3.9)

$$\sigma = \frac{My}{I}$$ Equation (3.10)

$$\tau = \frac{Tr}{J}$$ Equation (3.11)

M is the bending moment (Nm)

σ is the normal stress (N/m^2)

E is the Young's Modulus (N/m^2)

R is the radius of the neutral axis (m)

y is the distance from the neutral axis (m)

I is the second moment of area, in bending, about X or Z axis (m^4)

J is the second moment of area, in torsion, about Y axis (m^4)

τ is the shear stress, (N/m^2)

r is the radius (m)

T is the torque moment (Nm)

Based on the local coordinate system defined in Figure 3.21, the normal stress at point A, B and C are a result of the axial load F_y and the bending moment M_x, M_z and M_x respectively. Depending on the direction of the bending moment, the stress at point A due to a negative M_x moment with respect to the local coordinate system will be positive due tension and negative at point C due to compression. Furthermore the shear stress due to the torques and shear loads was also considered. The shear load F_z will create a minimum zero shear at point A and the opposing side of the tube at C but a maximum at point B (Figure 3.22). Hence the Fx shear force will cause a maximum shear stress at point C but no stress at point A and B, again the same equation is used to determine the same maximum shear force from F_z load.
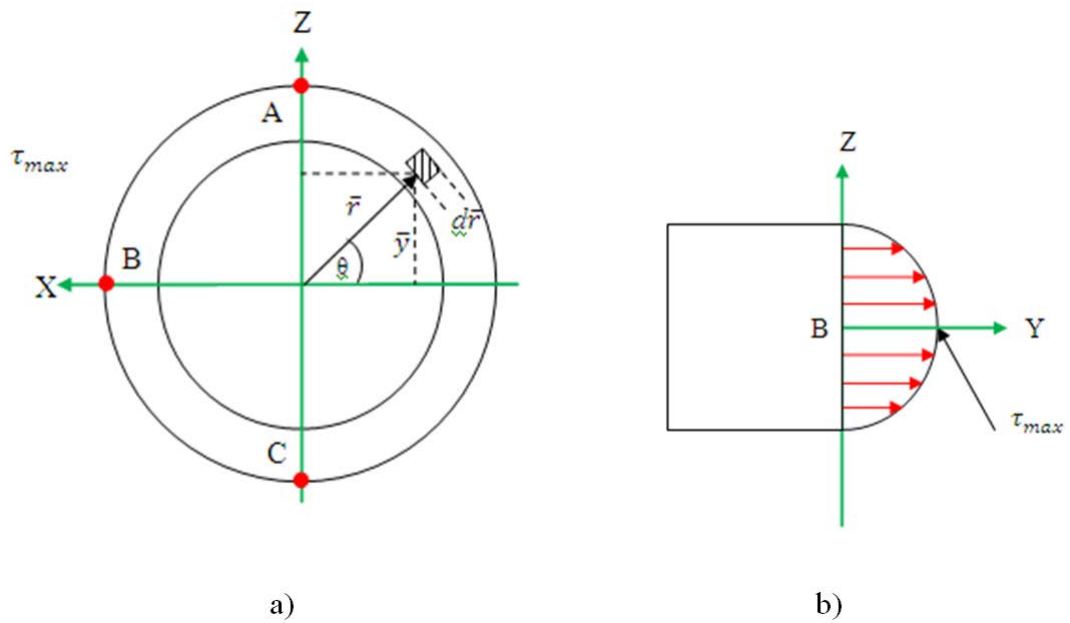
Figure 3.22 Normal stress at point A, B and C on the BA
a) x,z coordinate, b) y,z coordinate

The first moment of area and max transverse shear force

$$\bar{y} = \bar{r}\sin\theta \qquad \text{Equation (3.12)}$$

The elemental area

$$dA = \bar{r}\,d\bar{r}\,d\theta \qquad \text{Equation (3.13)}$$

The first moment area

$$A\bar{y} = \int \bar{y}\,dA \qquad \text{Equation (3.14)}$$

$$A\bar{y} = \int_0^\pi \int_{r_{inner}}^{r_{outer}} \bar{r}^2 \sin\theta\,d\bar{r}\,d\theta \qquad \text{Equation (3.15)}$$

$$\tau A\bar{y} = \frac{2r_o^3}{3} - \frac{2r_i^3}{3} \qquad \text{Equation (3.16)}$$

Therefore the maximum shear force of Fz is given by

$$\tau_{max} = \frac{F_z A\bar{y}}{2rI} \qquad \text{Equation (3.17)}$$

$$\tau_{\max\ (z)} = \frac{32F_z}{\pi r_o\left(D_i^4 - D_o^4\right)}\left[\frac{3r_i^3}{3} - \frac{2r_o^3}{3}\right] \qquad \text{Equation (3.18)}$$

As shown, plane stress is considered on the surface at positions A, B and C, and the transverse shear stress is considered to be complementary to the surface longitudinal shear stresses and thus equal and opposite to it.

Consider a rectangular element of material of unit thickness, taken from points A, B and C (Figure 3.22), and subjected to tensile and shear stress. Normal stresses and shear loads acting are defined as shown in Figure 3.23 - Figure 3.25
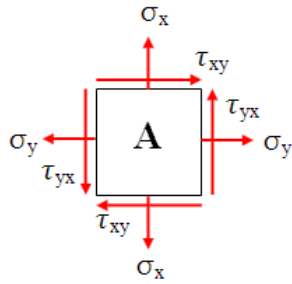
Figure 3.23 Point A

$$\sigma_y = \frac{M_x y}{I} + \frac{F_y}{A}$$

$$\sigma_x = 0$$

$$\tau_{yx} = \frac{M_y r}{J} + \tau_{\max\ (x)}$$
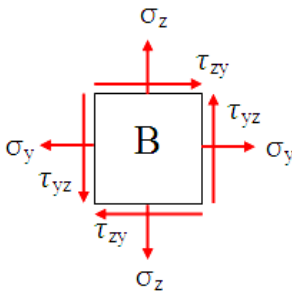
$$\tau_{xy} = \tau_{yx}$$

Figure 3.24 Point B

$$\sigma_y = \frac{M_z y}{I} + \frac{F_y}{A}$$

$$\sigma_z = 0$$

$$\tau_{yz} = \frac{M_y r}{J} + \tau_{\max\ (z)}$$

$$\tau_{zy} = \tau_{yz}$$
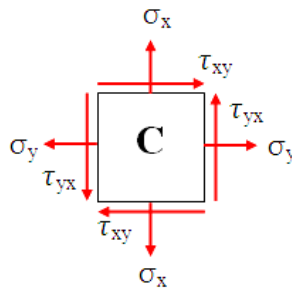
Figure 3.25 Point C

$$\sigma_y = \frac{M_x y}{I} + \frac{F_y}{A}$$

$$\sigma_x = 0$$

$$\tau_{yx} = \frac{M_y r}{J} + \tau_{\max\ (x)}$$

$$\tau_{xy} = \tau_{yx}$$

There is a certain orientation, with respect to the defined local coordinate system at position A, B and C, in which the normal stress are at a maximum and minimum. These planes are known as the principal planes and completely define the state of stress at these points. Once these principal stresses are known the equivalent stress can be calculated and then compared to the yield stress of the material determined from the uni-axial tensile test.

In three dimensions the symmetric stress tensor used to define the three normal orthogonal stresses and six orthogonal shear stresses is shown below (Young and Budynas, 2002).

$$\begin{bmatrix} \sigma_x & \tau_{xy} & \tau_{xz} \\ \tau_{yx} & \sigma_y & \tau_{yz} \\ \tau_{zx} & \tau_{zy} & \sigma_z \end{bmatrix}$$

The axial normal stress at position A, B and C is readily obtained from the bending and axial loads, however the normal hoop stress acting in each element is considered to be zero as the bending or shear force will not create a normal stress in this direction. Finally if the third normal stress acting is also consider to be zero, as the bending moments and shear forces also do not induce surface normal stress on the tube face, plane stress can be considered.

$$\begin{bmatrix} \sigma_x & \tau_{xy} \\ \tau_{yx} & \sigma_y \end{bmatrix}$$

Mohr's circle is convenient method to determine the principal normal stress, however due to the large volume of data being evaluated in this study, a more appropriate method involves the eigenvalues, relating to the principal normal stress, and eigenvectors, relating to the direction of the principal axes at each point A, B and C, to be determined (Young and Budynas, 2002).

Using the MATLAB eig.m function the principal eigenvalues were solved for and directly substituted in the von Mises equation below.

$$\sigma_e = \frac{1}{\sqrt{2}} \left[(\sigma_x - \sigma_y)^2 + (\sigma_y - \sigma_z)^2 + (\sigma_z - \sigma_x)^2 \right]^{\frac{1}{2}} \qquad \text{Equation (3.19)}$$

$$\sigma_e = \frac{1}{\sqrt{2}} \left[(\sigma_x - \sigma_y)^2 + (\sigma_y - \sigma_z)^2 + (\sigma_z - \sigma_x)^2 \right]^{\frac{1}{2}} \qquad \text{Equation (3.20)}$$

When σ_e reaches σ_y, the yield strength determined from the uniaxial tensile test, the material is deemed to have yielded. In two dimensions the von Mises equation is reduced to (Benham and Crawford, 1996):

$$\sigma_e = \frac{1}{\sqrt{2}} \left[(\sigma_x - \sigma_y)^2 + (\sigma_y)^2 + (\sigma_x)^2 \right]^{\frac{1}{2}} \qquad \text{Equation (3.21)}$$

3.6.2 Backrest Angle Tube

Only the axial force and torque were determined on the backrest angle tube (BT, Figure 3.26Figure 3.25). The stress on the BT was defined by the force (Fy) divided by the cross section area:

$$\sigma_y = \frac{F_y}{A}$$

Equation (3.22)
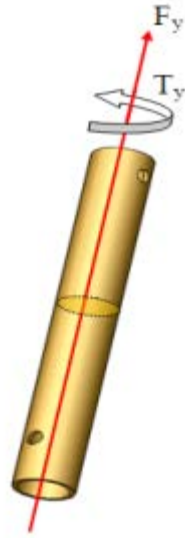
Figure 3.26 Measured force on BT

3.6.3 Gas Spring Base
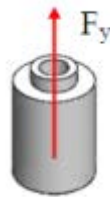
Figure 3.27 Measured force on GB

The uniaxial force (Fy) and the stress (σ_y) were determined on the gas spring base as follows:

$$\sigma_y = \frac{F_y}{A}$$

Equation (3.23)

3.6.4 Foot Calf Support Lower Assembly

On the foot calf support lower assembly (FA) the axial force (Fy) and the bending moments (Mx and Mz) on the footplate (Figure 3.28) were measured.
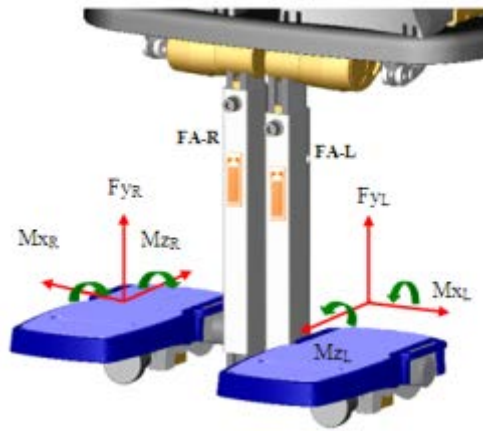
Figure 3.28 Schematic diagram of the footrest
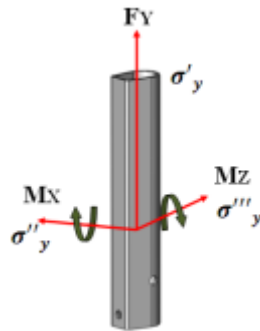
Figure 3.29 Measured force on FA

The stress on the FA (σ_y) was the combination of the stress in the axial direction (σ'_y), bending stress Mx (σ''_y) and bending stress Mz (σ'''_y):

$$\Sigma\sigma_y = \sigma'_y + \sigma''_y + \sigma'''_y$$

$$\Sigma\sigma_y = \frac{Fy}{A} + \frac{MxYz}{Ix} + \frac{MzYx}{Iz} \qquad \text{Equation (3.24)}$$

3.7   CONCLUSION

The development of a fully mobile, strain-gauged seating system focussed on maximising force information, whilst reducing the size and weight of the DAQ. All units were housed in a basket with a cover and then installed underneath the seat without external connection wires or cross cables.

Our DAQ offered several advantages when compared to previous methods. As mentioned before, since the system is a standalone, it allowed for testing in everyday locations, not only in a laboratory environment. Furthermore, the DAQ did not limit participants in their ADLs. The transducers were attached to the seating frame and appeared flush with the surface of the wheelchair components, and no transducers or any physical contact was made on the participants.

The major advantage of using strain-gauge technology is the ability to determine the magnitude and direction of the force exerted on the component. Therefore this technology has been used not only for static positions but it also recorded data at certain instants of dynamic measurements. Assuming static equilibrium, the strain data can be converted into force and moments acting on the backrest and footrests in three dimensions. The position of the resultant force on the backrest, termed the COP, can be also determined.

A variety of component coordinate systems were establishedand set when the strain gauges were attached. Each three dimensional coordinate system, x, y, and z was oriented in the same orientation as the strain-gauge bonding diagram of the six circuits (Magnissalis, 1992). To eliminate any misunderstanding of coordinate systems, the orthogonal coordinate system will be shown along with the schematic of wheelchair components and load data.

CHAPTER 4
CALIBRATION OF THE
STRAIN GAUGES

4.1   INTRODUCTION

Strain gauges were arranged on the metal framework of the wheelchair, the backrest angle tube assembly (BA), backrest angle tube (BT) on the rigid backrest system or gas spring base (GB) of the dynamic backrest. The twenty channels of strain gauge output were amplified and then underwent analogue to digital conversion using the Catman system (Catman®Easy V3.1.2.21 HBM, Darmstadt, Germany). The discrete values were then stored in the ultra-mobile PC. Ideally, each Wheatstone bridge arrangement would only produce an output signal when a load was applied in the appropriate direction. However, crosstalk signals were inevitable and expected due to the activation of the non-corresponding arrangements, due to minor misalignment of the gauges.

Crosstalk or unwanted correlation between strain gauge circuitry is an important factor which can severely affect the validity of a measurement system. Thus crosstalk should either be minimised or incorporated and accounted for during the calibration process. The calibration process correlates strain outputs from the strain gauge acquisition system to known applied loads on the wheelchair components by repeatedly applying forces and measuring the resulting change of the transducer outputs. To achieve this process, an Instron testing machine was used to test a wide range of loads in tension, compression and torsion on the framework of the wheelchair. The components were loaded within their elastic limit so material yield was not reached, as this would damage the material structure and the strain gauges. A

linear response between load and output was assumed, enabling the associated linear equations between output and applied loads on components to be used to determine the coefficients of the linear stress strain relationship. After calibration, the strain output data can be processed by using calibration matrices to determine forces and moments acting on the components.

4.2   CALIBRATION COEFFICIENTS

The forces and strains on each component were assumed to be related through:

$$S_i = \sum_{j=1}^{6} C_{ij} F_j$$

or $\hspace{4cm}$ $[S] = [C]\ [F]$ $\hspace{3cm}$ Equation (4.1)

$[S]$ = column matrix (6x1) of output signal proportional to strain

$[C]$ = square matrix (6x6) constraining calibration factor C_{ij}

$[F]$ = column matrices (6x1) of input applied loads

In matrix notation:

$$[S] = \begin{bmatrix} SF_X \\ SF_Y \\ SF_Z \\ SM_X \\ SM_Y \\ SM_Z \end{bmatrix}, \qquad C_{ij} = \begin{bmatrix} C_{11} & C_{12} & C_{13} & C_{14} & C_{15} & C_{16} \\ C_{21} & C_{22} & C_{23} & C_{24} & C_{25} & C_{26} \\ C_{31} & C_{32} & C_{33} & C_{34} & C_{35} & C_{36} \\ C_{41} & C_{42} & C_{43} & C_{44} & C_{45} & C_{46} \\ C_{51} & C_{52} & C_{53} & C_{54} & C_{55} & C_{56} \\ C_{61} & C_{62} & C_{63} & C_{64} & C_{65} & C_{66} \end{bmatrix}, \qquad [F] = \begin{bmatrix} F_X \\ F_Y \\ F_Z \\ M_X \\ M_Y \\ M_Z \end{bmatrix}$$

The resultant matrix, should have a leading diagonal (when i = j) of dominant coefficients. Thus the main channel, which is the channel that corresponds to the applied load, should give the largest coefficient or response. Therefore when i ≠ j the coefficients correspond to the five cross talk effects and should ideally be zero (Magnissalis, 1992b). The coefficient matrix that converts the Catman strain outputs to a known applied load is the inverse *of* the calibration matrix.

$$[F] = [C]^{-1}. [S] \qquad \text{Equation (4.2)}$$

$$[F] = [M]. [S] \qquad \text{Equation (4.3)}$$

[M] = square matrix (6x6) inverse calibration matrix (C_{ij}),

Written metrically is

$$\begin{bmatrix} F_x \\ F_y \\ F_z \\ M_x \\ M_y \\ M_z \end{bmatrix} = \begin{bmatrix} M_{11} & M_{12} & M_{13} & M_{14} & M_{15} & M_{16} \\ M_{21} & M_{22} & M_{23} & M_{24} & M_{25} & M_{26} \\ M_{31} & M_{32} & M_{33} & M_{34} & M_{35} & M_{36} \\ M_{41} & M_{42} & M_{43} & M_{44} & M_{45} & M_{46} \\ M_{51} & M_{52} & M_{53} & M_{54} & M_{55} & M_{56} \\ M_{61} & M_{62} & M_{63} & M_{64} & M_{65} & M_{66} \end{bmatrix} \begin{bmatrix} SF_x \\ SF_y \\ SF_z \\ SM_x \\ SM_y \\ SM_z \end{bmatrix}$$

$F_x = M_{11} . SFx + M_{12} . SFy + M_{13} . SFz + M_{14} . SMx + M_{15} . SMy + M_{16} . SM_Z$

$F_y = M_{21} . SFx + M_{22} . SFy + M_{23} . SFz + M_{24} . SMx + M_{25} . SMy + M_{26} . SM_Z$

$F_z = M_{31} . SFx + M_{32} . SFy + M_{33} . SFz + M_{34} . SMx + M_{35} . SMy + M_{36} . SM_Z$

$Mx = M_{41} . SFx + M_{42} . SFy + M_{43} . SFz + M_{44} . SMx + M_{45} . SMy + M_{46} . SM_Z$

$My = M_{51} . SFx + M_{52} . SFy + M_{53} . SFz + M_{54} . SMx + M_{55} . SMy + M_{56} . SM_Z$

$Mz = M_{61} . SFx + M_{62} . SFy + M_{63} . SFz + M_{64} . SMx + M_{65} . SMy + M_{66} . SM_Z$

The physical process of determining the strain gauge output *(S)* for a known applied load *(F)* using the Instron testing machine will now be discussed in section 4.3.

4.3 CALIBRATION USING THE INSTRON MACHINE

An Instron E10000 test system (Illinois Tool Works Inc. High Wycombe, UK) is a material testing instrument used for a wide range of testing in both static and dynamic testing applications (Instron, 2009). The Instron testing machine consists of three main units including a) load frame, b) controller and c) software application running on a computer as shown in Figure 4.1.
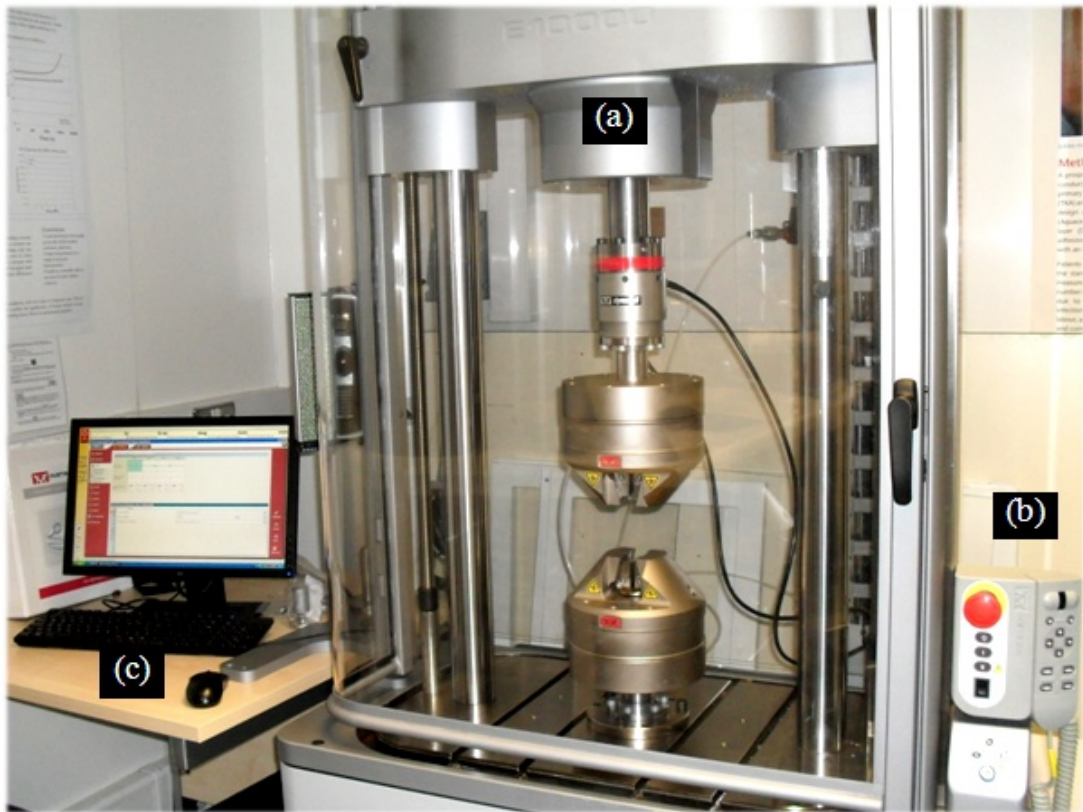
Figure 4.1 Instron testing machine and controller

- The load frame comprises of a table and crosshead. The crosshead can be moved by a drive system allowing testing of a wide range of materials in tension or compression. This particular machine also has a torsion actuator allowing torque moment to be applied on a specimen. A 1 kN/10Nm load cell was attached to the actuator measuring the load acting on the specimen.

- A computer communicates with the controller though customised software that also provided the graphical user interface (GUI) with the Instron system. The GUI provides the means by both which testing were monitored in real

time and specific software application modules were run. For this study, they were connected to provide application for set-up and running the static or dynamic test packages by the Wavematrix software V1.5 (Illinois Tool Works Inc. High Wycombe, UK).

- The Wavematrix software provides simultaneous recording of displacement and load from load cell. The calibration of the force transducers mounted on the chassis components were recorded with the CatmanEasy® software.

- Both sets of force data were compared and analysed.

Using the Instron machine the components to be calibrated were positioned then various loads were applied in load control.

All the loading processes of calibration were carried out six times to ensure repeatability; the recorded signals were then averaged. All signals were recorded with the DAQ system and related to the six degrees of freedom: F_x, F_y, F_z, M_x, M_y and M_z. Linear stress strain relationships were assumed to determine the material loading at the location of the strain gauges for each loading configuration as shown in Table 4.1.

Table 4.1 Details of the calibration test required for each strain gauged component

Component	Force Measurement
Backrest Angle Tube Assembly (BA)	Shear force, axial force, bending and torsion moment
Backrest Angle Tube (BT)	Axial force, torsion moment
Foot Calf Support Lower Assembly (FA)	Axial force, bending moment
Gas spring Base in dynamic system (GB)	Axial force

4.3.1 Bespoke Testing Rigs

It was necessary to design bespoke testing rigs for each component. This was because the components were irregular in shape and it was not possible to apply the loads in the principal directions of the components with simple grips.

For example, BA was a u-shape tube which was required to be calibrated in six degrees of freedom. The BA could not be directly gripped by the jaws of the Instron and therefore bespoke grips were manufactured for these tests as shows in Figure 4.2
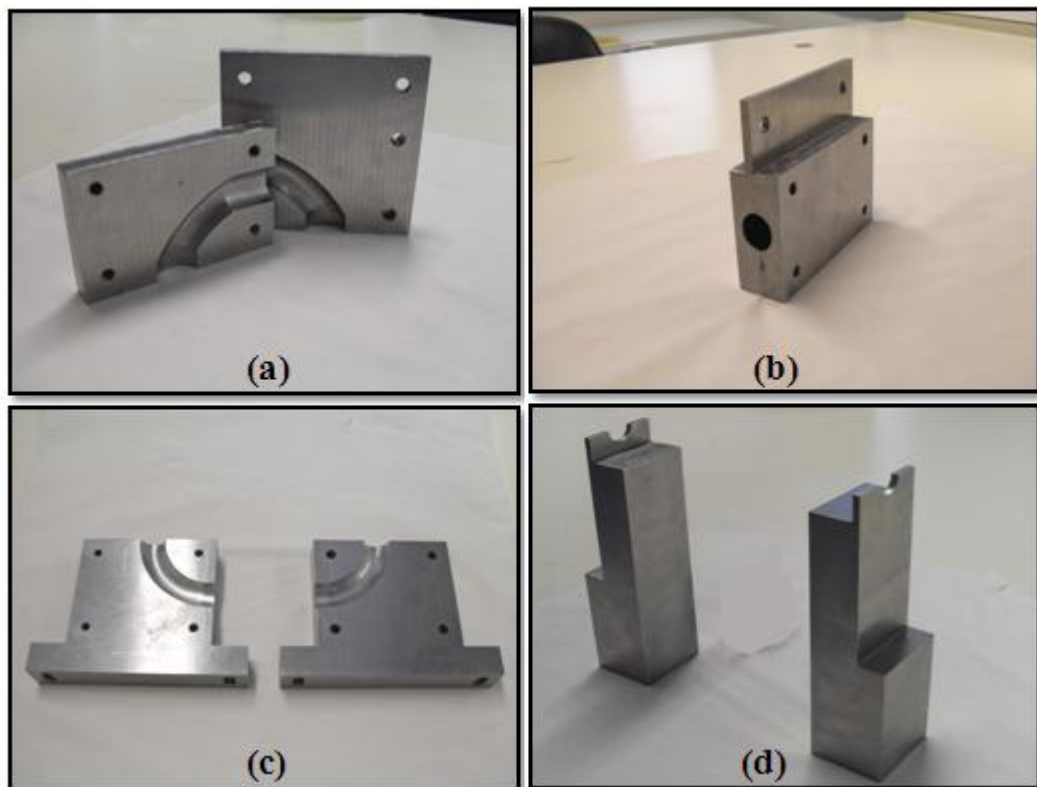
Figure 4.2 Bespoke grips for BA: (a), (b) upper grips for torsion test, (c) lower grips for torsion test and (d) holders for shear and bending moment test

4.3.2 Safety factors

Before calibration, the safe maximum load was first estimated from the material's yield strength and the component's cross-sectional area to ensure the component's elastic limit was not exceeded. A safety factor of 5 was deemed appropriate to ensure that all calibrations were within the elastic limit of the material (Juvinall and Marshek, 1991).

The maximum forces for the calibration were calculated using the following formulas (Benham and Crawford, 1996) including the safety factor (all calculations are detailed in Appendix A). The maximum loads of testing are listed below in Table 4.2

$$F = \sigma_y \, A \qquad\qquad \text{Equation (4.4)}$$

$$M = \frac{\sigma_y I}{y} \qquad\qquad \text{Equation (4.5)}$$

$$T = \frac{\tau J}{r} \qquad\qquad \text{Equation (4.6)}$$

Table 4.2 Material properties (William and Callister, 2007) and maximum testing loads

| Component | Material | Young's Modulus (GPa) | Yield Strength (MPa) | Maximum testing load | | |
				Axial (N)	Bending (N)	Torsion (Nm)
BA	Mild Steel	200	250	300	300	15
BT	Al 6061-T6	69	276	300	NA	10
FA	Al 6061-T6	69	276	100	100	NA
GB	Al 6061-T6	69	276	500	NA	NA

4.3.3 Shear Force Calibration

A shear force calibration was only done for the BA. To generate shear force on the BA, it was placed in three point bending. The load (W) was applied through a cross-section of the specimen then all other cross-sections of it were subjected to this load simultaneously and transducers recorded together the required shear force and bending moment.
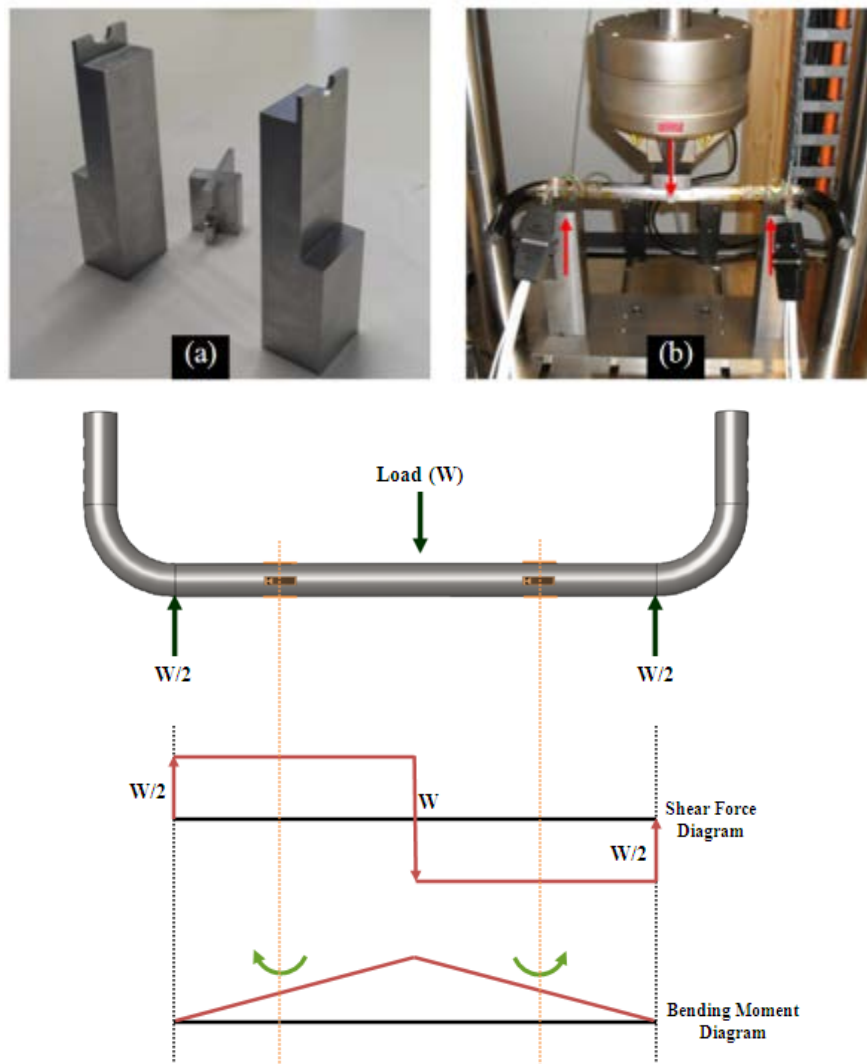
Figure 4.3 Three point bending calibration
(a) grips, (b) testing in Instron, and shear force and bending moment diagram of the three point bending method

Figure 4.3 depicts the expected shear force and bending moments withstood by the tube section along the length of the tube. From these diagrams we can estimate the force and moment at each transducer position.

Figure 4.3 (a) and (b) show that BA was placed on top of two fittings that had a custom design to hold it in place and also to not damage the force sensors on it. The component was loaded around its mid-point up to -300 N using a crosshead speed of 10 N/sec. When the maximum load was reached, the load was reduced back to zero using the speed. The specimen was rotated through 90 degrees to produce the orthogonal shear force. The reference force directions were +Fx at 0 degrees, +Fz at 90 degrees, -Fx at 180 degrees and –Fz at 270 degrees of the BA cross section.

4.3.4 Bending Moment Calibration

For the calibration of the bending moments, Mx and Mz, on the BA, the BA was positioned horizontally, similarly to the shear force test, and loaded by using a four point bending method in the X or Z direction as can be seen in Figure 4.4. The load (W) was applied and the force data from strain gauges were recorded. The crosshead speed was 10N/sec and the load was applied within a range of 0 to -300 N.
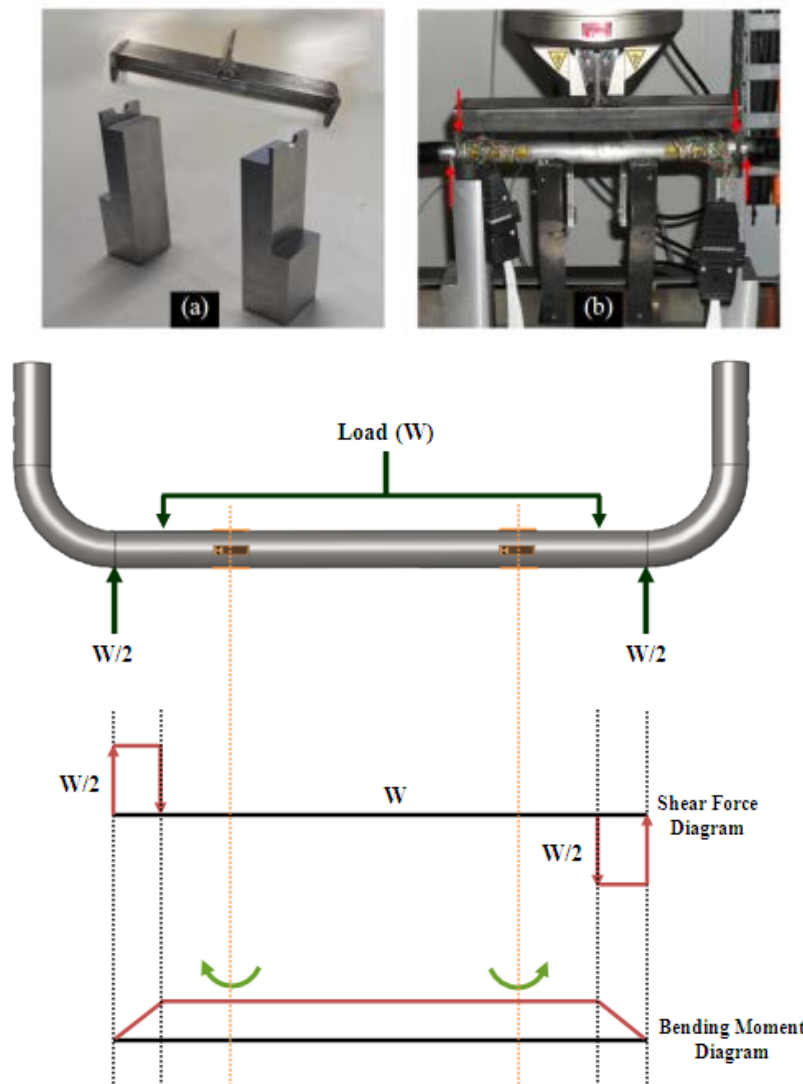
Figure 4.4 Four point bending calibration: (a) grips, (b) testing in Instron and shear force and bending moment diagram of the three point bending method

This four point bending method produced only the required bending moment Mx and Mz while shear forces were zero. Similarly to the shear force calibration, when the specimen was turned through 90 degrees it enabled the the orthogonal bending moment to be calculated. Because of the specimen's shape, it was not possible to turn the component to all desired angles and, for this test, Mx was applied in the positive, and Mz in the negative, directions only.

For the bending calibration of the FA, the specimen was placed on the Mygo seat as shown in Figure 4.5. Then the load was applied by hanging deadweights from 0 to 100 N at 0.12 m from the strain gauges along X axis, in the lateral side of footrest, to generate bending moments, Mz, from 0-12 Nm. After that, the load from 0-100 N was changed the position to 0.13 m at the front side of footrest (Z axis) to generate the orthogonal bending moment, Mx, from 0-13 Nm.
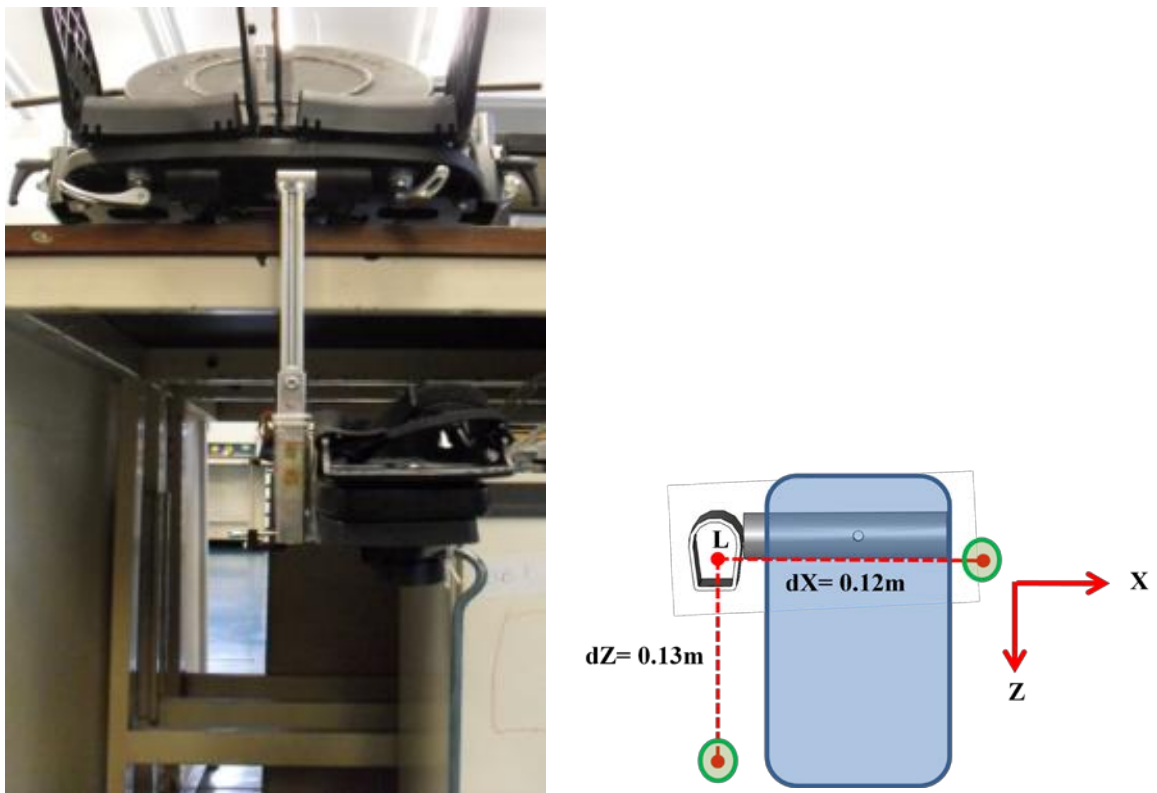
Figure 4.5 Calibration of bending moments on FA by dead weight
and top view shows distances along X and Z axes of FA-L

4.3.5 Axial Force Calibration

The axial force on the BA is denoted by Fy. To impose a negative Fy load on the component, the BA was placed vertically in the Instron machine and then the crosshead was moved down to compress load through the end of tube (Figure 4.6). The load was decreased to -300 N by steps of 100 N and, after having reached the maximum compressive load, the force was returned to zero using the same steps and the cycle was repeated. A similar tension test provided a positive Fy.

The BT was calibrated identically to the BA by placing it vertically in the Instron machine and by attaching the ends to with upper and lower special grips (Figure 4.7).
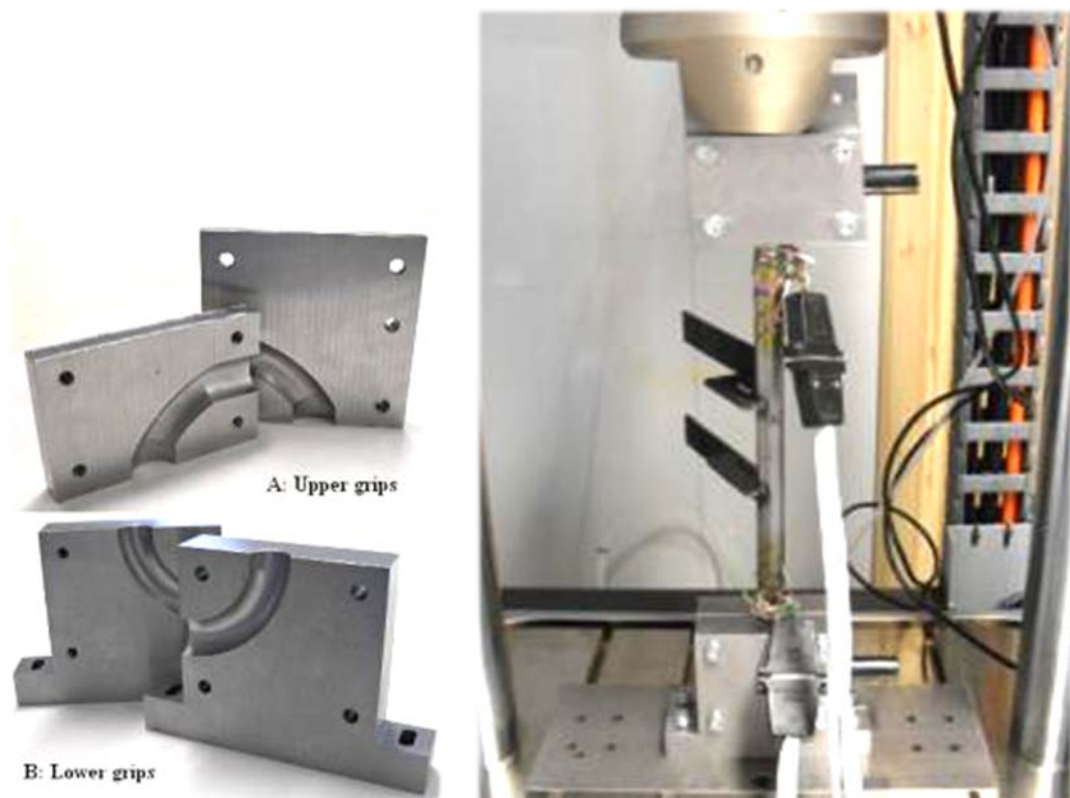
Figure 4.6 Calibration of axial and torsion on BA using special designed grips in the Instron

Figure 4.7 Calibration of axial and torsion on BT using special designed grips in the Instron

Figure 4.8 Calibration of axial force on GB

Figure 4.8 depicts the manufactured gas spring base (GB) in the Instron prior to the compression test. The load was applied from 0 to -500 N and, due to the limitation of its shape, GB could be calibrated only in compression.

Figure 4.9 Calibration of axial force on FA by deadweight

The FA was assembled on the seat and calibrated using an axial force. To generate the tensile force, a 30 mm G clamp was used to hang deadweights in the midline of the FA as shown in Figure 4.9. Each side of the FA was calibrated using tensile forces from 0 to 100 N in steps of 10 N. The loading-unloading cycle was repeated and recorded.

Difficulties arise, however, when the length of footrest is adjusted, since the axial force calibration of the FA was found to be affected by this adjustment. Adjustment is necessary according to the length of user's legs, as shown in Figure 4.10. The top tube is slotted in FA and the length of the FA is locked by a screw. The length of the FA may be reduced by sliding the top tube inside the FA (Figure 4.10b). For some users who require a longer length of FA, the top tube can be slid out until the maximum length as shown in Figure 4.10c is achieved. These adjustments made the FA less uniform and influenced the strain gauge calibration, especially with regards to axial force. This problem is discussed and detailed in section 4.4.2.
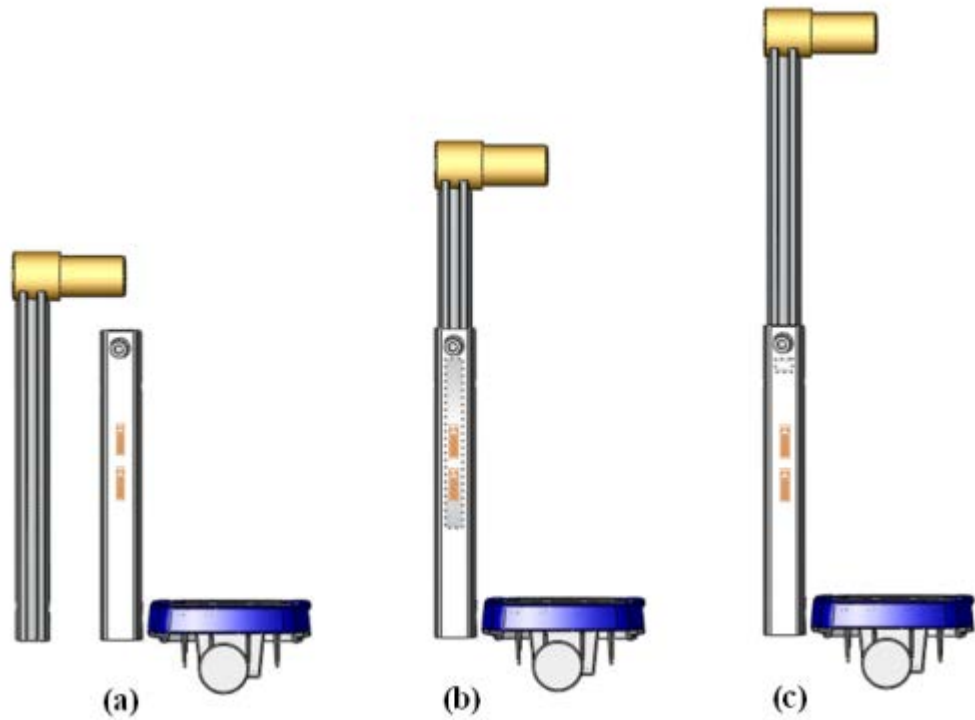
Figure 4.10 Adjusting the length of the FA

4.3.6 Torsion Calibration

For the torsional calibration of the BA, the specimen was mounted, using bespoke grips, on the crosshead of the Instron in the same position as for the axial force calibration (Figure 4.6). The positive My moment testing was achieved by rotating the crosshead clockwise in the loading range of 0 to 15 Nm in increments of 5 Nm. Then the application of an opposite torque was performed using moments of 0 to -15 Nm in the same increments.

The BT was calibrated in torsion using bespoke grips (Figure 4.7) using the range of 0-10 Nm and a crosshead speed of 2 Nm.

4.4   RESULTS

4.4.1 Signal Outputs

The signal outputs in strain (um/m) were plotted against the applied loads (N, Nm). The graphs display a typical and repeatable form, which includes a strong main channel signal with smaller cross-talk signals which occurred due to the activation of the non-corresponding gauges. The linearity of the main channel is confirmed with an R^2 value above 0.98 in all graphs. Most of the tests were loaded in both positively and negatively. However, some bending tests were loaded only one-way cycle due to the limitation of the component's shape which could not be easily placed in the Instron. A summary of the calibration methods, correspondence signal channels and illustrated result figures is in Table 4.3.

Table 4.3 Summary of the calibration methods and illustrated result figures

Part	Calibration	Load (N, Nm) Maximum	Correspondence signal[1]	Result
BA	Shear Force	300	Channel 1 Fx1	Figure 4.11
	(Horizontal)	300	Channel 7 Fx2	Figure 4.12
	Shear Force	300	Channel 3 Fz1	Figure 4.13
	(Vertical)	300	Channel 9 Fz2	Figure 4.14
	Bending moment	300	Channel 4 Mx1	Figure 4.15
	(Horizontal)	300	Channel 10 Mx2	Figure 4.16
	Bending moment	300	Channel 6 Mz1	Figure 4.17
	(Vertical)	300	Channel 12 Mz2	Figure 4.18
	Axial force	300	Channel 2 Fy1	Figure 4.19
		300	Channel 8 Fy2	Figure 4.20
	Torque moment	15	Channel 5 My1	Figure 4.21
		15	Channel 11 My2	Figure 4.22
BT	Axial force	300	Channel 19 Fy	Figure 4.23
	Torque moment	10	Channel 20 My	Figure 4.24
GB	Axial force	500	Channel 19 Fy	Figure 4.25
FA-L	Bending moment	30	Channel 13 Mx_L	Figure 4.26
	Bending moment	50	Channel 14 Mz_L	Figure 4.28
	Axial force	50	Channel 15 Fy_L	Figure 4.30
FA-R	Bending moment	30	Channel 16 Mx_R	Figure 4.27
	Bending moment	50	Channel 17 Mz_R	Figure 4.29
	Axial force	50	Channel 18 Fy_R	Figure 4.31

[1] *The main signal corresponding to the testing load (details of amplifier channels in section 3.4.3 Data processing)*

- *Backrest Angle Tube Assembly (BA)*
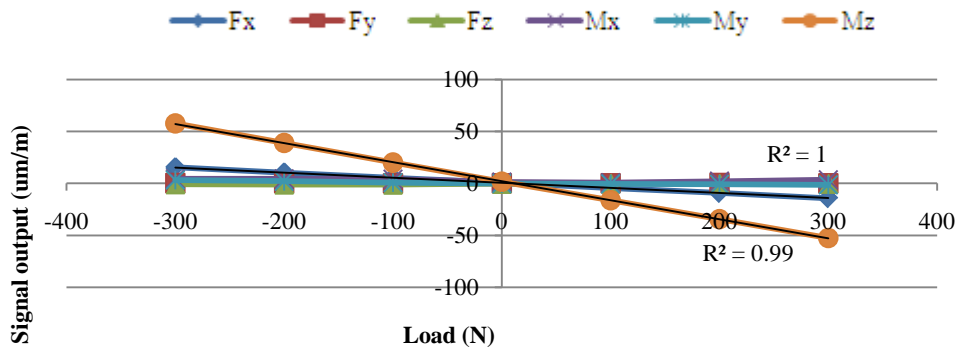
Figure 4.11 Three point bending Fx_1 and Mz_1 (BA1)
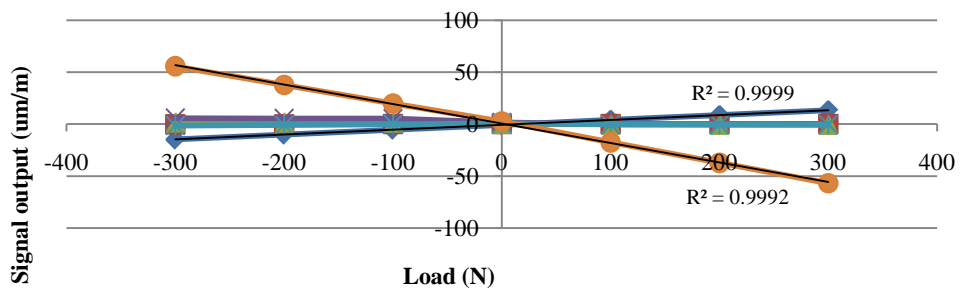
Figure 4.12 Three point bending Fx_2 and Mz_2 (BA2)
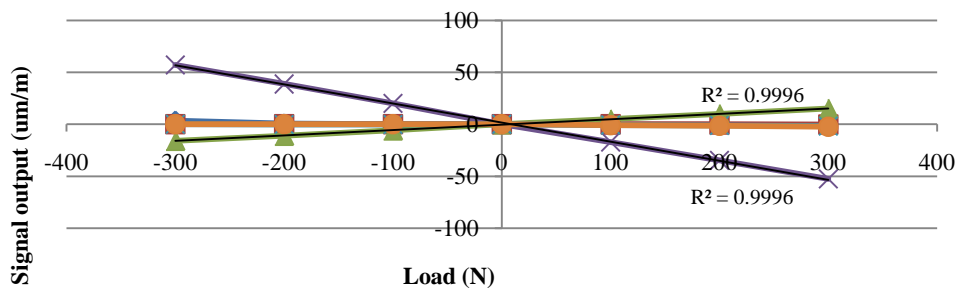
Figure 4.13 Three point bending Fz_1 and Mx_1 (BA1)
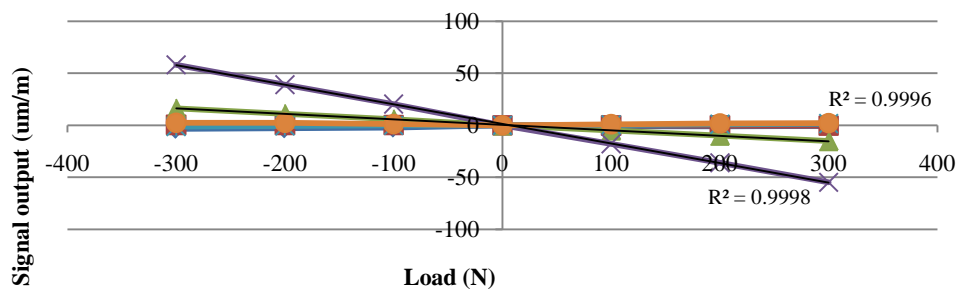
Figure 4.14 Three point bending Fz_2 and Mx_2 (BA2)
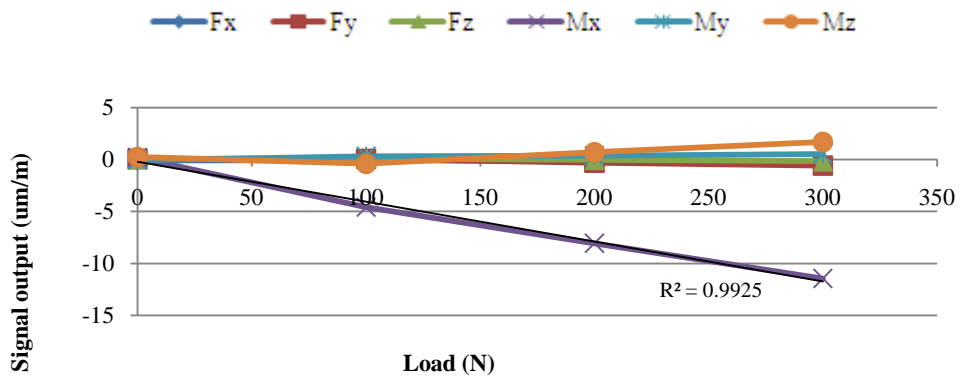
Figure 4.15 Four point bending Mx_1 (BA1)
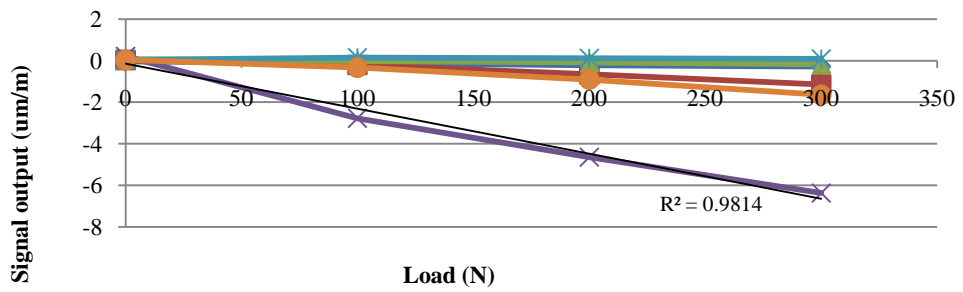
Figure 4.16 Four point bending Mx_2 (BA2)
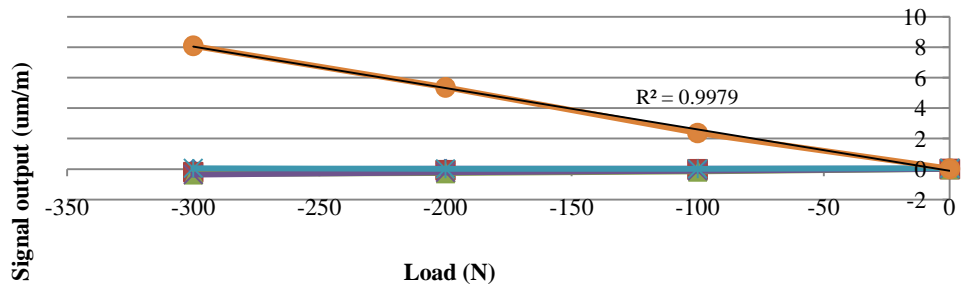
Figure 4.17 Four point bending Mz_1 (BA1)
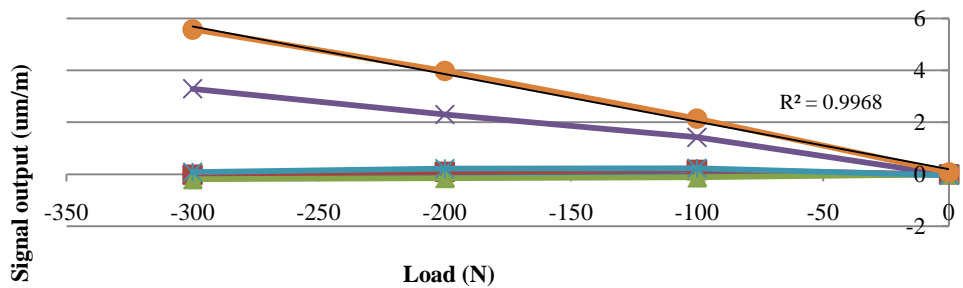
Figure 4.18 Four point bending Mz_2 (BA2)
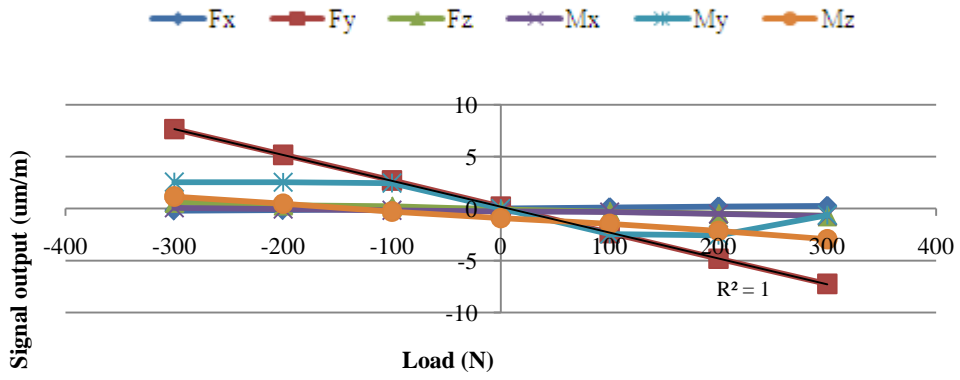
Figure 4.19 Axial force Fy₁ (BA1)
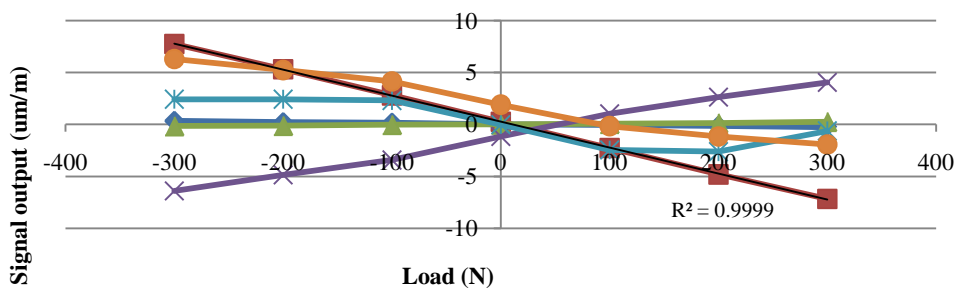
Figure 4.20 Axial force Fy₂ (BA2)
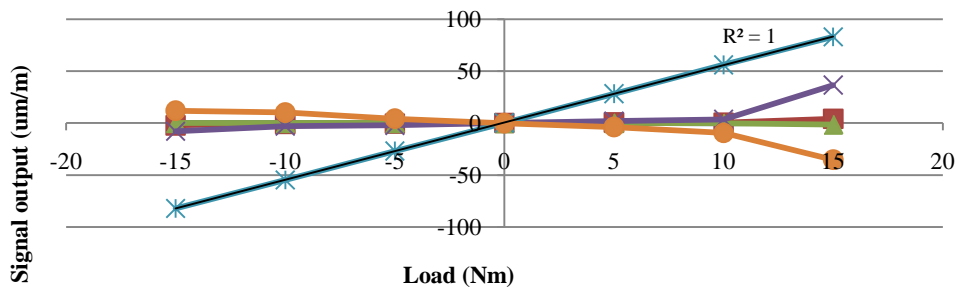
Figure 4.21 Torsion My₁ (BA1)
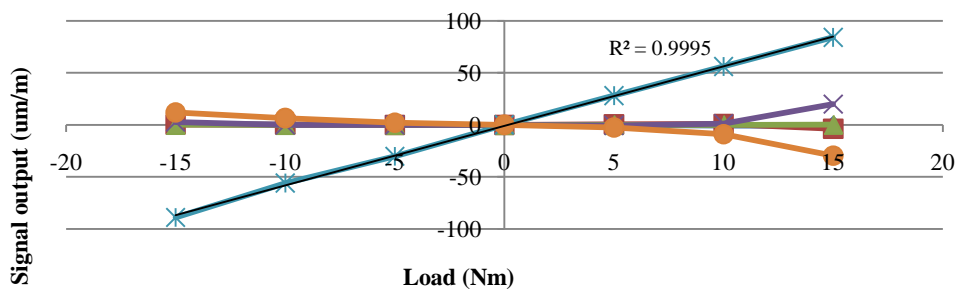
Figure 4.22 Torsion My₂ (BA2)

- *Backrest Angle Tube (BT)*
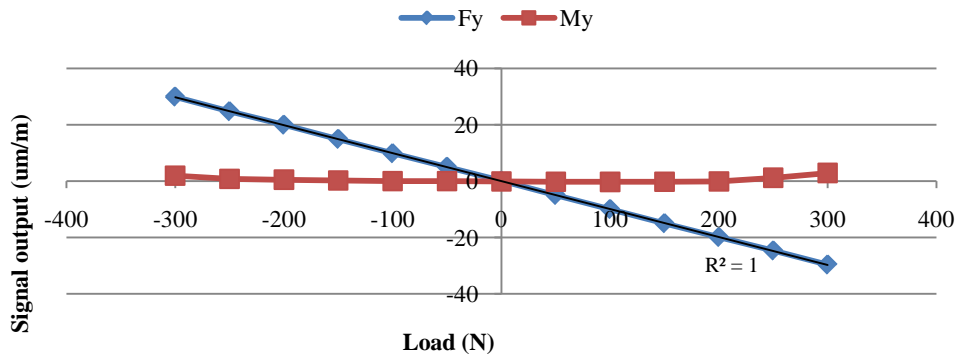
Figure 4.23 Axial force Fy (BT)
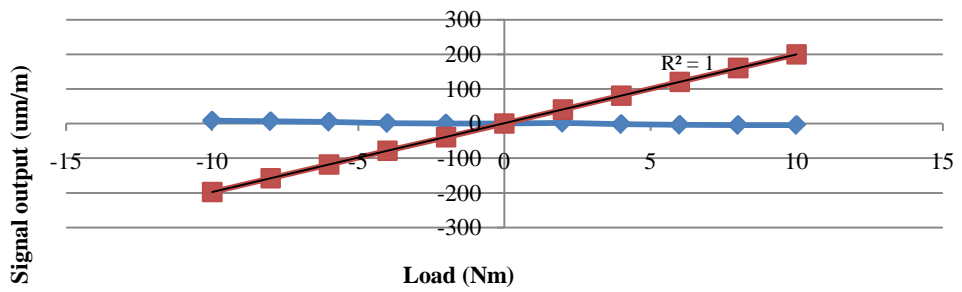
Figure 4.24 Torsion My (BT)

- *Gas spring Base for the dynamic system (GB)*
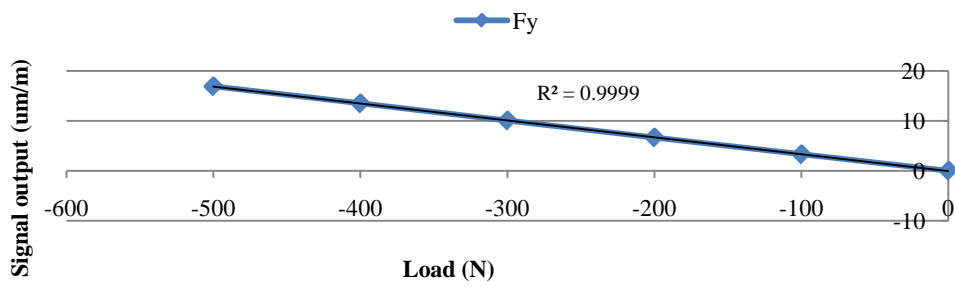
Figure 4.25 Axial force Fy (GB)

- *Foot Calf Support Lower Assembly (FA)*
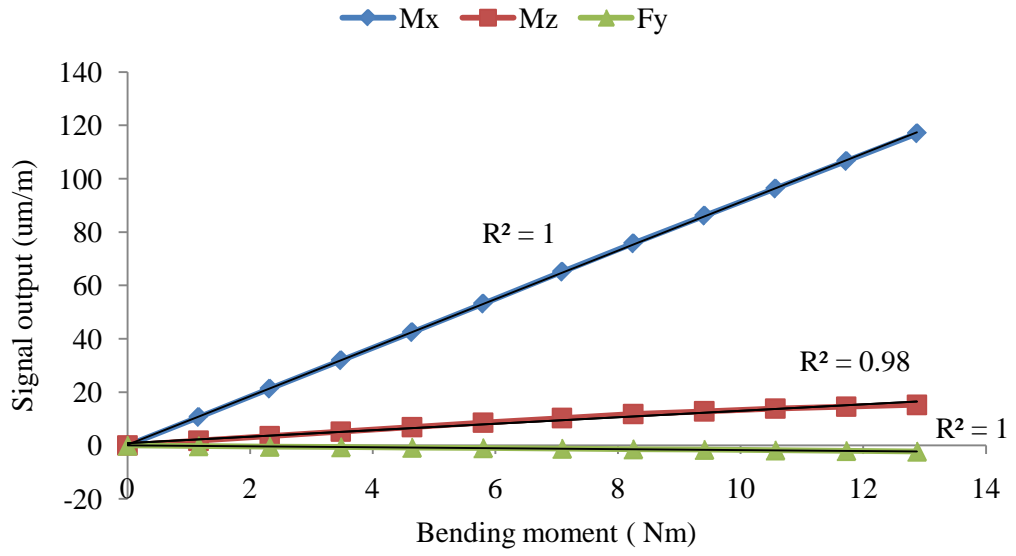
Figure 4.26 Bending Mx (FA-L)
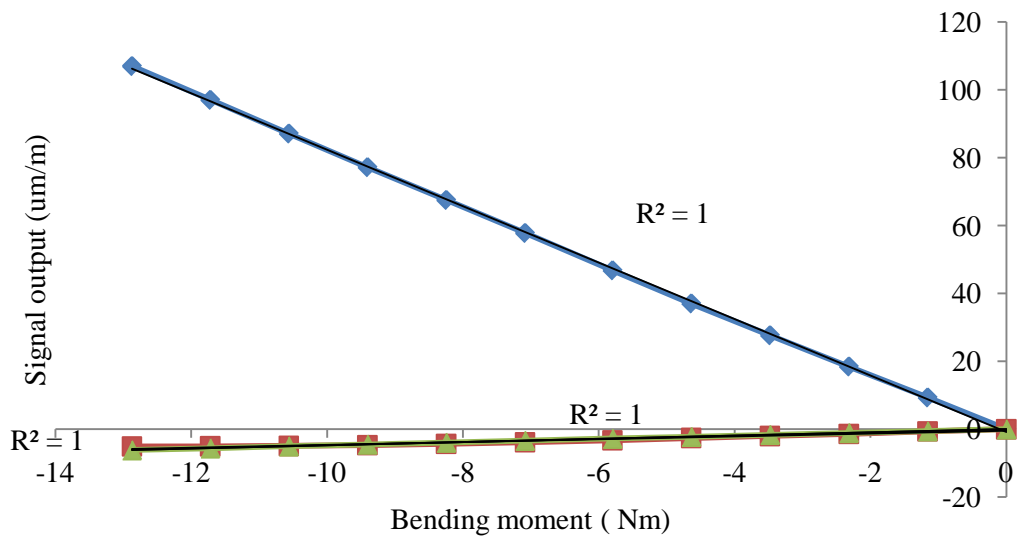
Figure 4.27 Bending Mx (FA-R)
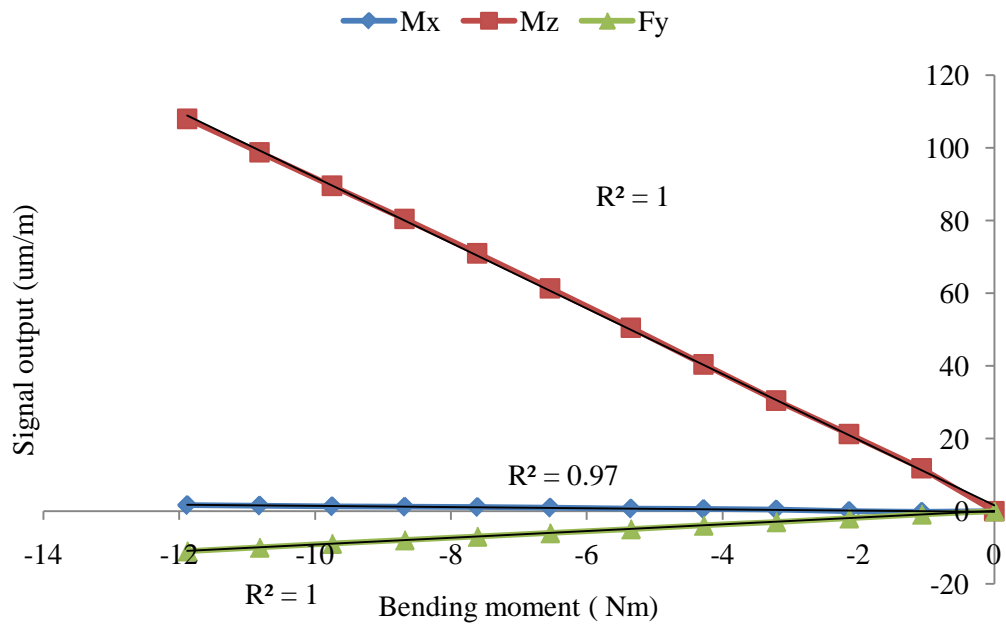
Figure 4.28 Bending Mz (FA-L)
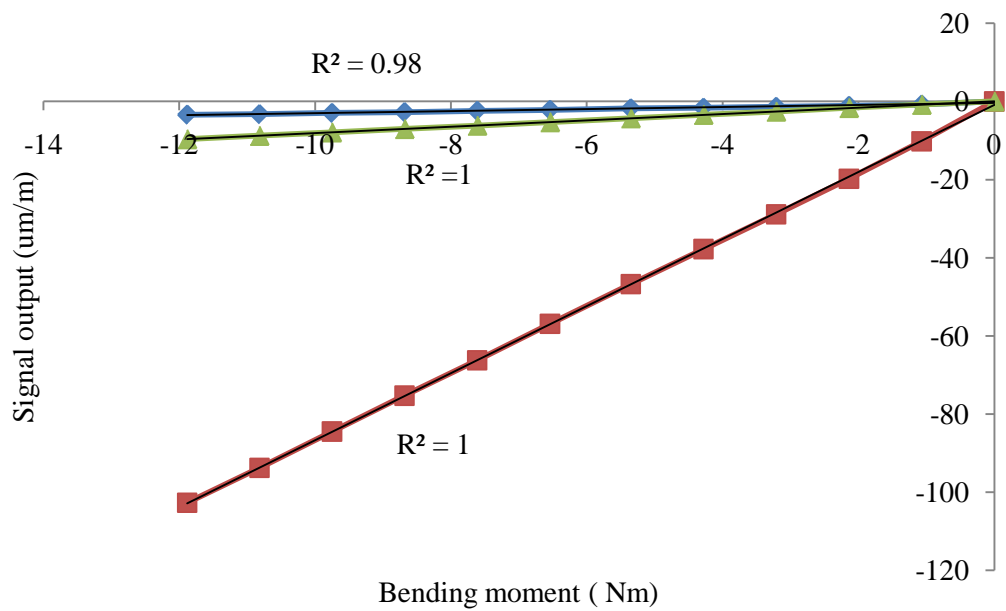
Figure 4.29 Bending Mz (FA-R)
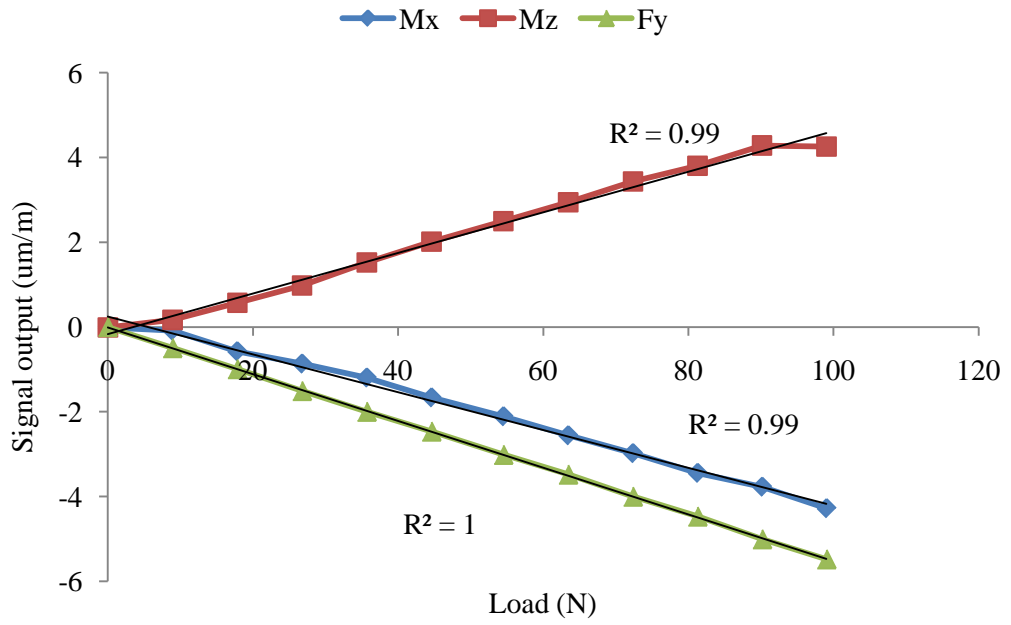
Figure 4.30 Axial Fy (FA-L)
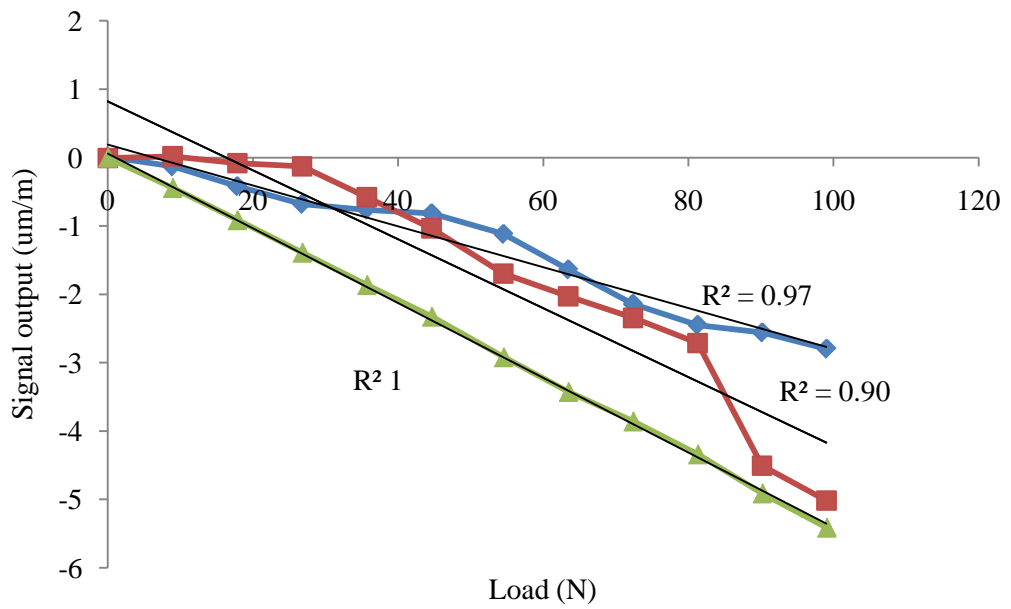
Figure 4.31 Axial Fy (FA-R)

A problem was found in the axial calibration of the FA. Due the thickness of the FA, the load at 100 N generated a strain output of less than 7 um/m (Figure 4.30-Figure 4.31). This amount was small when compared to bending moment calibration. With 100 N load on the footplate, the strain output in the bending moment was above 100 um/m (Figure 4.26 - Figure 4.29). Since the signal output of Fy was approximately similar to the crosstalk, Mx and Mz, this significantly affected the matrix coefficient of FA. Consequently, to convert the strain to force and moments on the FA, the crosstalk would be ignored, and only the coefficient of the main channel would be used.

4.4.2 Coefficient Matrices

The graphical results in section 4.4.1 displayed linear relationships between the gauge readings and actual loads. Unfortunately some cross-talk signals occurred due to activation of the non-corresponding gauges and a complete calibration matrix for each component was therefore required to include cross-talk effects into the load determination.

The gradients for the positive and negative applied loads were calculated and then averaged. The calibration matrix, *[C]* in Equation (4.1) was determined for the rigid and dynamic seating systems, using 20 and 19 channels respectively.

Table 4.4 shows the completed matrix of the now inverted *[C]* to give the 6x6 *[M]* matrix. They allow the applied load to be calculated when the signal outputs are known.

From Equation (4.1) $\quad\quad\quad\quad [S] = [C]\,[F]$

From Equation (4.7) $\quad\quad\quad\quad [F] = [M]\,[S]$

Table 4.4 Coefficient matrices of BA, FA-L and R, BT, and GB

BA

Force [F]	Coeficient matrices [M]						Signal [S]
BA1							
Fx1	10.62	2.46	1.71	-0.14	0	0.91	SFx1
Fy1	0.38	-40.29	1.02	-0.09	0.02	0.06	SFy1
Fz1	-0.7	4.55	-10.07	0.82	-0.02	-0.04	SFz1
Mx1	-0.2	1.38	-0.03	0.11	-0.01	-0.01	SMx1
My1	0.08	-3.15	-0.28	-0.02	-0.18	-0.04	SMy1
Mz1	0.03	-0.77	-0.39	0.04	0	-0.1	SMz1
BA2							
Fx2	-11.98	-10.9	3.99	0.68	0.07	1.35	SFx2
Fy2	1.02	-35.03	-0.58	-0.24	0	-0.27	SFy2
Fz2	-0.19	-17.04	12.07	1.24	0.04	0.46	SFz2
Mx2	0.34	4.68	-0.53	-0.21	-0.01	-0.12	SMx2
My2	-0.48	-5.29	0.55	0.17	-0.17	0.16	SMy2
Mz2	-0.56	-3.73	0.85	0.19	0.01	0.26	SMz2

[F]	[M]	[S]
FA-L		
FL Mx	0.11	SFL Mx
FL Mz	-0.15	SFL Mz
FL Fy	-19.52	SFL Fy
FA-R		
FR Mx	-0.12	SFR Mx
FR Mz	0.17	SFR Mz
FR Fy	-19.13	SFR Fy
BT		
BT Fy	-0.1	SBT Fy
BT My	19.53	SBT My
GB		
GB Fy	-0.03	SGB Fy
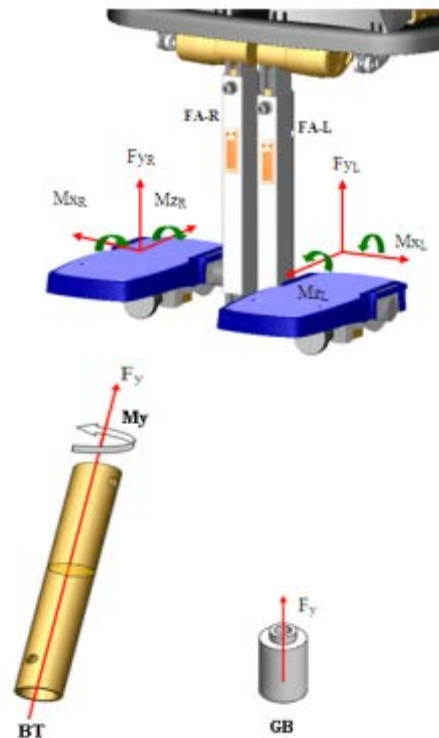
4.5   VALIDATION OF THE CALIBRATION MATRIX

The purpose of this section is to describe the method to verify the prediction ability of the calibration matrices. The results of the applied force and predicted force are compared and the percentage difference calculated.

The validation tests were carried out by applying various known loads to each wheelchair component. Strain data were simultaneously recorded and the calibration matrix of each part was used to estimate the force acting on it.

The tests were carried out by separating the strain-gauged Mygo chair system into two parts: the seat and the footrest (Figure 4.32). The seat consisted of two components, the backrest angle tube assembly (BA) and the backrest angle tube (BT) / gas spring base (GB), which involved 14 channels for the rigid system and 13 channels for the dynamic backrest system. Left and right footrests were tested independently with each side having 3 channels to validate.

Figure 4.32 Seat and footrest
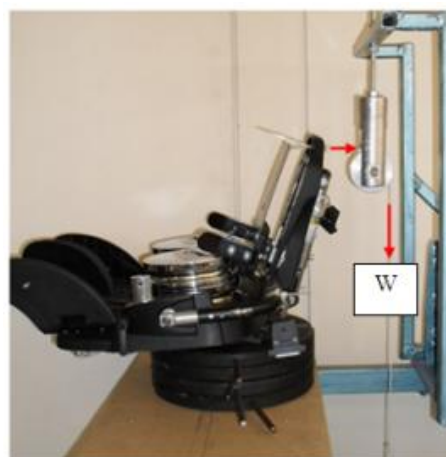
Figure 4.33 Application of known load on the backrest

4.5.1 Seat

The set-up of the seat to validate the calibration matrix of BA and BT/GB is shown in Figure 4.33. The backseat was pulled in the direction which the user leans his or her back on the backrest. Strain data was resolved into forces and moments in 14 channels in the rigid backrest system and 13 channels in the dynamic backrest system. A load of 98 N was applied on the rigid backrest seating system by hanging a weight via a pulley to direct the force at a 90 degree angle to the horizontal. Due to the limited testing area available, the dynamic backrest seat was loaded with about 78.5 N. Following calibration, static equilibrium was used to determine the magnitude of the contact force applied on the backrest. The percentage of difference between predicted and applied load was calculated by,

$$\% \, difference = \frac{predicted \; load - applied \; load}{applied \; load} \; x \; 100 \qquad \text{Equation (4.8)}$$

The results were plotted as the one to one of predicted load by the calibration matrix and percentage of difference which are shown in Figure 4.34 and Table 4.5

FB Rigid

y = 10.87x - 5.5462
R² = 0.983

Applied force (N)	0.00	9.81	19.62	29.43	39.24	49.05	58.86	68.67	78.48	88.29	98.10
◆ Predicted FB	0.00	12.68	25.86	40.38	55.55	70.15	68.97	80.24	90.83	100.41	111.35

FB Dynamic

y = 12.621x - 21.01
R² = 0.9857

Applied force (N)	0.00	9.81	19.62	29.43	39.24	49.05	58.86	68.67	78.48
◆ Predicted FB	0.00	3.57	12.69	24.54	38.61	53.74	68.15	82.33	95.22
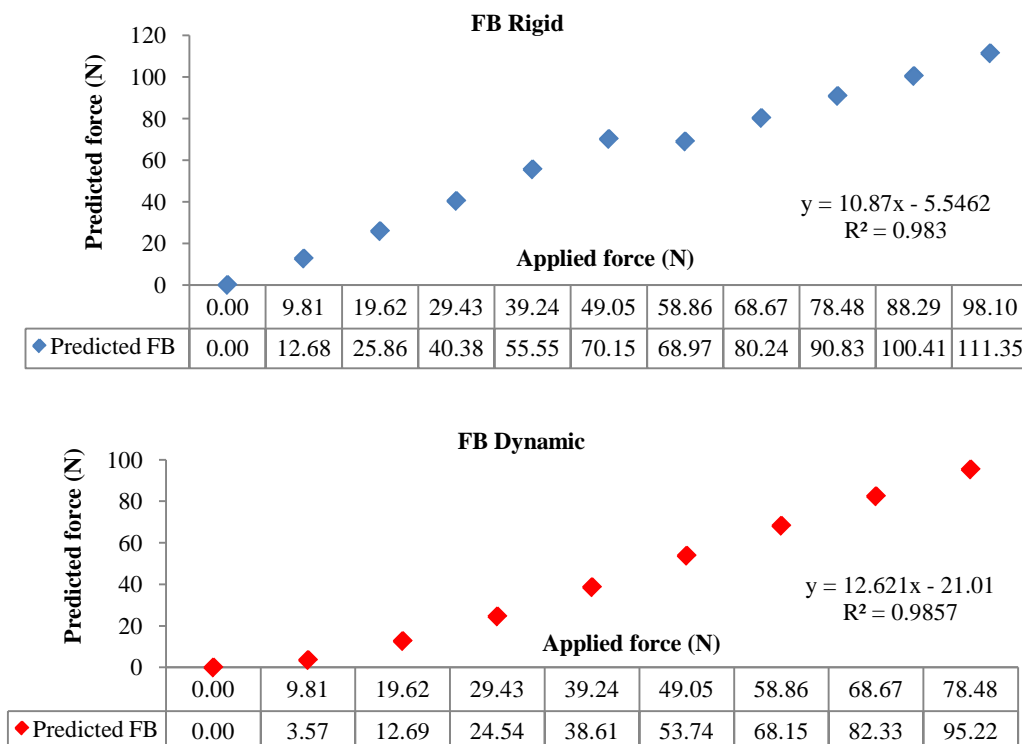
Figure 4.34 Predicted and applied forces on the backrest

Table 4.5 Percentage of difference between predicted and applied forces on the backrest

Backrest	Applied force (N, x)	Predicted force (N, y)	% difference
Rigid	98.1	111.35	13.51
Dynamic	78.48	95.22	21.33

The relationship between the applied force and the predicted force on seating systems were linear with $R^2 = 0.98$. The results of the percentage difference between the applied force and the predicted on the rigid seating system was 14 percent and the dynamic system was 21 percent. There were some potential reasons which indicated this error was slightly high. For example, the strain gauges were not precisely attached on the right position, the measuring components do not have a uniform shape and there were many connections to each part

4.5.2 Footrest

As mentioned in section 4.3.5, the length of the footrest affected its axial force calibration. In particular, there was a difference when the strain gauge location on the FA overlapped with the top (internal) tube, compared to when the footrest was extended and this overlap did not occur. Therefore in this section, the footrest was validated in these two conditions.

Each side of footrest was loaded using deadweight to generate bending moments Mx and Mz, and an axial force, Fy. The footrest was loaded at 100 N at the point which was 0.08 m from the midline, along X axis and 0.15 m along Z axis as shown in Figure 4.35.
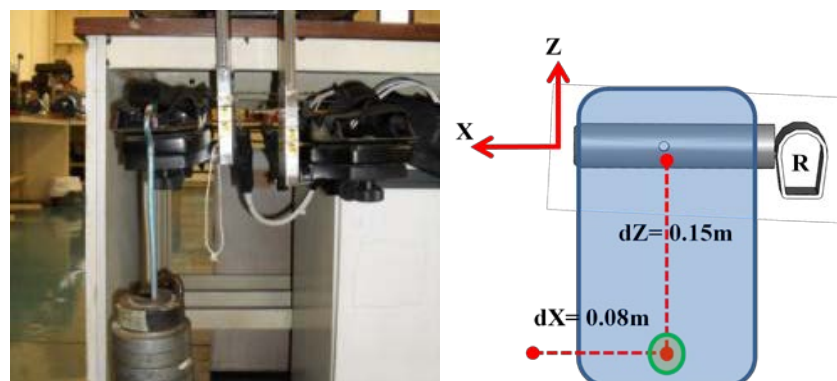
Figure 4.35 Multi direction loading test on each footrest

FA-L

	0.00	1.16	2.32	3.48	4.64	5.80	7.09	8.25	9.41	10.56	11.72	12.87
Mx	0.00	1.06	2.11	3.18	4.21	5.25	6.40	7.43	8.43	9.41	10.36	11.36

$y = 1.0378x - 0.9807$
$R^2 = 0.9997$

	0.00	-1.07	-2.14	-3.21	-4.28	-5.35	-6.54	-7.61	-8.68	-9.75	-10.82	-11.88
Mz	0.00	-1.14	-2.25	-3.32	-4.36	-5.38	-6.56	-7.59	-8.60	-9.58	-10.48	-11.36

$y = -1.0403x + 0.877$
$R^2 = 0.9989$

	0.00	8.92	17.83	26.77	35.69	44.61	54.51	63.44	72.36	81.27	90.16	99.03
Fy	0.46	-21.53	-46.34	-74.86	-104.1	-135.1	-166.4	-196.1	-223.3	-233.6	-223.1	-206.1

$y = -22.544x + 10.67$
$R^2 = 0.9231$

Figure 4.36 Predicted vs applied loads in Mx, Mz and Fy on the left footrest- FA-L
when the top tube was inside (shorten)

84

FA-R

	0.00	-1.16	-2.32	-3.48	-4.64	-5.80	-7.09	-8.25	-9.41	-10.56	-11.72	-12.87
◆ Mx	0.00	-1.14	-2.12	-3.19	-4.27	-5.37	-6.61	-7.74	-8.87	-10.00	-11.14	-12.27

$y = -1.1192x + 1.2143$
$R^2 = 0.9997$

	0.00	-1.07	-2.14	-3.21	-4.28	-5.35	-6.54	-7.61	-8.68	-9.75	-10.82	-11.88
◆ Mz	-0.01	-0.96	-1.73	-2.58	-3.41	-4.23	-5.10	-5.90	-6.68	-7.42	-8.19	-8.94

$y = -0.8111x + 0.6771$
$R^2 = 0.9994$

	0.00	8.92	17.83	26.77	35.69	44.61	54.51	63.44	72.36	81.27	90.16	99.03
◆ Fy	0.32	-19.14	-47.70	-72.71	-102.9	-132.2	-162.0	-187.2	-212.3	-238.7	-265.0	-289.1

$y = -26.978x + 31.272$
$R^2 = 0.9991$
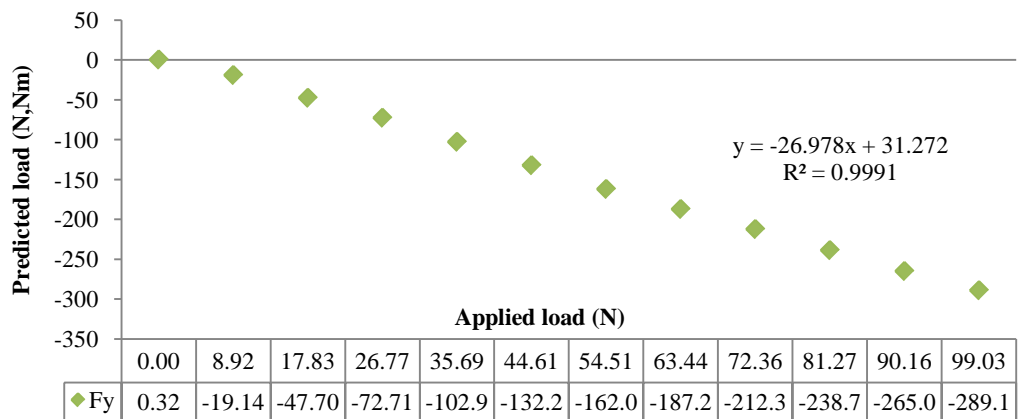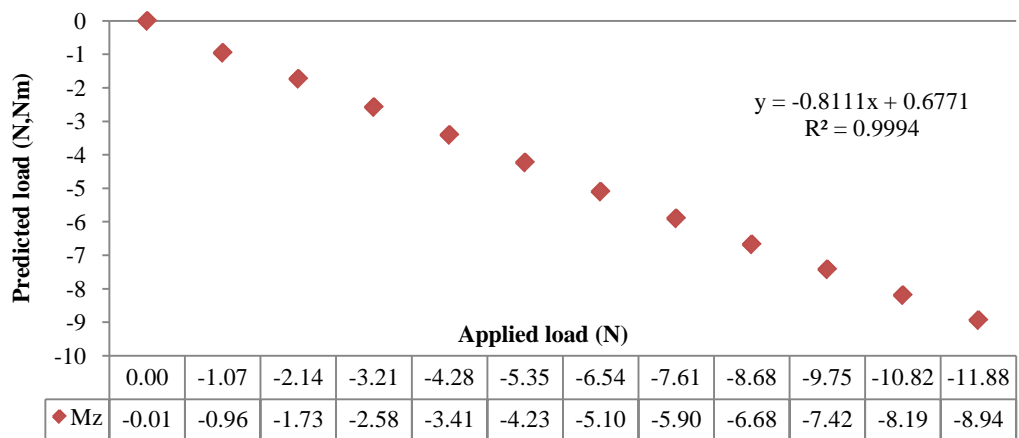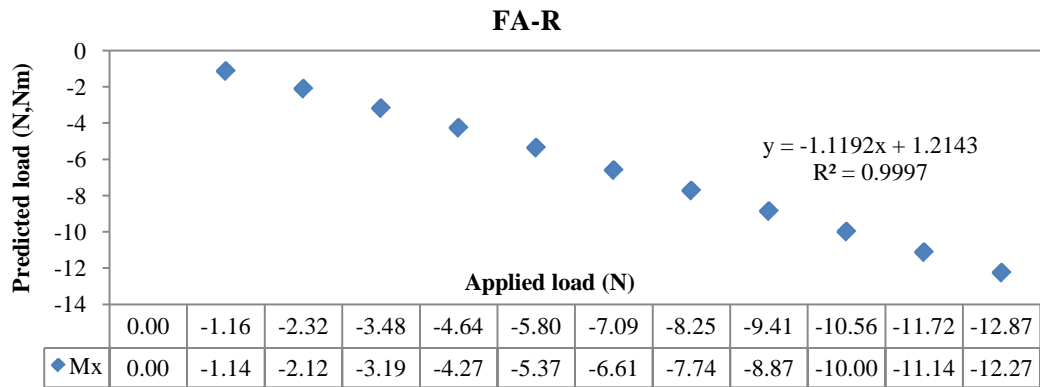
Figure 4.37 Predicted vs applied loads in Mx, Mz and Fy on the right footrest- FA-R
when the top tube was inside (shorten)

FA-L

	0.00	1.16	2.32	3.48	4.64	5.80	7.09	8.25	9.41	10.56	11.72	12.87
Mx	0.00	1.45	2.88	4.33	5.76	7.16	10.07	10.13	12.65	12.95	15.15	15.82

$y = 1.4873x - 1.4714$
$R^2 = 0.9917$

	0.00	-1.07	-2.14	-3.21	-4.28	-5.35	-6.54	-7.61	-8.68	-9.75	-10.82	-11.88
Mz	0.00	-1.09	-2.21	-3.31	-4.35	-5.28	-7.20	-7.15	-8.83	-8.93	-10.3	-10.6

$y = -0.9967x + 0.7015$
$R^2 = 0.987$

	0.00	8.92	17.83	26.77	35.69	44.61	54.51	63.44	72.36	81.27	90.16	99.03
Fy	0.78	8.19	16.14	23.50	32.21	41.83	62.83	63.17	80.34	83.39	99.16	104.1

$y = 9.8756x - 12.883$
$R^2 = 0.9889$
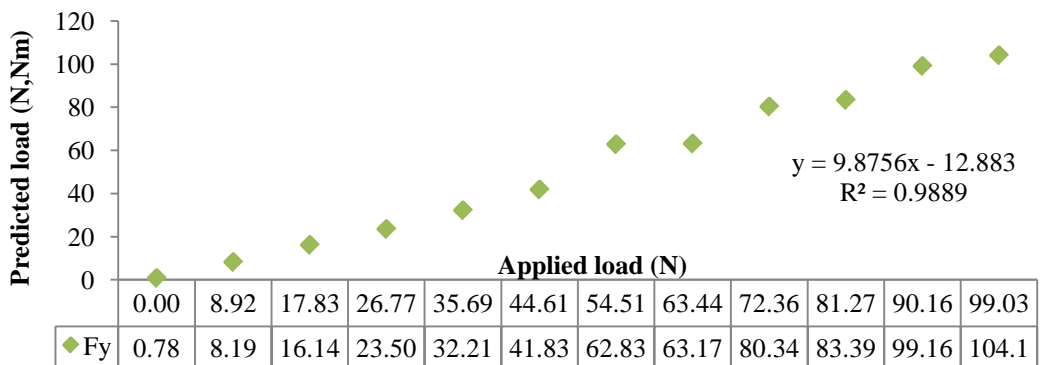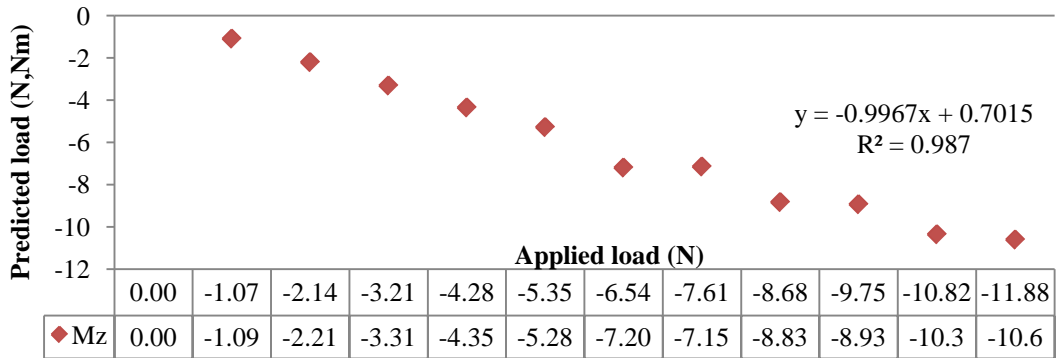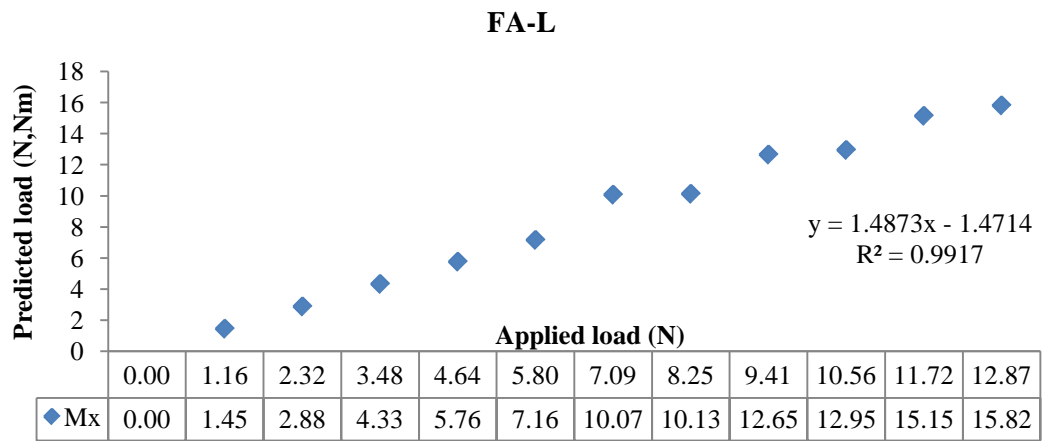
Figure 4.38 Predicted vs applied loads in Mx, Mz and Fy on the left footrest- FA-L when the top tube was outside (lengthen)

FA-R

	0.00	-1.16	-2.32	-3.48	-4.64	-5.80	-7.09	-8.25	-9.41	-10.56	-11.72	-12.87
◆ Mx	0.00	-1.31	-2.67	-4.09	-5.53	-6.98	-8.63	-10.0	-11.5	-13.0	-14.4	-15.9

$y = -1.4644x + 1.6621$
$R^2 = 0.9997$

	0.00	-1.07	-2.14	-3.21	-4.28	-5.35	-6.54	-7.61	-8.68	-9.75	-10.82	-11.88
◆ Mz	-0.01	-1.01	-1.97	-2.90	-3.77	-4.69	-5.69	-6.60	-7.50	-8.40	-9.28	-10.2

$y = -0.9265x + 0.8482$
$R^2 = 0.9999$

	0.00	8.92	17.83	26.77	35.69	44.61	54.51	63.44	72.36	81.27	90.16	99.03
◆ Fy	0.05	16.59	32.62	49.20	65.89	82.91	101.56	118.89	135.19	152.70	170.23	187.09

$y = 17.092x - 18.357$
$R^2 = 0.9998$
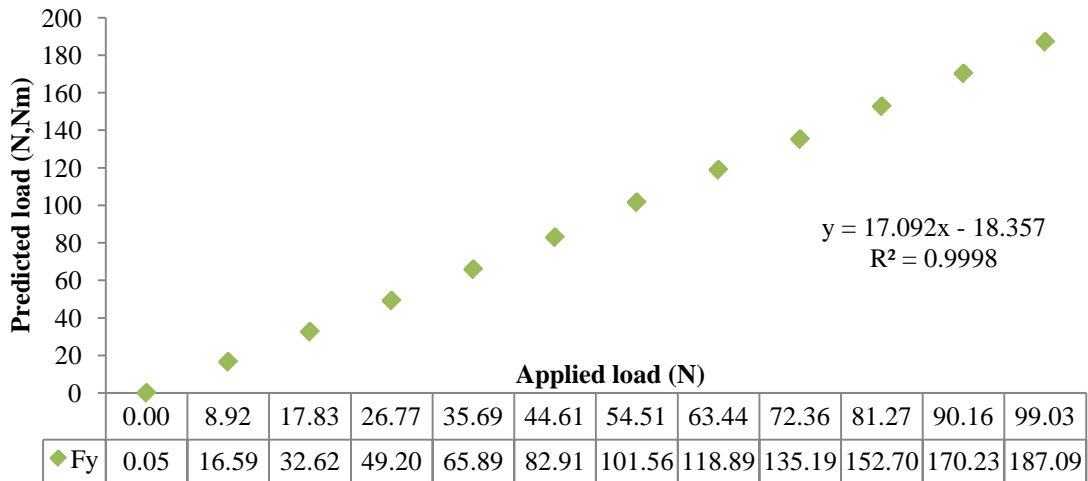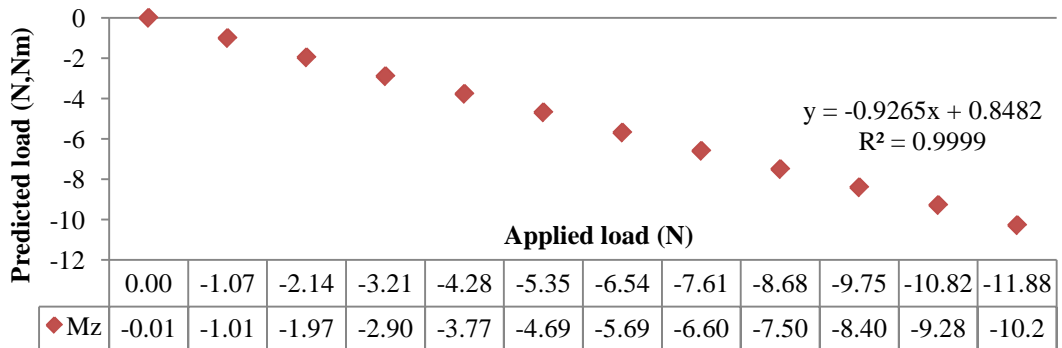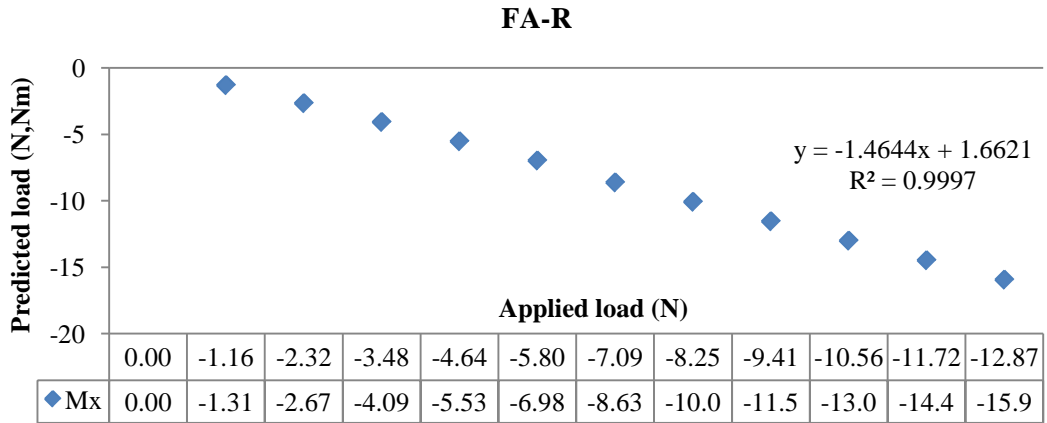
Figure 4.39 Predicted vs applied loads in Mx, Mz and Fy on the right footrest- FA-R when the top tube was outside (lengthen)

Figure 4.36 to Figure 4.39 present the relationship of the applied loads and the predicted loads. A quantitative evaluation of the patterns could be obtained by the linear regression of the data which is shown in Table 4.6

Table 4.6 Percentage of difference between predicted and applied forces on the footrest

Footrest	Applied force (x)	Predicted force (y)	% difference
Condition 1: The top tube was inside			
Left			
FL Mx	12.87	11.36	-11.73%
FL Mz	-11.88	-11.36	-4.38%
FL Fy	99.03	-206.10	-308.11%
Right			
FR Mx	-12.87	-12.27	-4.66%
FR Mz	-11.88	-8.94	-24.75%
FR Fy	99.03	-289.10	-391.93%
Condition 2: The top tube was outside			
Left			
FL Mx	12.87	15.82	22.92%
FL Mz	-11.88	-10.60	-10.77%
FL Fy	99.03	104.10	5.12%
Right			
FR Mx	-12.87	-15.90	23.54%
FR Mz	-11.88	-10.20	-14.14%
FR Fy	99.03	187.09	88.92%

Table 4.6 shows the percentage of error of force and moments on FA-L and FA-R in two conditions when the footrest was shortened and lengthened. The % error of the axial force determination was extremely high. This was because the footrest had been adjusted the length by slotting the top tube into FA as explained in Figure 4.10. The span of top tube affected the strain measurement of FA especially on axial force channel. Therefore the calibration coefficient of this channel cannot be used to convert the axial force on the footrest. However, the % error of bending moments in both conditions was not as high as the axial force. The maximum error was about 25

percent. Thus the calibration coefficient of these will be used to convert the strain data to bending moments on FA-L and FA-R.

To work around the problem of axial force measurement on the footrest, the COP of footrest was estimated and then used them to calculate the axial force. The sizes of participants' feet were average afterwards the COP was approximated to be at about the midpoint of the footrests as shown in Figure 4.40.
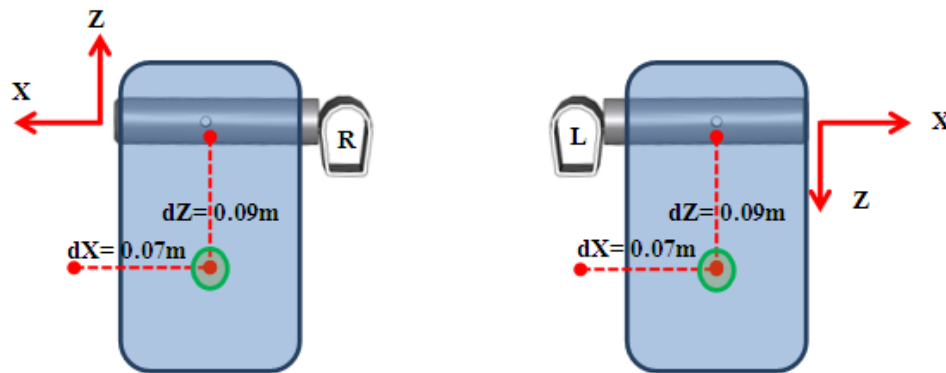
Figure 4.40 Estimated COP on footrest, FA-R and FA-L

The axial force, Fy, can then be determined by:

$$Mx = Fy_1 \times dZ$$
<div align="right">Equation (4.9)</div>

$$Mz = Fy_2 \times dx$$
<div align="right">Equation (4.10)</div>

$$Fy = \sqrt{Fy_1{}^2 + Fy_2{}^2}$$
<div align="right">Equation (4.11)</div>
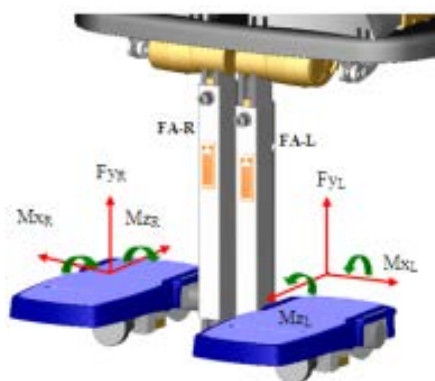
Mx, Mz are the bending moment in x, and z axis (Nm)

Fy is the axial force (N)

dx, dz are the distance along x and z axis (m)

Table 4.7 Percentage of difference on the axial force calculated by determining COP

Footrest	Linear regression	Applied force (x)	Predicted force (y)	% difference
Condition 1: The top tube was inside				
Left				
FL Mx	y = 1.0378x - 0.9807	12.87	11.36	-11.73%
FL Mz	y = -1.0403x + 0.877	-11.88	-11.36	-4.38%
FA-L Fy		**99.03**	**118.17**	**19.33%**
Right				
FR Mx	y = -1.1192x + 1.2143	-12.87	-12.27	-4.66%
FR Mz	y = -0.8111x + 0.6771	-11.88	-8.94	-24.75%
FA-R Fy		**99.03**	**121.52**	**22.70%**
Condition 2: The top tube was outside				
Left				
FL Mx	y = 1.4873x - 1.4714	12.87	15.82	22.92%
FL Mz	y = -0.9967x + 0.7015	-11.88	-10.60	-10.77%
FA-L Fy		**99.03**	**158.95**	**60.50%**
Right				
FR Mx	y = -1.4644x + 1.6621	-12.87	-15.90	23.54%
FR Mz	y = -0.9265x + 0.8482	-11.88	-10.20	-14.14%
FA-R Fy		**99.03**	**150.90**	**52.38%**

Table 4.7 presents the percentage error of the axial force determined by Equation (4.9) to Equation (4.11). When the footrest was shortened, the percentage error was reduced from -308 percent to 19 percent on FA-L and from -392 percent to 22 percent on FA-R. But when the footrest was extended at the maximum length, percent error on FA-L was increased from 5 percent to 60 percent. However, percentage error on FA-R was decreased from 89 percent to 52 percent.

4.6   DISCUSSION AND CONCLUSION

Before the strain gauges mounted on the chassis components can be used in the measurement of forces and moments, they must be calibrated. Difficulties in the calibration were expected due to minor inaccuracies in strain gauge positioning combined with stress concentrations resulting from machining tolerances of components. Therefore an output signal from a uni-directional force was not only produced by the main channel but it was a combination of signals from other strain gauges. This extent of crosstalk was evaluated by deriving a calibration matrix for each component.

The axial calibration of the BA is an example of the complexity in the calibration process. As can be seen from the results, a significant crosstalk was generated. This happened because the shape of BA was complicated with corners, and the specimen could not properly align when testing in Instron. When an axial force had been exerted on BA, the output signal of corresponding load (Fy1 and Fy2) was generated in combination with bending moments (Mx and Mz). However, the axial force, Fy, on the BA was not used to calculate the resultant force on the backrest thus the amount of force on the backrest (FB) was reliable.

On the backrest, the predicted force was an overestimation of the actual force: +14% error for the rigid system and +21% for the dynamic system. These are a cumulative error which could therefore be considered to be the upper boundary of the actual loads experienced during ADL.

The predicted axial force on the footrest was extremely different from the applied force. This was because the transducer was affected by the length adjustment of footrest (detailed in section 4.3.5). An improved estimation of the axial force in the footrests was achieved using the bending moments applied to each footrest and an assumption regarding the centre of pressure of the applied force on the footrest. Whilst not ideal, this was the only way in which the axial force on the footrest could be estimated with the strain gauges in the prescribed position. This approximation was highly variable which have an effect on the reliability of results. Alternative solutions to this problem, such as redesigning the strain gauge positioning, were not possible in the timeframe.

CHAPTER 5
GAS SPRING
CHARACTERISTICS

5.1   INTRODUCTION

The dynamic backrest mechanism is achieved using a gas spring on the backrest to provide damping and a means to adjust the backrest inclination with ease. As it replaces the back angle inner extrusion of the rigid backrest seating system, both end sides of the gas spring are fitted in joints of the backrest and seat. Various sizes of gas springs (sizes refer to stiffness) are available and the selected gas spring should depend on user's body weight and the severity of the extensor spasms experienced.

Gas springs used on dynamic seating systems have two functions. Firstly, when the gas spring is in unlocked position, the backrest can be adjusted easily to the preferable reclining position. When this adjustment had been done, the gas spring is locked to give firm support. However, when user extends their body, the backrest can be displaced backward dependent on the stiffness of the gas spring in the locked position.

This chapter provides an overview of the gas spring characteristics used on the Mygo wheelchair system determined though systematically loading the gas spring in the Instron tensile test rig. The aim of which was to understand the response of the gas spring when in use, especially when gas springs are in the locked position because these characteristics are not provide by their manufacturer. Another aim is to determine equations to describe the displacement of the gas springs based on the compressive load.

5.2   GAS SPRING
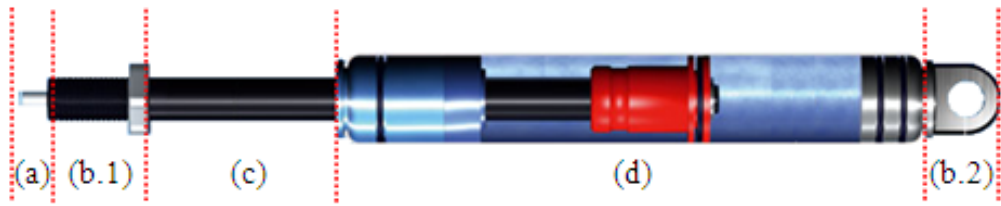
Figure 5.1 Gas spring components: (a) release pin (b) connecting parts, (c) stroke
area and (d) body (Bansbach, 2012)

The gas spring consists of four main parts, as can be seen in Figure 5.1, namely
the body or rod, stroke area, release pin and connecting parts. Inside the gas spring
body, high pressure nitrogen gas is compressed by a piston rod up to 300 bar,
depending on size of the gas spring (Bansbach, 2012). The release pin controls a
bypass valve allowing the Nitrogen gas to leak and allow the piston to freely travel at
any point of the stroke length. The pin can also be released (locked) at any point
along the stroke length to seal the gas behind the piston.

The gas spring is attached to the dynamic backrest seat by the set of assembly
parts as shows in Figure 5.2. When the security lock is released the lever is free to
push the release pin, enabling the gas to leak past the piston head allowing the
backrest to be fully adjustable. The piston can be moved along the stroke length to
the desired position allowing a suitable backrest orientation for the user to be set.
After adjusting the seat orientation, the pin again is released to lock the gas spring. In
this locked position, the dynamic system provides a small amount of backrest motion
under applied loads.
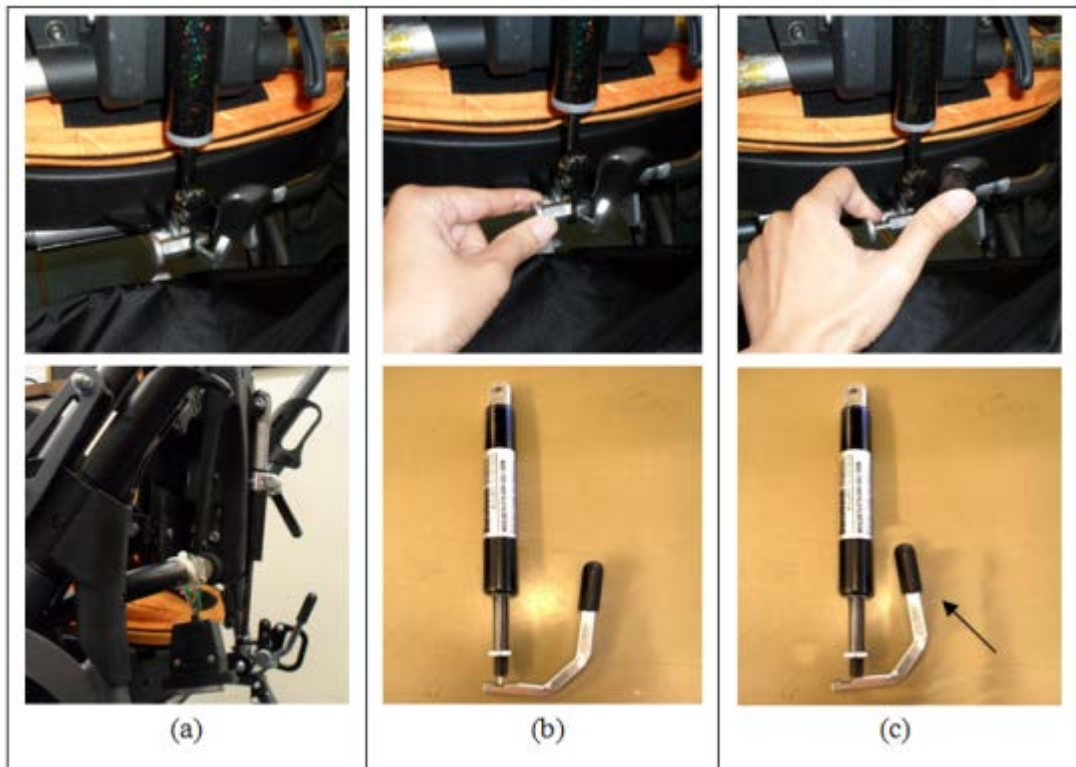
Figure 5.2 Dynamic backrest assembly parts
(a) the pin locks the lever to operate the gas spring in the locked position. (b) Pull the security lock (c) push the lever up to operate gas spring in the unlocked position

5.3 METHOD

The dynamic Mygo seating system utilises the gas springs labelled size 50, 100 and 150 N. It was hypothesised that these labels indicate the force required to move the piston in the gas spring in the unlocked position. The force-displacement characteristics of the gas springs in the locked position are unknown.

Compression tests of the locked Bansbach gas springs, Germany, were performed on the Instron testing machine (Illinois Tool Works Inc. High Wycombe, UK). The specimen was positioned as shown in Figure 5.3 and preconditioned by a series of loading-unloading cycles prior to the following test procedure below.

1. The gas spring was placed vertically in a custom-made jig which was positioned in the Instron E10000 testing machine (as in chapter 4, bespoke testing rigs were made to characterise the components). When positioned, the push rod was facing down and the resting stroke length of the gas spring was set at approximately

50% of its movement range (on the chair, the resting length of gas spring depends on the degree of backrest recline)

2. The gas springs were tested in two conditions:

    a. Firstly, the gas spring was locked, as the release pin fitted through a hole in the bottom plate, Figure 5.3(a).

    b. The second testing condition of testing involved testing the gas spring in the unlocked condition. For testing in the unlocked position, the release pin was flush to the flat plate, Figure 5.3(b).

3. We loaded each spring to less than 1000 N. Therefore the Instron specimen protection settings ensured that the spring was compressed to this safe maximum limit.

4. The piston rod was compressed in displacement control with a maximum intended displacement of 30 mm at rates of 1, 3, 5 and 10 mm/s.

5. The gas spring was also allowed to return at the selected test speed until the piston rod was back to the original position.
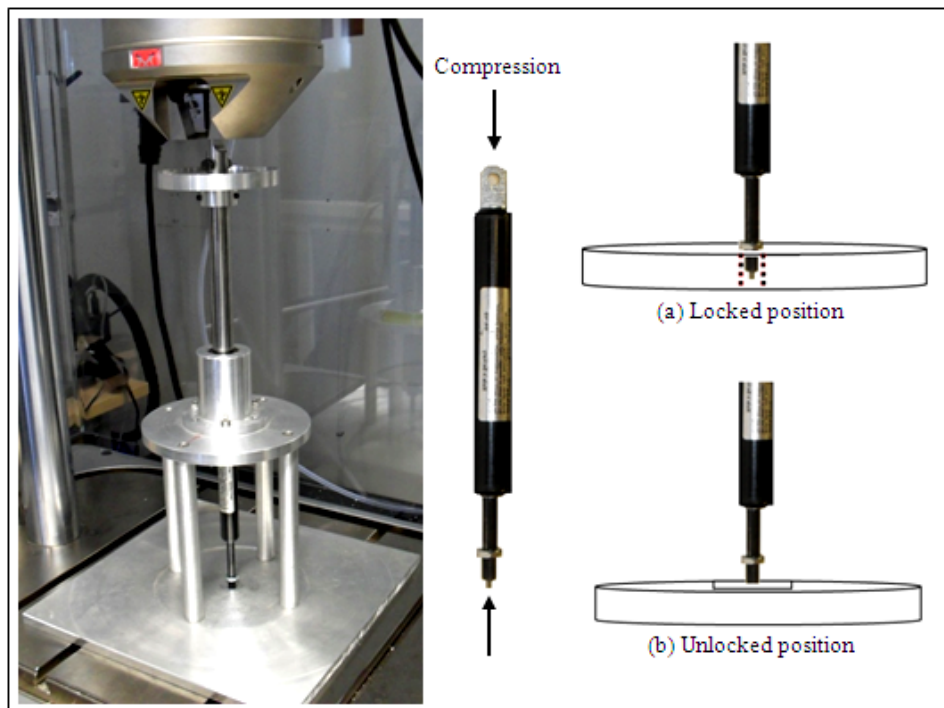
Figure 5.3 The gas springs were positioned by the custom-made jig in Instron testing machine for the compression test in (a) Locked and (b) Unlocked positions

5.4 RESULTS

5.4.1 Threshold Force

The results indicated that a threshold force in the gas spring was required to overcome internal friction and initiate motion when compressing it. Figure 5.4(a) shows the threshold forces and their relationship among those three sizes when they were compressed in the unlocked position. The results of the 1 mm/s test were representative of the other testing rates, which clearly showed that when the gas spring was in unlocked position, the threshold force changed linearly, depended on the size of gas springs. However, when in the locked position the threshold force of the selected gas springs remained constant in small range, approximately 60-70 N, as can be seen in Figure 5.4(b) in locked position.
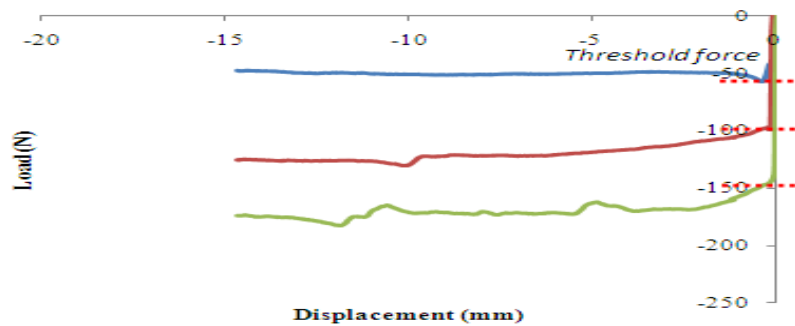
(a)
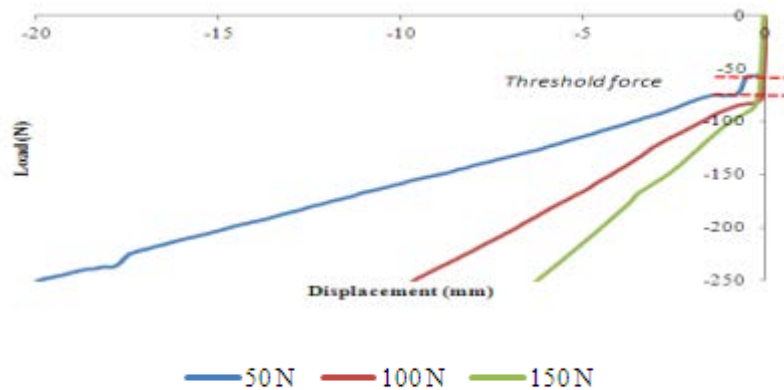
(b)

Figure 5.4 Relationship of the displacement and load when the gas springs were compressed (a) in unlocked position and (b) in locked position; the red dotted lines show the threshold force of gas springs

96

5.4.2 Stiffness

After threshold had been reached, the gas springs were continually compressed to 30 mm displacement to verify the linear relationship of displacement and load. When gas springs were in the unlocked position, the springs compressed without stiffness (Figure 5.4(a)). In the locked position, the stiffness of the gas springs above the threshold force depended on the spring size (Figure 5.5).
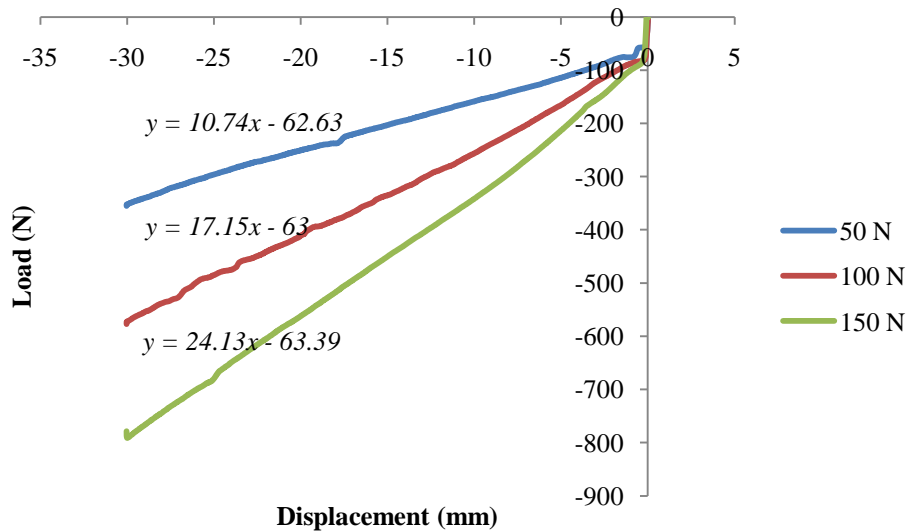
Figure 5.5 Stiffness of the gas spring

The stiffness can be used to determine the displacement of the gas springs as shown in Equation (5.1).

$$\text{Displacement (mm)} = \text{Load (N) / stiffness (N/mm)} \qquad \text{Equation (5.1)}$$

The dynamic backrest gas spring can be compressed by a maximum of 60 mm (stroke length), and this maximum range leads to the backrest being reclined to a maximum of 20 degrees, as the recline of backrest linearly depended on the displacement of gas springs as shown in Figure 5.6 - Figure 5.7.
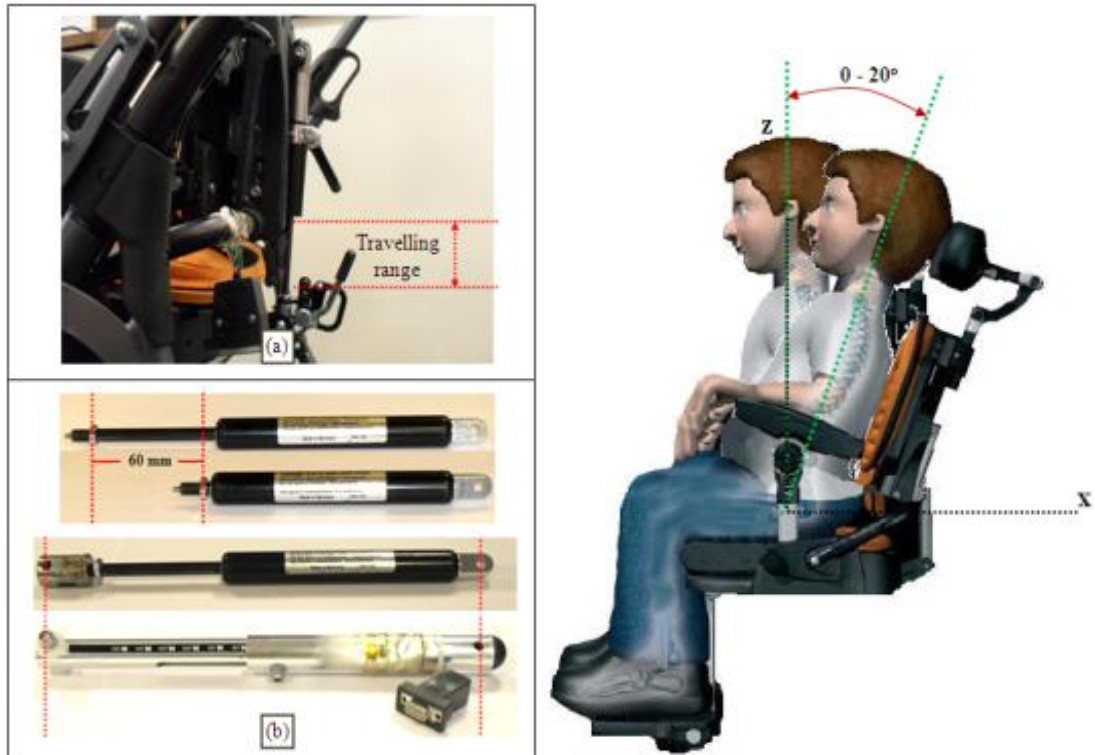
Figure 5.6 (a) Travelling range of the gas spring and comparison between the displacement length of gas spring and (b) the angle of the back tube

Displacement (mm)	Degree changed (deg)
0	0
15	5
30	10
45	15
60	20

(a)

$y = 0.3333x$

(b)
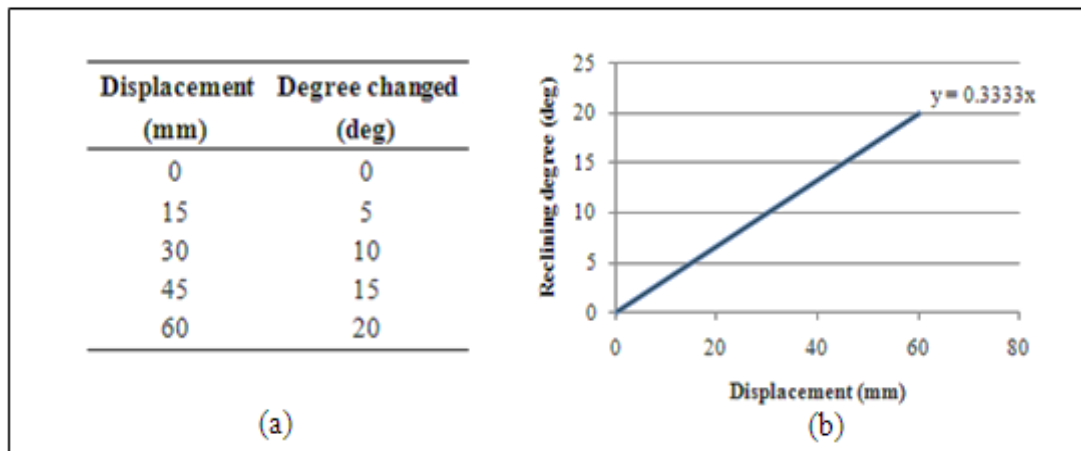
Figure 5.7 (a) Linear relationship of the displacement of gas spring and the changed degree of the backrest and (b) the linear equation

5.4.3 Hysteresis

Figure 5.8 displays a typical hysteresis of a gas spring during a loading/unloading cycle (50 N spring compressed by 30 mm). The area within the loading/unloading loop is equal to the energy lost during the cycle. The energy absorbed by the gas spring at the tested compression rates is plotted then calculated, the hysteresis of each gas spring are shown in Table 5.1, these outcomes indicate debatable energy absorption depending on size of gas springs.
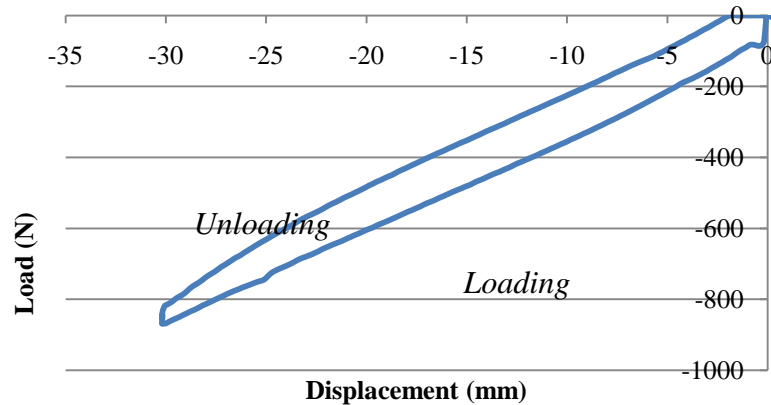
Figure 5.8 Displacement and load of gas spring when loading and unloading
(50 N spring)

Table 5.1 Hysteresis of three sizes of gas spring in different speed of compression

Size (N)	Speed (mm/s)	Hysteresis (Nm) Work (Joule)
50	1	9.48
	3	9.63
	5	9.59
	10	9.46
100	1	16.78
	3	17.11
	5	17.08
	10	17.37
150	1	23.62
	3	24.00
	5	24.38
	10	25.44

5.4.4 Speed Effect

The effect of compression speed on the stiffness characteristics of the spring was assessed by compressing the gas springs 30 mm at different speeds 1, 3, 5 and 10 mm/s when they were in the locked position. Threshold forces, stiffness and hysteresis were compared among all different speeds. The threshold forces were slightly increased when the displacement rate or speed were increased. However, stiffness and hysteresis remained constant and independent of different displacement rates as can be seen in Figure 5.9.
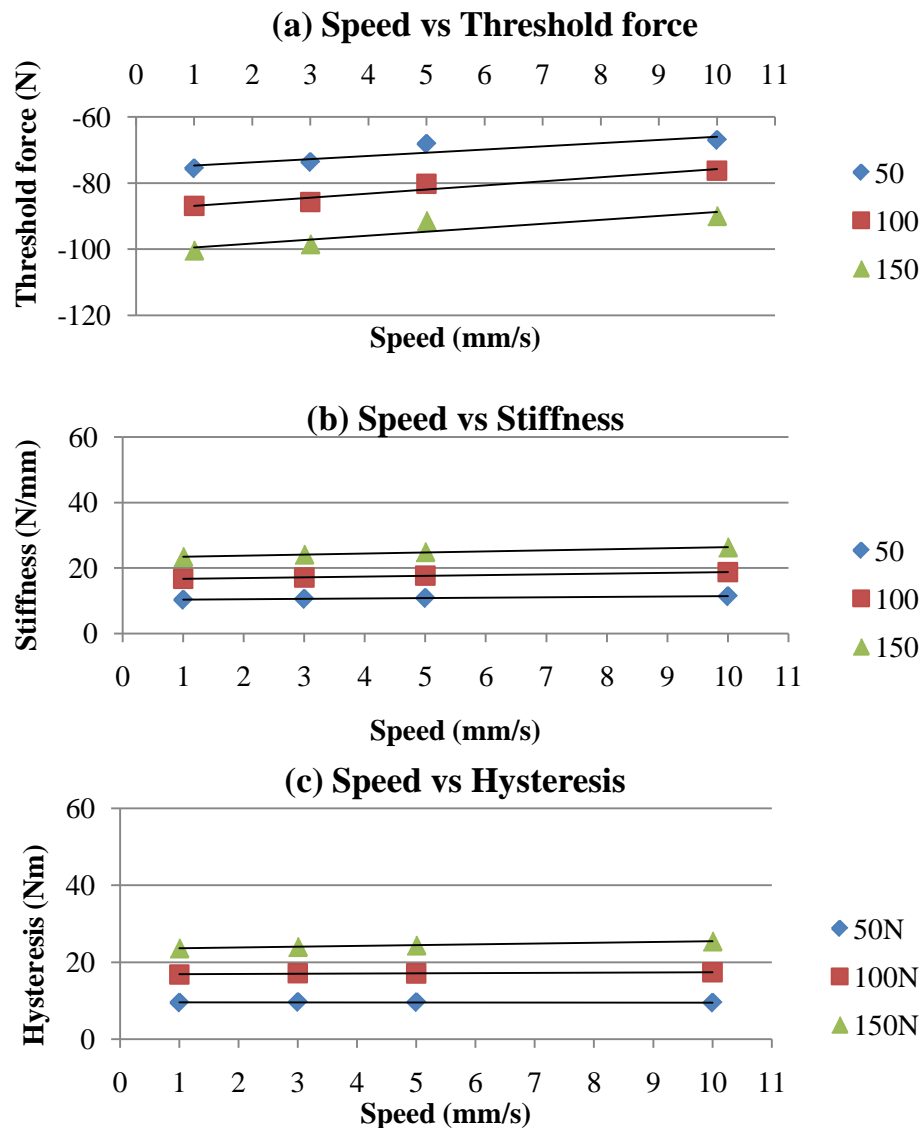
Figure 5.9 Relationship of speed and (a) threshold force, (b) stiffness and (c) hysteresis when 50, 100 and 150 gas springs were compressed at different speeds

5.5 STRESS ANALYSIS OF GAS SPRING

The gas spring is designed to be loaded in the axial direction however the orientation of the gas spring on the Mygo seating system may subject the rod of the gas spring to low bending moments, potentially causing low cyclic fatigue and the rod to break. Furthermore, the rod of the gas spring is attached to the chair using a non tapered design that will inevitably lead to high stress concentrations on application of the low bending moments. Shear forces applied to the backrest by a user changing position or driving the chair will induce a bending moment around the lower attachment point of gas spring Figure 5.10.
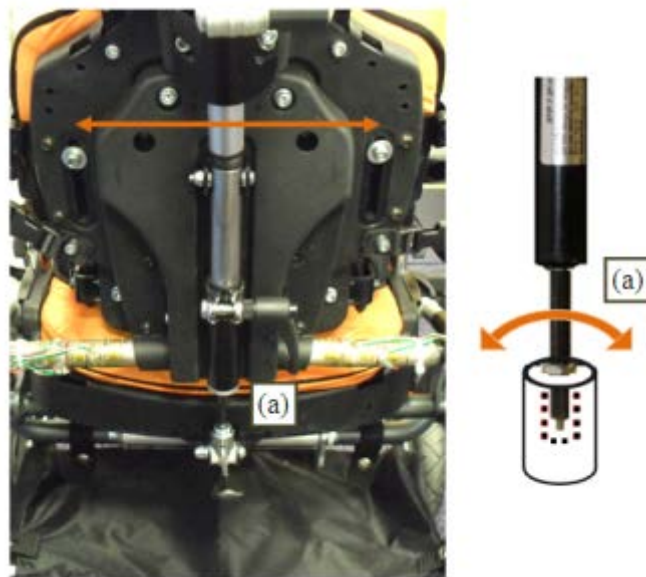
Figure 5.10 (a) High stress concentrations due to threads and joints with no tapers

The rod is made from mild steel, the Modulus of elasticity or Young's Modulus, E is 200 GPa and yield strength, Y is 250 MPa (William and Callister, 2007). The geometry dimensions are shown in Figure 5.11. The axial force, bending moment and torsion moment were determined by those data, in a similar fashion to chapter 3.
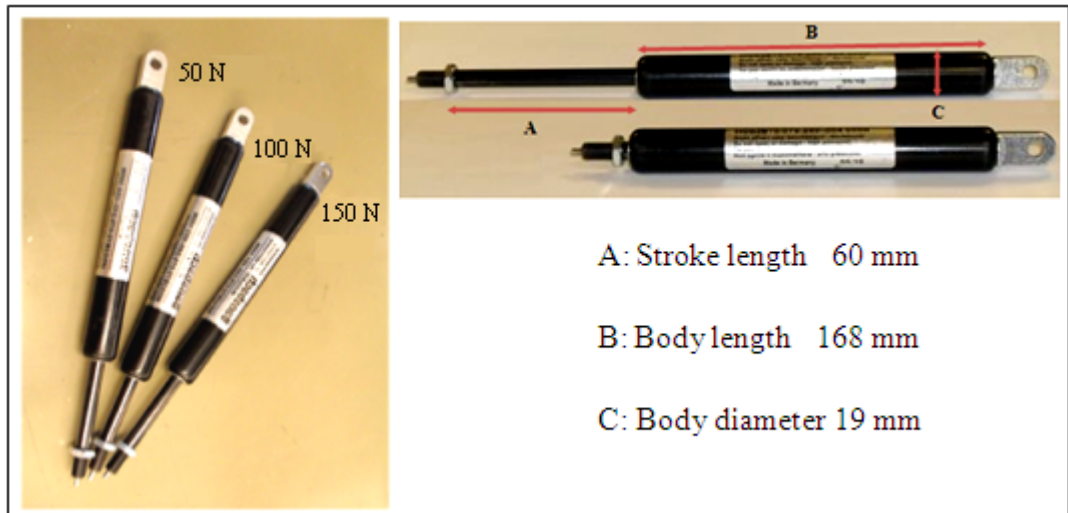
Figure 5.11 Three sizes of Bansbach gas springs, Germany and size details

The area of force in tension or compression

$$A = \frac{\pi}{4} (D^2)$$

Equation (5.2)

The second moment of area in bending

$$I = \frac{\pi}{64} (D^4)$$

Equation (5.3)

The second moment of area in twisting

$$J = \frac{\pi}{32} (D)$$

Equation (5.4)

Where

A is the area (m^2)

I is the second moment of area, in bending, (m^4)

J is the second moment of area, in twisting, (m^4)

D is the dimension of the material (m)

- *Axial force (F)*

$$Fmax = \sigma_y \times A \hspace{3cm} \text{Equation (5.5)}$$

Where:

      F is the axial force (N)

      σ_y is the yield stress (N/m^2)

      A is the cross section area (m^2)

$$Fmax = 12.56 \text{ kN}$$

- *Bending moment (M)*

$$M = \frac{\sigma_y I}{y} \hspace{3cm} \text{Equation (5.6)}$$

$$Mmax = 12.56 \text{ Nm}$$

$$M = F \times distance \hspace{3cm} \text{Equation (5.7)}$$

When maximum M is 12.56 Nm, and the gas spring length is 0.28 m thus maximum F is,

$$F = 12.56/ \, 0.28$$

$$= 45 \text{ N}$$

Where:

      M is the bending moment (Nm)

      y is the distance from the neutral axis (m)

      I is the second moment of area, in bending (m^4)

Using simple stress strain relationships, Equation (5.6), the maximum bending moment can be applied to the gas spring rod (Figure 5.10) is approximately 12.56 Nm. The gas spring length is 0.28 m when he backrest angle is about 90 degree reclining. Therefore from Equation (5.7), the maximum force is 45 N.

From these calculations, it is noticeable that the gas spring cannot stand high bending moments which could be generated when the backrest is moved or the wheelchair was driven. Furthermore, repetitive motion below these critical forces could fatigue the spring rod and cause it to fail (Benham and Crawford, 1987).

At the end of the gas spring rod is an external thread which is intended to screw into the gas spring base (GB). As the stressed area in the thread root is the weakest point of the specimen (Chalupnik, 1968), hence this connection point has the potential to fail when the backrest gets a high imparted force from a user or when wheelchair is driven.

5.6   CONCLUSION

The compression tests on the Bansbach gas springs set out to determine their stiffness in the locked position, which were unknown and uncharacterised by the manufacturer. Results showed the three gas springs rated as 50, 100 or 150 N were able to approximately resist an initial maximum load of 50, 100 or 150 N. The data gained from this test include the threshold force, stiffness and hysteresis characteristics. These data are useful for determining the suitable size of the gas spring for each individual.

- *The two characteristics in compression*

During compression after the threshold force was reached the velocity dependent damping thus hysteresis by the gas spring was shown to be minimal. After the threshold force had been reached, the gas spring behaviour was that of a linear spring response.

In the unlocked position, the threshold force required to initiate movement is the internal friction that needs to be overcome and was approximately equal to the size or rating of the gas spring, as expected.

On the wheelchair, however, the gas springs were used and compressed when they were in the locked position. Threshold forces were such that the user needs to place force more than 60-70 N on the backrest to overcome the internal friction and to activate the compressive movement of the gas spring. After the threshold force had

been reached, the gas spring loading response depended on their rating (stiffness). Importantly their response was linear, allowing a clear prediction between applied force and displacement for each spring type. These relationships were found to be independent of speed, enabling the range of recline of the backrest angle to be estimated when gas spring was compressed by the applied extensor load.

The energy lost in gas springs was proportional to their hysteresis, the greater the area enclosed in the hysteresis loop, the greater the energy lost. Hysteresis was slightly increased when the stiffness of gas springs was increase.

CHAPTER 6
STRESS ANALYSIS
OF RIGID AND DYNAMIC
SEATING SYSTEMS
DURING ACTIVITIES OF
DAILY LIVING

6.1   INTRODUCTION

This chapter provides details of the test protocols and results of the stress analysis of the rigid and dynamic seating systems. The investigation into the long-term effects of dynamic seating will be detailed in the next chapter.

This project was classified as a research study of a medical device (Mygo™ seating system) which has a CE marking by the manufacturer. James Leckey Design Ltd. as manufacturer with sole responsibility declares that the Mygo™ Seating System conforms to the requirements of the 93/42/EEC Guidelines, Medical Device Regulations 2002 and EN12182 Technical aids for disabled persons and test methods. The study was not intended for CE marking purpose, thus the approval by Medicines and Healthcare Products Regulatory Agency (MHRA) was not required. However, the research did involve the NHS in some capacity (WestMARC) and thus the study protocol was reviewed and granted approval by the West of Scotland Research Ethics Committee 5 (REC 5) and the NHS Research and Development Central Office (NHS R&D).

The primary objective of the study was to identify the forces imposed on the seating systems by the child during ADLs and especially during an extensor spasm. A secondary aim was to compare two backrest designs by means of imparted force throughout the day. Twelve children were recruited after the study protocols had been approved by REC and NHS R&D. They were children who have CP and have been prescribed a Mygo seating system by WestMARC or James Leckey Design Ltd.

The methodology was primarily observational, the only intervention imposed was the following: certain chassis components had strain gauges attached to allow chassis forces to be determined and the placement of the data acquisition unit under the seat. The monitoring period was between 2 and 6 hours[*] while the participants performed their ADLs normally without interruption. In the meantime the researcher discreetly followed and simultaneously logged an activity diary in order to associate recorded forces with activity. At the end of the agreed time, the child was returned to their normal chair and the data was downloaded and analyzed in conjunction with the activity diary.

The output signals from the transducers on the wheelchair framework were amplified and collected via the mobile DAQ. The data were continuously streamed to an ultra mobile PC for storage. The stored strain measurements were then was used to inverse engineer the loads applied by the body to generate these forces in the components.

Results of imparted force on the chair's components were analysed and presented in two ways: external contacts force and internal stress in material. The external contact forces were determined by static equilibrium method. The maximum and average forces on critical positions, backrest and footrest were presented. And according the applied forces on each component, the von Mises equivalent stress were concluded the yield criterion on material which were under the complex stress condition.

---

[*] *Agreed by the child's parents in advance*

107

6.2 PARTICIPANT RECRUITMENT

The population of interest in this study were children with CP. Each child had been prescribed a Mygo Seating system by either WestMARC or James Leckey Design Ltd. This ensured the participants were fully familiar with the chair and that the chair itself would not act as a stimulus for extensor spasm. The inclusion and exclusion criteria of recruitment are shown below.

- Inclusion criteria

Children between 4 and 10 years old, which have been prescribed a Mygo by WestMARC and James Leckey Design Ltd.

- Exclusion criteria

Children who are within 6 months of a prior surgical procedure, or have a current illness, or are on temporary medication.

The University prepared unaddressed envelopes which contained the participant information sheet. These envelopes were passed to WestMARC and to James Leckey Design Ltd. who put on the address of potential participants that were stored in their databases. At this point the University had no knowledge of the names and addresses of those invited to participate.

The information sheet (Appendix C) provided a detailed explanation of the study in which the research aims, benefits, risks and what participation involves were highlighted. In addition it was clarified that taking part to this project is voluntary and children have the possibility to withdraw at any time without consequence. A consent form was also given to children and their parents with whom they can subsequently confirm their agreement to participate in the study after due reflection. If an invitee agreed to volunteer, participants agreed to take part, the researcher arranged to visit them to obtain informed consent (parent) and assent (child) and to arrange a time and a date for the participation[*]. A specially designed assent form was created in order for the child to assent to the research. Where possible, consent was taken from the child by making a mark on the consent form near or in a "yes" box.

---

[*] *Under Scottish law, consent is required from the parent/guardian for research on under 12s. It is also desirable, although not legally requested, to get the child's assent, and we attempted this whenever possible.*

The "yes" box and "no" box were separated as much as possible. If this was not possible, a verbal consent was taken and parents/carers confirmed this on their own form.

In addition, if the agreed time and date included a visit to a school or other similar premises, we also provided the information sheet for the community based activity that was encountered for permission to do the investigation in their establishment. There was no time limit that each child was expected to be sat in the chair, and as such, the length of the exercise for each child was determined by the child and parent. Figure 6.1 shows the summary of recruitment process and testing protocol.
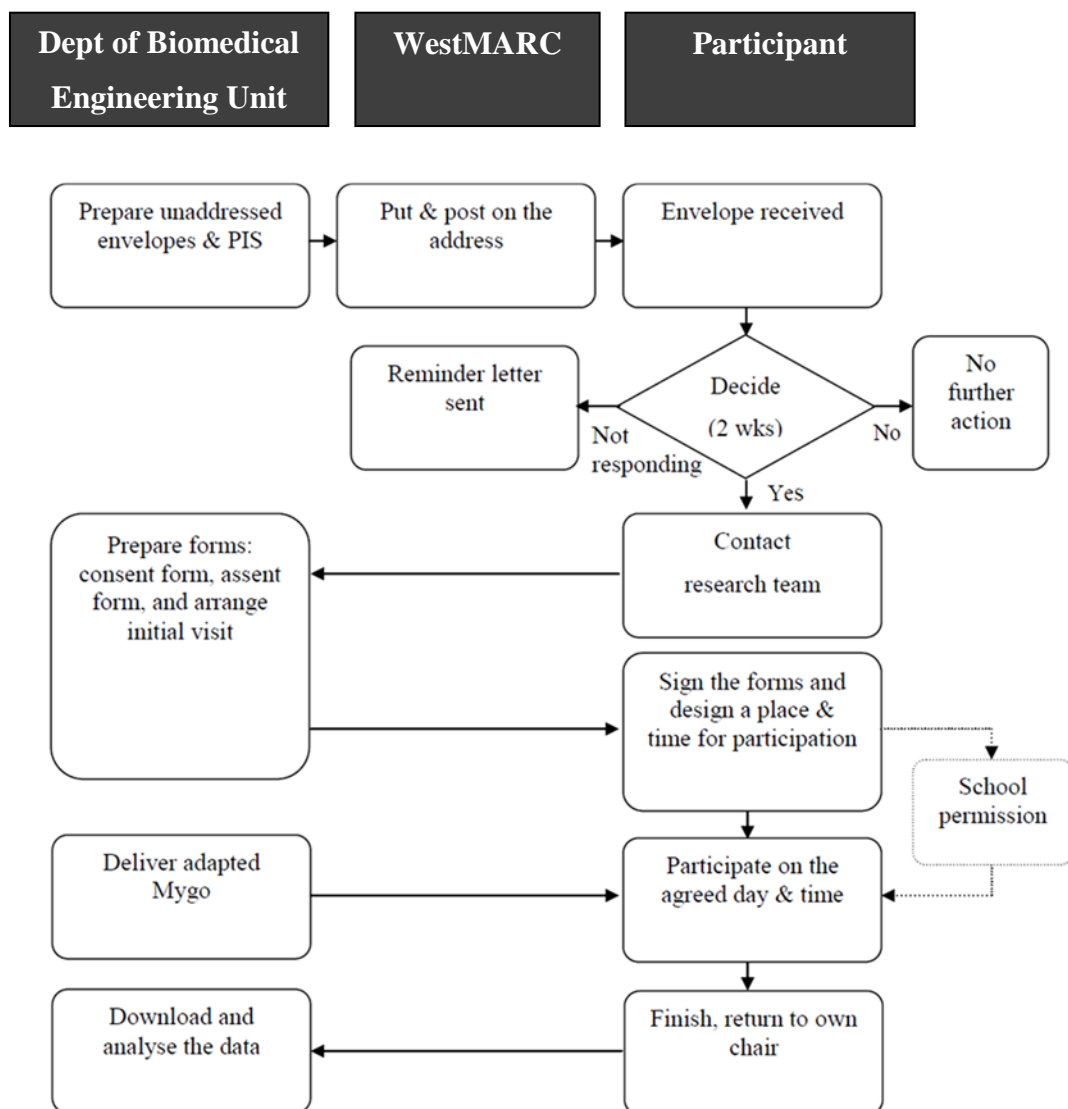
Figure 6.1 Diagram of the recruitment and testing process

6.3   THE MYGO SEATING SYSTEM

The seating system that was used for this study was the Mygo Seating System by James Leckey Design Ltd. The seat can be used with a variety of base units to support the child activities at home, school or other community places.

The components of the Mygo seating system are separated to two sections including a seat and mobility base (Figure 6.2). The seat consists of the contoured headrest, backrest, pelvis and hip supports, armrest and footrest. All these components are adjustable to match with individual needs. In addition, the support structures or seat frames are the main components of the seat, these parts are also adjusted in depth and recline the back support. The seating is situated on the chassis which provides the mobility for the seating system.

The Mygo has two different backrest systems. Un-adapted, the Mygo is a rigid backrest system. Since 2010 the dynamic backrest option has been offered to children who have extensor spasms (Leckey, 2010).

6.3.1 Rigid Backrest System

The rigid or non-dynamic backrest system was used for the study. The backrest angle in the rigid backrest system is adjustable: it can be manually changed in depth and angle, prone 10° (80° from seat cushion) to recline 25° (115° from seat cushion) to accommodate posture, growth and angle positioning. During the test the backrest angle was adjusted match with the child own chair and the angle of recline noted.

Strain data from one hundred strain gauges were collected from five areas of the seat including a) right side of FA, b) left side of FA, c) BT, d) left side of BA and e) right side of BA these were connected to DAQ via the pin connecters. All cabling and devices were well kept in the basket then put under the seat as shown in Figure 6.3

Figure 6.2 (a) Mygo seating system, (b) seating and supporting structures and (c) mobility base (Leckey, 2010)

Figure 6.3 The set-up of the strain gauged Mygo seating in the rigid backrest system

6.3.2 Dynamic Backrest System

To convert the chair into a dynamic seating system, a gas spring was inserted into the back tube on the backrest of the chair as can be seen in Figure 6.4. The size of the gas spring used depended on the load of each user; their weight and their extensor force. There were three sizes of gas springs which were classified by the extension forces: 50, 100 and 150 N. The gas spring system permitted the forward and backward movement of the backrest as the occupant extended and retracted their body. However, the movement of the dynamic backrest system was able to be locked[*] to maintain the rigidity during an intentionally induced period such as when propelling the chair over rough surfaces or on transportation.

The output signals from ninety six strain gauges of the dynamic backrest seating system were amplified and collected via the mobile DAQ which housed under the seat.

(a)　　　(b)
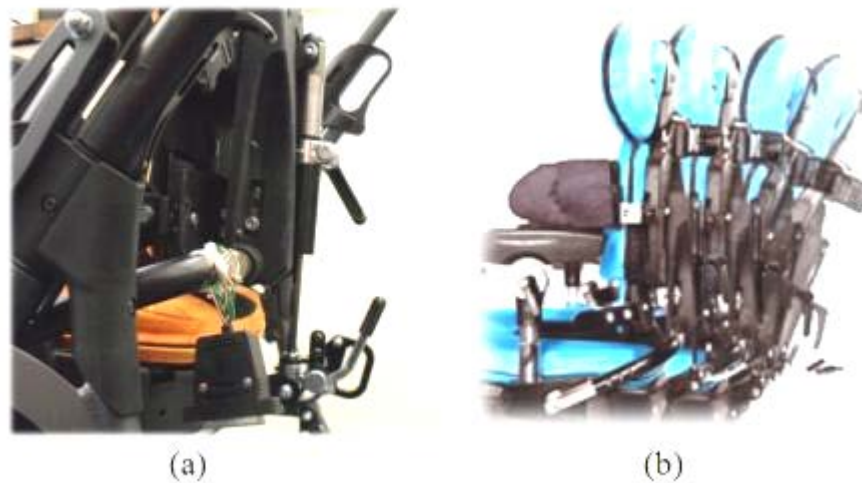
Figure 6.4 Dynamic backrest system
(a) gas spring is put inside the back tube and (b) dynamic movement of the
backrest

---

[*] *Externally locked, this is different to locking the gas spring which still allow motion.*

Figure 6.5 Major adjustments on strain gauged chair follow the measurement of head position, shoulder width, seat height, hip width, seat depth and footrest height

6.4   TEST PROCEDURE

Similar protocols were used with the two different types of seating systems. Hence, both investigations were offered to participants' parents to be done on the same day.

On the testing day, participation involved the child sitting in the modified Mygo seating system throughout a typical morning or afternoon. Chair measurements including the shoulder width, seat height, hip width**,** seat depth**,** footrest height and backrest angle had been taken in order to match their own chair with that of the strain gauged chair (Figure 6.5). Accessorises, such as a tray, harness or knee pads, were added to cater for an individual's needs. All these adjustments to the chair were done with the assistance of qualified clinical scientists from WESTmarc.

The DAQ was battery operated, and was contained within the seating system with no exposed or trailing wires. Data acquisition started immediately after the major adjustments of the strain gauged chair were finished. This was done so that the stresses exerted on seating a child could be determined. The child was lifted and fitted in the chair by a parent or other specialist, minor chair adjustments were done, and data was continually collected until the finish of the agreed time. The participants then continued their day as normal. In the meantime the researcher discreetly followed and simultaneously logged an activity diary in order to associate

recorded forces with an activity. It was intended that this project should cause a minimal amount of disruption, because the main aim was to collect data about normal activities. During the testing process, the researcher worked together with the child's teacher/PT/carer to understand whether the child was comfortable throughout testing. In addition they could help to observe the incidence of extensor spasms. At the end of the agreed time, the child was returned to their normal chair and the data was downloaded and analysed in conjunction with the activity diary. There was no minimum or maximum specified time that we would expect the child to be seated in the wheelchair and no specified place to do the trial. Typically, the monitoring lasted 2 to 6 hours in total. This time often included the child being lifted in an out of the seat a number of times and to include travel to and from a school or alike.

Participate on the agreed day & time, deliver adapted Mygo

Physical measurement of child

Adjust the modified Mygo chair

Turn on DAQ

Transfer the child to the modified Mygo chair

Minor adjustment to the modified Mygo chair

Collection of data using the Catman software and record activities by hand

Finish, return the participant to their own chair
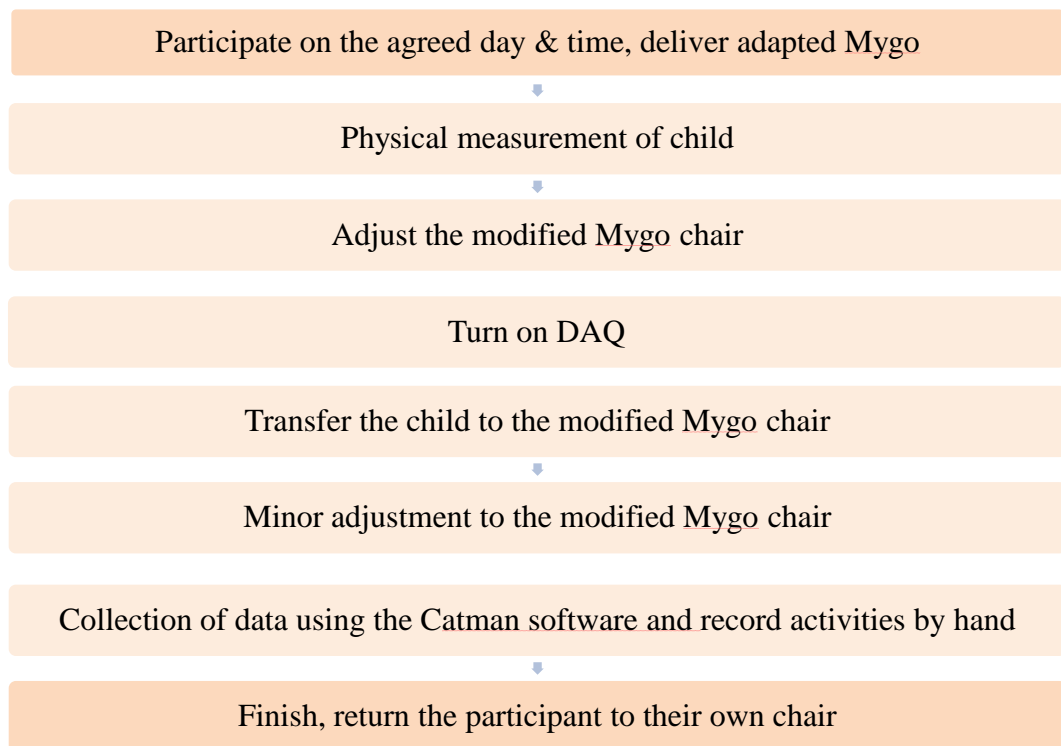
Figure 6.6 Experiment protocol

6.5   DATA ANALYSIS

The data analysis utilised the calibrated wheelchair components and calculations as described in previous chapters.

6.5.1 Data Collection

The outputs from strain gauges were amplified via twenty channels using an HBM strain gauge amplifier, in which each channel corresponded with a specific measurement as shown in Table 6.1.

Table 6.1 The HBM amplifiers collected data in 20 channels from the Mygo wheelchair

Catman strain channel	Component	Force/Moment
1		Shear Force (Fx1)
2		Axial Force (Fy1)
3	BA	Shear Force (Fz1)
4	(left side)	Bending Moment (Mx1)
5		Torsion Moment (My1)
6		Bending Moment (Mz1)
7		Shear Force (Fx2)
8		Axial Force (Fy2)
9	BA	Shear Force (Fz2)
10	(right side)	Bending Moment (Mx2)
11		Torsion Moment (My2)
12		Bending Moment (Mz2)
13		Bending A (Mx_l)
14	FA-L	Bending B (Mz_l)
15	(left side)	Axial force (Fy_l)
16		
		Bending A (Mx_r)
17	FA-R	Bending B (Mz_r)
18	(right side)	Axial force (Fy_r)
19		Axial (Fy)
20	BT/GB	Torsion (My)

Data were sampled at 10 Hz using commercial software (CatmanEasy® version 3.1.2.21) which was developed specifically for the HBM DAQ system. Data collection during the investigation was visualised in real time on the ultra mobile PC. All devices were powered by the two 12V 8Ah lithium ion batteries DC regulated supply.

At the end of each test, data from the ultra-mobile PC were exported to MS Excel then uploaded into MATLAB R2001a (The MathWorks Inc., Massachusetts, US). Finally, strain magnitudes could then be used to determine surface stresses using the calibration matrices determined from applying known loads detailed in chapter 4.

6.5.2 Management of Confidentiality Issues

Personal details (Name, address and telephone number) had been used to contact the patients, arrange transportation if required during the study, for notifying them of trials arrangements or to send them information about research results. This information was passed between the University and WestMARC via email.

Each participant was issued with a unique reference number which used to name and store scientific measurements. The data were kept anonymous with no references to personal details and retained in a locked cabinet at the University of Strathclyde. Access also has been maintained for the duration of the study in order to enable long-term follow-up studies should additional resources become available.

6.5.3 Statistical Methods

The force data was collected and associated with participant's activities during ADL. Descriptive statistics were used to summarise the results. Mean and peak forces and moments were calculated. Statistical analyses were performed using Minitab 16 statistical software (Minitab Inc, State College, PA, USA). Twelve participants used the rigid and dynamic backrest systems. The data from both the rigid and dynamic systems were analysed and compared. The data from the twelve participants were normally distributed, and therefore the paired t-test was used to determine if there was any significant differences in an of the variables between the two systtems. Results were considered to be statistically significant if the level of significance (p) was $p < 0.05$.

6.6   RESULTS 1: PILOT TEST

The main goal of the pilot experiment was to establish the validity of the DAQ system and calibration matrix used to calculate force data. It was hoped that this pilot test would give some idea of the parameters required to characterise seated child activity, and an understanding of any problems involved in the main study with CP children. Average and peak forces on the seat when it was driven were also determined.

6.6.1 Pilot Participants

After ethical approval, a pilot experiment was performed. After parental consent, two able-bodied girls (aged 4 and 6) assented and volunteered to perform this initial testing (Table 6.2). The girls were measured for height and weight before sitting on the strain gauged Mygo seating system. The DAQ was initiated and zeroed, sampling frequency set at 10 Hz. After a minute of data collection the child was sat on the wheelchair. The seat back angles, headrest, lateral supporters, harness and foot rest where all adjusted to provide further comfort. After a quiet sitting period, the wheelchair was propelled around the University campus by the parent for approximately 12 minutes over a tiled path, a bumpy path, up and down steps and up and down a 10° ramp. The researcher observed the child and simultaneously logged an activity diary to match the applied forces with the activity.

Table 6.2 Pilot participant data

Participant	Sex	Age (Year)	Weight (N)
A	Girl	4	172
B	Girl	6	191

6.6.2 Imparted Force on A Moving Wheelchair

The results of this pilot experiment were based on data obtained from two normal children. The resultant force and moment during each activity were calculated assuming static equilibrium of the chassis. The magnitude of the resultant force acting on the backrest and footrest are given in Table 6.3 and the normalised force by participants weight are given in Table 6.4.

Table 6.3 Resultant force acting on backrest, left and right footrest for each activity

Force (N)	Static sitting	Bumpy path	Up stairs	Down ramp	Down stairs	Tiled path
Backrest						
Average	76	92	84	98	126	90
SD	5	14	13	12	60	8
Peak	193	252	224	274	353	197
Footrest-left						
Average	5	5	2	7	4	5
SD	1	2	1	3	0	4
Peak	26	30	20	17	18	27
Footrest-right						
Average	5	7	5	9	12	6
SD	2	1	0	3	12	0
Peak	44	29	20	21	28	32

Figure 6.7 Backrest and footrest coordinate system

Table 6.4 Normalised force acting on backrest, left and right footrest for each activity

Force (BW)	Static sitting	Bumpy path	Up stairs	Down ramp	Down stairs	Tiled path
Backrest						
Average	0.42	0.51	0.46	0.54	0.69	0.49
SD	0.00	0.08	0.07	0.07	0.33	0.04
Peak	1.06	1.38	1.23	1.50	1.94	1.08
Footrest-left						
Average	0.03	0.03	0.01	0.04	0.02	0.03
SD	0.01	0.01	0.01	0.02	0.00	0.02
Peak	0.14	0.16	0.11	0.09	0.10	0.15
Footrest-right						
Average	0.03	0.04	0.03	0.05	0.07	0.03
SD	0.01	0.01	0.00	0.02	0.07	0.00
Peak	0.24	0.16	0.11	0.12	0.15	0.18
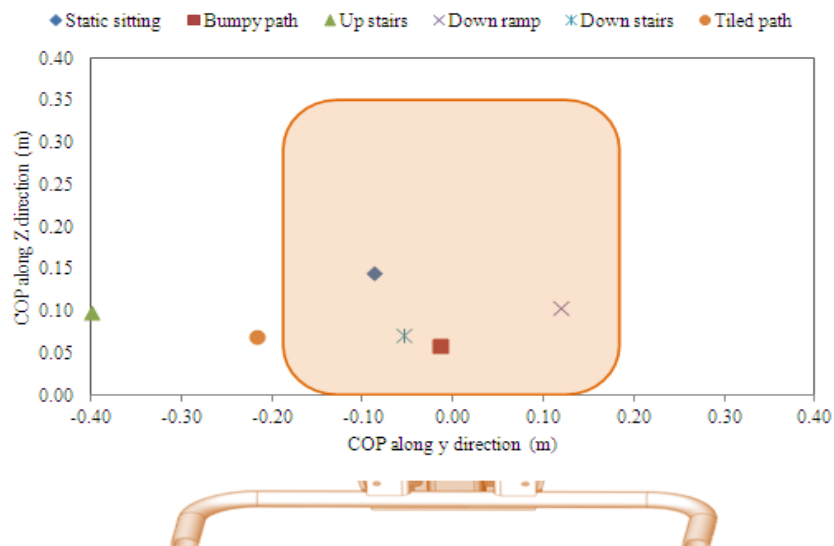
COP	Static sitting	Bumpy path	Up stairs	Down ramp	Down stairs	Tiled path
Lateral deviation of COP from midline (m)						
Average	-0.09	-0.01	-0.46	0.12	-0.05	-0.22
SD	0.23	0.08	0.10	0.84	0.10	0.05
Vertical deviation of COP from BA (m)						
Average	0.11	0.15	0.06	0.10	0.10	0.07
SD	0.05	0.08	0.22	0.27	0.03	0.19

Figure 6.8 Pilot participants COP on the backrest in frontal view

Peak forces of up to 2 times bodyweight were observed on the backrest during down stairs travel. Whilst muscle activity may have been a factor in these peak loads, we attribute the peak loads to the inertial loads on the chair, due to traversing rough terrain (e.g. bumping down steps). Traversing tiled path and bumpy surfaces and static sitting resulted in peak loads of up to 44 N on the footrest. Both participants were right-side dominant, which may explain the increased forces in the right footrest compared to the left.

The centre of pressure (COP) on the backrest was calculated by using static equilibrium. Figure 6.8 shows the point of COP and distance from the midline of reference y and z axes. These were determined by the average forces and moments of each activity on wheelchair. They fluctuated significantly since the able-bodied children were able to balance their positions on the wheelchair all the time in response to the environmental conditions.

The pilot test provided useful information and suggested that the system was able to collect sensible data with minimal technological difficulty.

6.7 RESULTS 2: COMPARISON OF RIGID AND DYNAMIC SYSTEMS

6.7.1 Project Participants

Table 6.5 Participants data: average and standard deviation of age, weight and testing period on the rigid and dynamic backrest seating systems

Participant	Sex	Age (Year)	Weight (N)	Testing period (hr.min)	
				Rigid	Dynamic
1	Girl	6	186	2.43	2.15
2	Girl	9	195	1.00	1.47
3	Girl	6	196	2.45	2.00
4	Girl	9	171	2.40	2.24
5	Girl	5	137	1.18	2.37
6	Boy	5	154	2.05	1.05
7	Girl	9	262	2.12	2.46
8	Boy	8	174	2.30	2.05
9	Boy	8	141	1.00	2.26
10	Boy	11	255	3.18	3.14
11	Boy	9	214	0.30	3.32
12	Girl	4	175	0.45	2.20
12	**5B, 7G**	**7.43**	**188**	**1.54**	**2.23**
	SD	**2**	**40**	**0.91**	**0.61**

Table 6.5 provides the details of experimental participant. Twelve children, five boys and seven girls, participated in total. The children, each with spastic CP, had an average age of 7 and half years, and weight of 188 N. Participants spent about two hours on the strain gauged Mygo seating on average.

6.7.2 Imparted Force during ADLs

This section summarises the peak and average force data from twelve children into three categories: on the rigid backrest seating, on the dynamic backrest systems and when travelling (e.g. in a minibus) with the rigid backrest system.

The data were collected when participants spent time during ADLs, such as attending the class and activity in the school, eating and travelling. During transportation, children used the rigid backrest system to avoid excessive movement, as recommended by the wheelchair provider, James Leckey Design Ltd. Most of participants did not present extensor spasms when testing. Table 6.6 shows the magnitude of the resultant force on the backrest and footrest of the rigid system, dynamic system and whilst travelling on the rigid system.

Table 6.6 Force magnitudes on the backrest, and left and right footrests

Force (N)	Rigid	Dynamic	Travelling
Backrest			
Average	114	129	126
SD	41	45	42
Peak	647	452	684
Footrest-left			
Average	14	10	13
SD	9	8	13
Peak	347	372	268
Footrest-right			
Average	15	8	9
SD	10	8	13
Peak	477	360	374

All participants were positioned in the midline of the backrest which can be seen from the average COP during the testing session. Figure 6.9 shows COP, on average the distance of COP in y axis on rigid and dynamic seating systems were not more than 0.1 m from the midline. The vertical COP along z axis was in the lumbar area, about 0.13-0.14 m from the seat base.
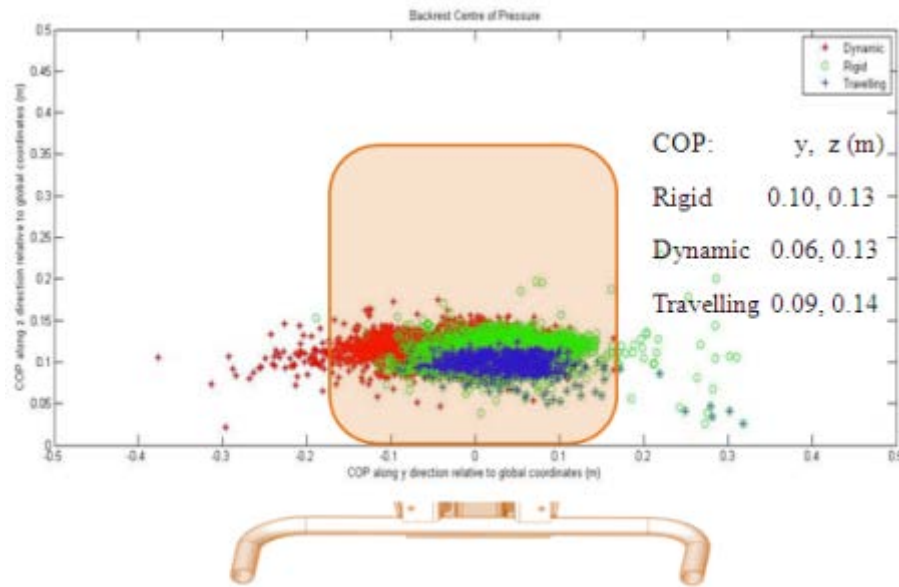
Figure 6.9 Participants COP on the backrest in frontal view

6.7.3 Comparison of the rigid and dynamic systems

On average, the force imparted on the backrest (FB) were similar, around 110-130 N (p = 0.14). The peak force on the rigid system was about 650 N and on the dynamic chair, the peak force was about 450 N. However, the paired t-test showed that these results were not statistically significant probably due to the between-subject variability.

Significant differences did exist between the forces on FA-R between the two seating systems. Overall, average and peak forces on the FA-R were slightly reduced when using the dynamic chair ($p < 0.05$).

Table 6.7 Comparison of imparted forces and moments on the rigid and dynamic backrest systems

Component	Average of force and moment (N, Nm)		P-value	Peak of force and moment (N, Nm)		P-value
	Rigid	Dynamic		Rigid	Dynamic	
Backrest angle (BA)						
Fx	53.82 ± 23.27	59.41 ± 23.44	0.06	325.17	220.87	0.21
Fy	-98.69 ± 90.04	-85.27 ± 134.80	0.74	-725.55	-583.05	0.39
Fz	-22.80 ± 22.12	-32.25 ± 32.21	0.14	-458.50	-356.12	0.78
Mx	8.95 ± 5.62	7.44 ± 8.25	0.48	71.21	55.79	0.12
My	-0.53 ± 1.94	0.31 ± 0.43	0.18	3.67	2.77	0.20
Mz	7.28 ± 5.99	5.68 ± 9.53	0.58	69.56	52.21	0.19
Back tube (BT)	-91.77 ± 40.38	-107.37 ± 47.90	0.19	-692.97	-528.61	0.92
Backrest (FB)	114.21 ± 41.11	128.76 ± 44.99	0.14	646.62	451.95	0.76
COP on y axis (m)	0.10 ± 0.09	0.06 ± 0.16	0.49	-	-	-
COP on z axis (m)	0.13 ± 0.02	0.13 ± 0.02	0.34	-	-	-
Footrest assembly - Left side (FA-L)						
Mx	1.18 ± 0.75	0.77 ± 0.73	0.04*	30.25	31.50	0.38
Mz	-0.98 ± 0.51	-0.79 ± 0.64	0.30	-25.01	-27.51	0.70
Fy	13.56 ± 7.29	9.94 ± 6.17	0.11	346.66	371.52	0.76
Footrest assembly - Right side (FA-R)						
Mx	-1.37 ± 0.88	-0.65 ± 0.72	0.02*	-42.71	-31.04	0.03*
Mz	-1.02 ± 0.85	-0.55 ± 0.45	0.04*	-33.52	-26.30	0.01*
Fy	14.90 ± 10.45	7.52 ± 6.02	0.03*	476.72	360.32	0.04*

Mean ± standard deviation

Force and moment in positive sign meant imparted same direction as the reference system, and negative sign was opposited

Axial force (Fy), positive sign meant the tension, and positive sign meant the compression

* $P < 0.05$ meant force on the rigid system was more than the dynamic system

124
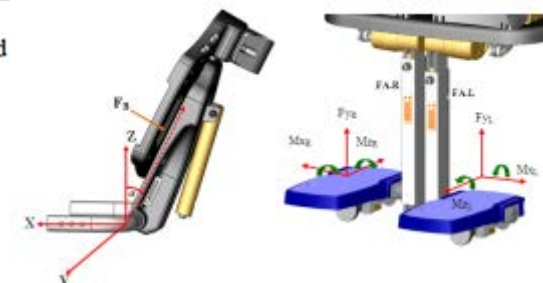
The data show that the children imparted asymmetric forces on the footrests. The use of the rigid seating system showed that children applied more force on the right side of footrest as can be seen clearly from the peak force. Whereas, the forces exerted on the left and right footrests were equal when using the dynamic seating system. A possible explanation for this might be that most participants were right-side dominant, which may explain the increased forces in the right footrest compared to the left. However, when using the dynamic seating system, the deformation of the chair, in terms of the reclining of the seat under load, may be responsible for reducing the right-sided forces.

6.7.4 Normalised Wheelchair Forces

Since the participants were different ages and weights, and genders, their physical statures varied. Therefore it was decided to analyse normalised data, in which the data were normalised with respect to bodyweight. In undertaking this normalisation, it is assumed that body strength varies linearly with body mass. Normalisation is important so that we can compare the results from a 4 year old with those of a 10 year old. Clearly a 10 year old will impart greater forces on the wheelchair than the 4 year old and it is hoped that normalisation will decrease the between-subjects variability associated with the ability to impart different levels of force on the chassis. Therefore, the differences between the two systems should be more readily ascertained.

The normalised forces were similar for each child suggesting this is a valid approach. The normalised forces which are shown in Table 6.8 can be used to estimate the imparted force by children on their own seating. The normalised of average force on the backrest was 0.6 times children's weight (BW) when using the rigid system and 0.7 BW when using the dynamic system. The normalised of peak forces were up to 3.5 BW on the rigid backrest system and 2.5 BW on the dynamic backrest system.

Table 6.8 Normalised forces imparted on each part of the seating

Force on wheelchair	Average						Peak	
	Rigid			Dynamic			Rigid	Dynamic
Force on backrest (FB)	0.60	$\pm$	0.20	0.69	$\pm$	0.24	2.54	2.52
Shear on the seat (Fx)	0.28	$\pm$	0.12	0.32	$\pm$	0.13	1.27	1.18
Shear on the backrest (Fz)	-0.13	$\pm$	0.11	-0.18	$\pm$	0.18	-1.80	-1.70
Perpendicular force (BT)	-0.49	$\pm$	0.20	-0.58	$\pm$	0.26	-2.72	-2.68
Force on left footrest (FA-L)	0.07	$\pm$	0.04	0.05	$\pm$	0.03	1.84	1.98
Force on right footrest (FA-R)	0.08	$\pm$	0.06	0.04	$\pm$	0.03	2.54	1.92
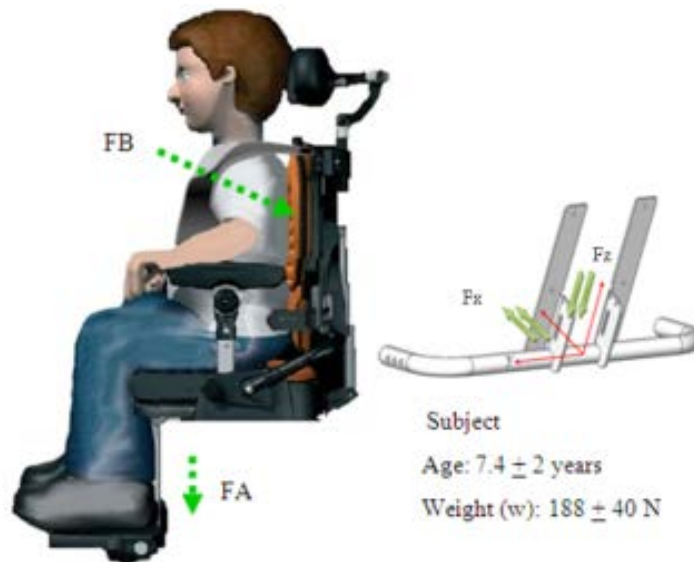
Figure 6.10 Direction of force on backrest (FB) and shear force on backrest angle tube assembly (BA) of the rigid and dynamic backrest system

Average tensile forces on the FA-L were similar in two seating systems, about 0.05-0.08 BW. But the peak force at the right side was 2.5 BW while the left side was lesser, 1.8 BW.

No statistical differences were found in the normalised forces and moments between each configuration.

6.7.5 Force Data for Gas Spring Selection

The rigid back strut is replaced by a gas spring allowing some flexibility in the movement of the backrest (Figure 6.11) in the dynamic seating configuration. The company provides three different sizes of gas spring: 50, 100 and 150 N which may be varied depending on the weight and the extensor thrust of each user.
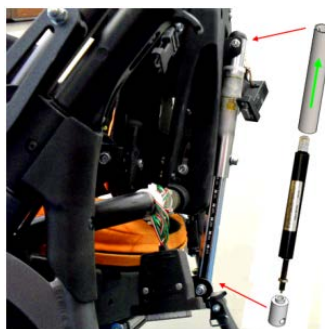
Figure 6.11 Dynamic components on the backrest

The study on the dynamic backrest system not only found the forces and moments on the dynamic seating system but also directly on the gas spring. These data will be used to consider the suitable size of gas spring for such users.

Figure 6.12 depicts the force acting on the gas spring base (GB) which represented the magnitude of force acting on the gas spring. Positive values indicate tension and negative values denote compression forces. Figure 6.13 shows the resultant of applied force after normalised by child's weight. On average 50 percent of the bodyweight is imparted on the gas spring (GB) and therefore the suitable size of gas spring for each user is able to be determined. More precisely, the peak applied force or severity of the extensor spasm should be used for this decision. The gas spring will be too soft for the user if its threshold force is less than the average imparted force. In this situation, the backrest will not able to bring the user back to the original position when a spasm has ceased. Also, the spring can be excessively stiff: if the resistance force threshold is more than the peak force when user performed the extensor thrust, then little movement, and thus potential benefit, will be seen.

Subject No.	1	2	3	4	5	6	7	8	9	10	11	12	Mean
■ Average	-94	-149	-150	-82	-36	-55	-66	-101	-156	-109	-201	-91	-107.
■ Peak	-220	-233	-295	-206	-116	-152	-336	-291	-380	-530	-499	-199	-287.
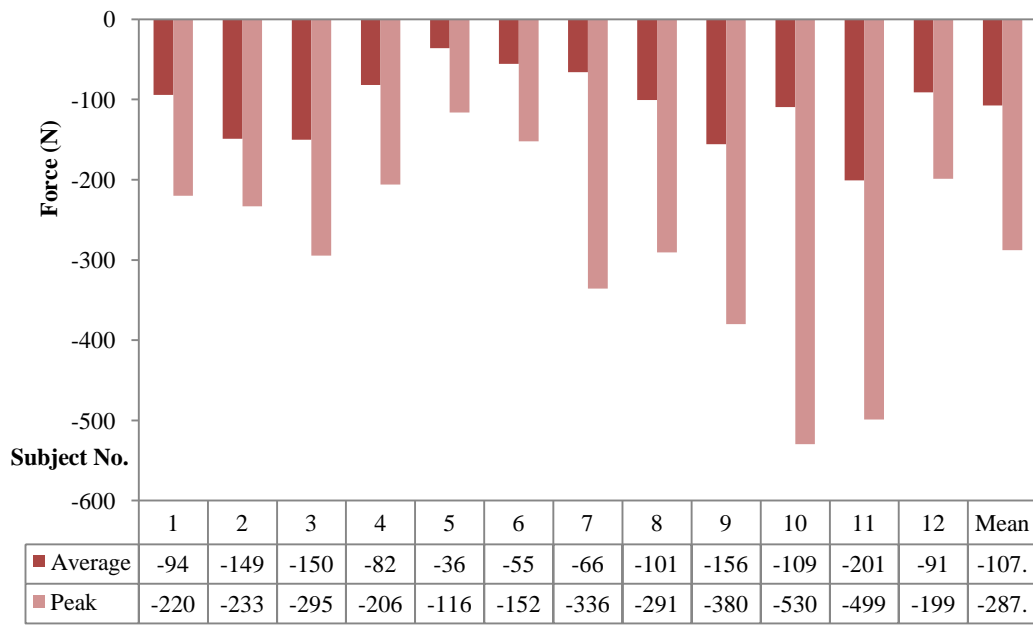
Figure 6.12 Imparted force on the gas spring base by all participants (N)
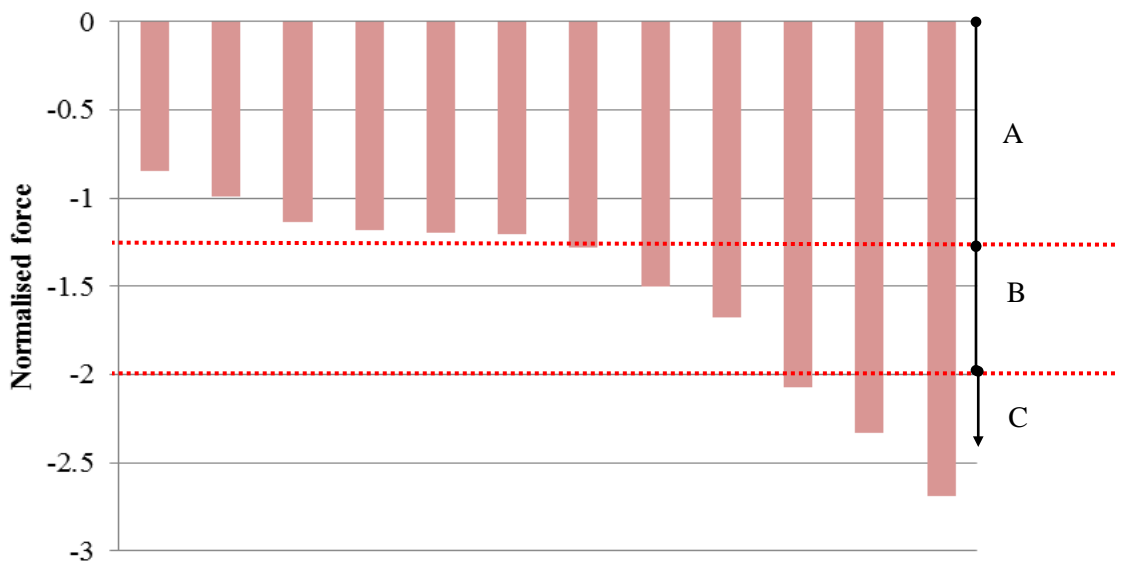
Figure 6.13 Normalised peak force on the gas spring base ranked
by increasing force (N/BW)

128

It is proposed that children could be divided into three groups by their maximum applied forces:

- A: Children who imparted force a force on the GB less than 1.25 times their weight are identified as a mild group
- B: Children who had extensor force between 1.25-2 times their weight are moderate
- C: Severe extensor group is described by children who impart a force greater than double their body weight

These findings suggest that, in general, a prescriber should consider a size of gas spring about 0.5 times the weight of the child, and 0.75 times bodyweight if the child experiences severe extensor spasms.

6.8   RESULTS 3: A CASE STUDY

This section reports the results from one individual who exhibited the highest forces on the Mygo. This individual is focussed upon, since he may be representative of those that might benefit the most from dynamic seating.

6.8.1 Participant

An eleven year old boy of 255 N bodyweight required a chair with 90 degrees of back angle and 10 degrees of tilt-in-space. He exhibited typical characteristics of a child with CP and experiences severe extensor spasms. He had a history of extensor spasms to such a severe extent that it has previously resulted in components of the Mygo wheelchair to either deform or break. As expected, he generated significantly high forces on the backrest and footrest when testing. Also his results were interesting, as the contact forces on the backrest apparently reduced when he used the dynamic seating system. Therefore his results will be considered separately in this section to show evidence of potential advantages that he and other such users could obtain from a dynamic system.

The test was conducted for about 6 hours and 32 minutes. In the morning, he sat on the dynamic backrest system for 3 hours and 14 minutes and then on rigid system in the afternoon for 3 hours and 18 minutes. He experienced extensor spasms during both sessions and more often when he was interacted with activities such as singing a song, games, and when attempted to communicate with teachers and friends.

Table 6.9 Participant details

Sex	Age (Year)	Weight (N)	Testing period (hr.min)	
			Rigid	Dynamic
B	11	255	3.18	3.14

6.8.2 Imparted Forces on the Rigid System

As explained in chapter 3, strain data from the DAQ were converted to forces and moments using a full calibration matrix. Table 6.10 shows the strain data from 12 channels of DAQ of the backrest, BA1 measured from the left side of BA and BA2 measured the right side of BA. The reference system of both sides is shown in Figure 6.14.

Strain data were multiply by the coefficient matrix, which was identified in chapter 4, to estimate the forces and moments acting on BA1 and BA2 as shown in Table 6.11. These forces and moments were used to calculate the resultant force and moment on the BA. These calculations were conducted by MATLAB, with the script of the calculation, and example of data, shown in Appendix B.

Table 6.10 Strain data from 12 channels of BA1 and BA2

	BA1			BA2		
Signal	**Fx1**	**Fy1**	**Fz1**	**Fx2**	**Fy2**	**Fz2**
Average	5.95	-0.93	-6.16	5.72	0.21	-3.35
Peak	25.64	-5.43	-41.34	24.70	5.39	-28.48

	BA1			BA2		
Signal	**Mx1**	**My1**	**Mz1**	**Mx2**	**My2**	**Mz2**
Average	-52.91	0.04	-104.60	24.37	1.20	106.80
Peak	-275.40	0.10	-354.80	168.70	9.81	430.00

Table 6.11 Forces and moments after converted by coefficient matrices

Force	BA1			BA2		
(N)	**Fx1**	**Fy1**	**Fz1**	**Fx2**	**Fy2**	**Fz2**
Average	72.66	-154.79	-89.85	-0.41	-396.61	37.57
Peak	305.21	-587.43	-452.31	-45.39	-1302.29	163.26

Moment	BA1			BA2		
(Nm)	**Mx1**	**My1**	**Mz1**	**Mx2**	**My2**	**Mz2**
Average	2.20	0.14	-5.25	17.66	1.62	22.47
Peak	11.90	0.57	-12.78	59.31	6.78	79.70

Table 6.12 Resultant forces and moments on BA

Force				BA		
(N)	**Fx**	**Fy**	**Fz**	**Mx**	**My**	**Mz**
Average	72.26	-241.82	-52.28	19.85	0.88	17.22
Peak	325.17	-725.55	-458.50	71.21	3.67	69.56

*Fx, Fz, Mx, My, Mx: positive number means force imparted same direction
of the global system, negative number means opposite direction.
Fy: positive means tension, negative means compression force*
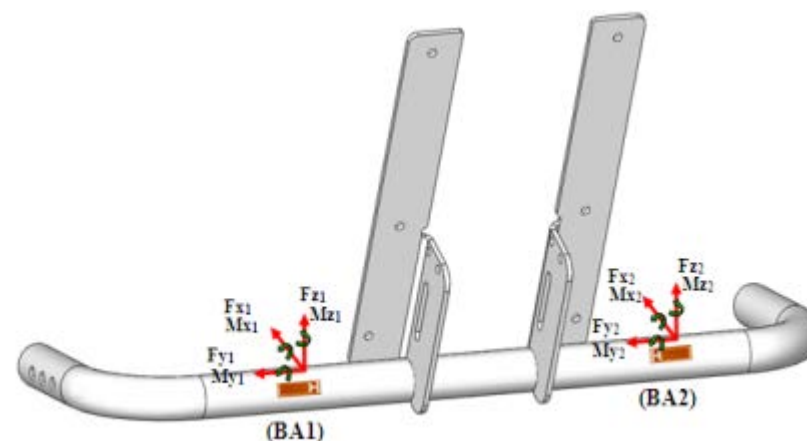
Figure 6.14 Measured positions, BA1 and BA2 on BA

Table 6.13 Strain data from a channel of BT

Signal	BT	
	Fy	My
Average	16.80	-2.89
Peak	68.58	-18.69

Table 6.14 Forces and moments after converted by coefficient matrices

Force	BT	
(N)	Fy	My
Average	-169.81	-0.17
Peak	-692.97	-1.01

Figure 6.15 Measured position on BT

Fy: positive means tension, negative means compression force
My: positive number means force imparted same direction
of the global system, negative number means opposite direction.

132

6.8.3 Imparted Forces on the Dynamic System

Table 6.15 Strain data from 12 channels of BA1 and BA2

Signal	BA1			BA2		
	Fx1	Fy1	Fz1	Fx2	Fy2	Fz2
Average	3.83	-1.32	-3.53	4.49	-0.89	-1.17
Peak	18.65	-5.16	-31.37	17.94	-4.42	-20.95

Signal	BA1			BA2		
	Mx1	My1	Mz1	Mx2	My2	Mz2
Average	-26.76	0.12	-63.86	9.36	0.36	60.63
Peak	-206.70	0.21	-274.40	120.70	7.63	301.40

Table 6.16 Forces and moments after converted by coefficient matrices

Force	BA1			BA2		
(N)	Fx1	Fy1	Fz1	Fx2	Fy2	Fz2
Average	45.95	-113.33	-51.91	17.98	-229.99	23.65
Peak	226.40	-500.95	-370.37	54.97	-1053.56	118.80

Moment	BA1			BA2		
(Nm)	Mx1	My1	Mz1	Mx2	My2	Mz2
Average	1.67	0.09	-2.80	8.64	0.70	10.24
Peak	11.06	0.52	-14.69	45.94	5.14	59.90

Table 6.17 Resultant forces and moments on BA

Force	BA					
(N)	Fx	Fy	Fz	Mx	My	Mz
Average	63.93	-116.66	-28.26	10.31	0.40	7.45
Peak	220.87	-583.05	-356.12	57.00	2.77	52.10

Fx, Fz, Mx, My, Mx: positive number means force imparted same direction
of the global system, negative number means opposite direction.
Fy: positive means tension, negative mean compression force
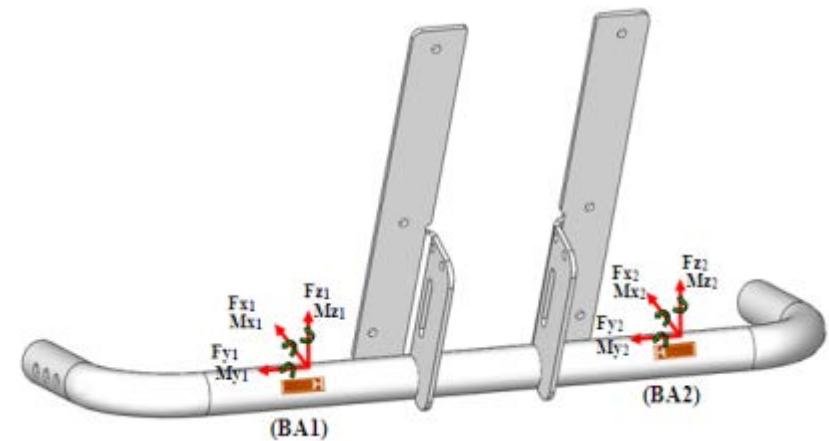
Figure 6.16 Measured positions, BA1 and BA2 on BA

Table 6.18 Strain data from a channel of BT

	GB
Signal	**Fy**
Average	3.69
Peak	17.90

Figure 6.17 Measured position on GB

Table 6.19 Forces and moments after converted by coefficient matrices

Force	**GB**
(N)	**Fy**
Average	-109.28
Peak	-529.65

Fy: positive means tension, negative means compression force

6.8.4 Comparison of Force on the Rigid and Dynamic Systems

With this one individual, there is strong evidence of a load reduction on the backrest when using the dynamic backrest system compared to the rigid system. The average force imparted on the backrest reduced by about 25 percent and the peak force also reduced approximately 30 percent when using the dynamic chair.
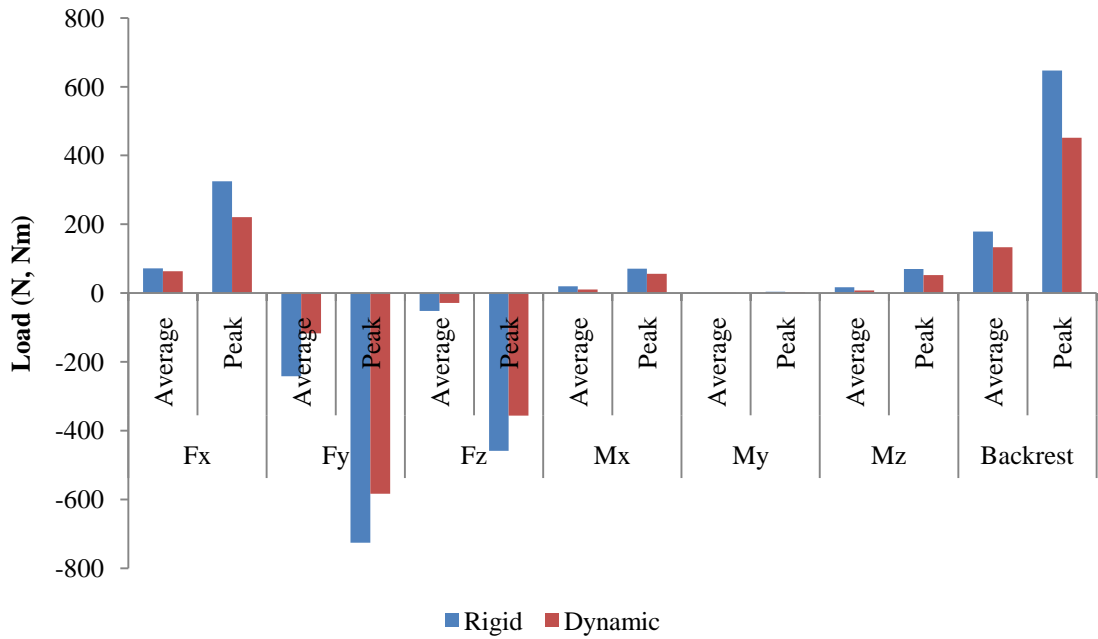
Figure 6.18 Comparison of forces and moments in six DOF at the backrest
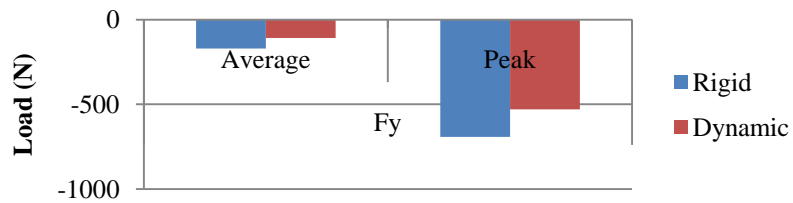
Figure 6.19 Comparison of compression forces at the backrest supports

Table 6.20 Comparison of reducing force and moment on the backrest

BA

	Fx		Fy		Fz		Mx		My		Mz	
	Average	**Peak**	**Average**	**Peak**	**Average**	**Peak**	**Average**	**Peak**	**Average**	**Peak**	**Average**	**Peak**
Rigid (N)	72.26	325.17	-241.82	-725.55	-52.28	-458.50	19.85	71.21	0.88	3.67	17.22	69.56
Dynamic (N)	63.93	220.87	-116.66	-583.05	-28.26	-356.12	10.31	57.00	0.40	2.77	7.45	52.10
Reducing force (N)	8.33	104.30	125.16	142.50	24.02	102.38	9.55	14.21	0.48	0.90	9.77	17.46
Percent of reduction	12%	32%	52%	20%	46%	22%	48%	20%	55%	25%	57%	25%

BT

	Average	Peak
Rigid (N)	-169.81	-692.97
Dynamic (N)	-109.28	-529.65
Reducing force (N)	60.53	163.33
Percent of reduction	36%	24%

Summation of force on the backrest

	Average	Peak
Rigid (N)	178.50	646.60
Dynamic (N)	133.60	452.60
Reducing force (N)	44.90	194.00
Percent of reduction	25%	30%

Figure 6.19 shows that, compared to the rigid backrest system, the force when using the dynamic system slightly decreased on the BT and GB. The average force reduced by about 35 percent, and the peak force reduced 25 percent approximately.

Table 6.20 summarises the forces and moments data on BA, BT and the resultant average and peak forces on the backrest in the two backrest systems. This table clearly shows the reduction in force observed on the dynamic backrest system compared to the rigid. However, since this is a case study, no statistical analysis can be performed other than descriptive statistics.

The average COP was oriented to the left side of the back rest; from which it can be inferred that most of the time the child leaned his trunk to left side or tilt to left lateral support. Interestingly, especially with the rigid system, there seems to be 3 clusters of COP, potentially inferring 3 preferred postures on the seat. Thus this user may shift his body periodically to relieve and change the position of the contact pressures when using the rigid system. However, these clusters are not so visible on the dynamic seat, potentially implying that the deformations afforded by the chair provide more continuous postural adjustments, possibly reducing the annoyance of high contact pressures being concentrated in specific places.

	Average	
	Y	Z
Rigid	0.11	0.12
Dynamic	0.21	0.14
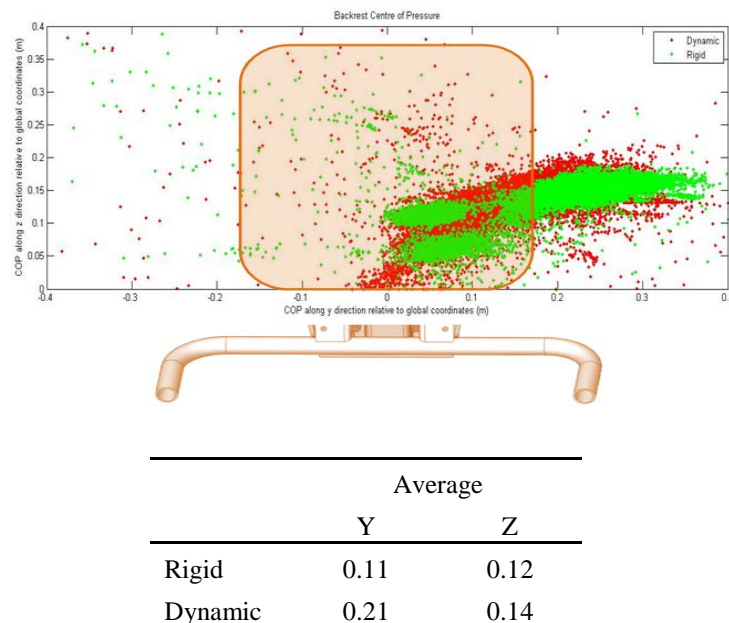
Figure 6.20 Average and peak COP on the rigid and dynamic backrest systems
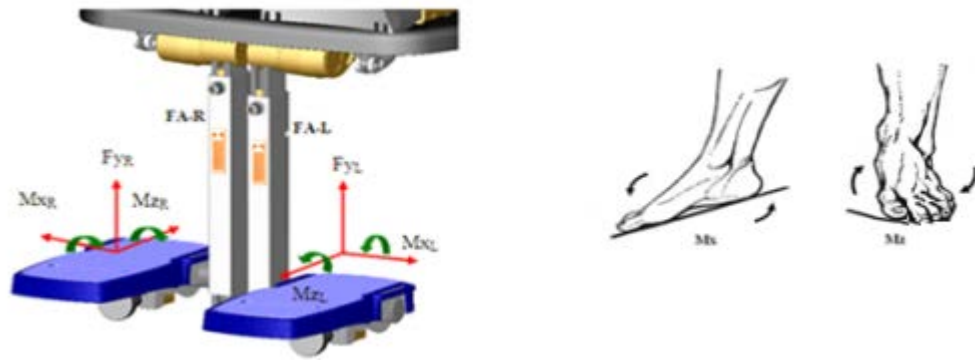
Figure 6.21 Schematic diagram of footrest and direction of imparted forces
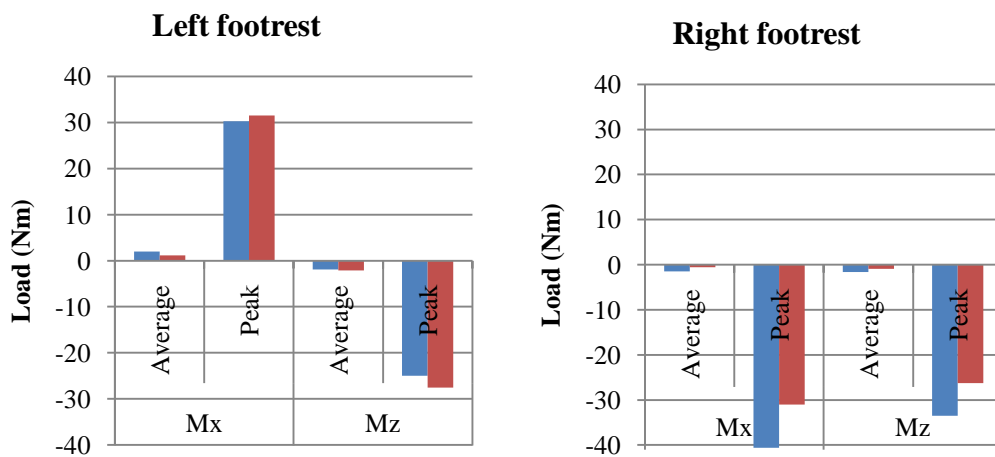
Figure 6.22 Comparison of moments at the footrest
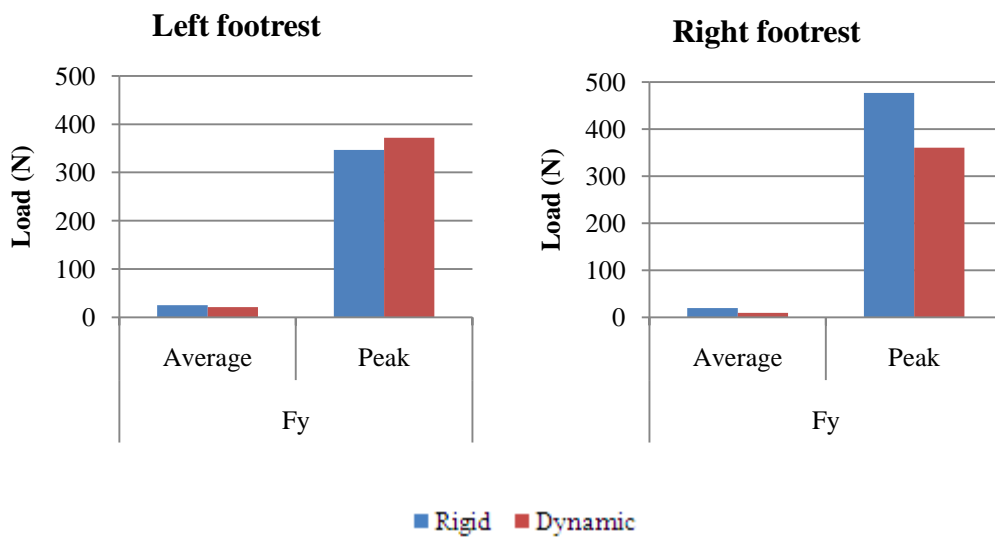
Figure 6.23 Comparison of force at the footrest

The forces and moments on the footrest show that the dynamic chassis exhibits reduced forces and moments on the right footrest, whilst the left footrest showed (smaller) increased forces compared to the rigid (Figure 6.22). This could mean that the individual is more balanced, or shares foot forces more equally, on the dynamic system compared to the rigid chassis.

6.8.5 Evidence of Extensor Spasms
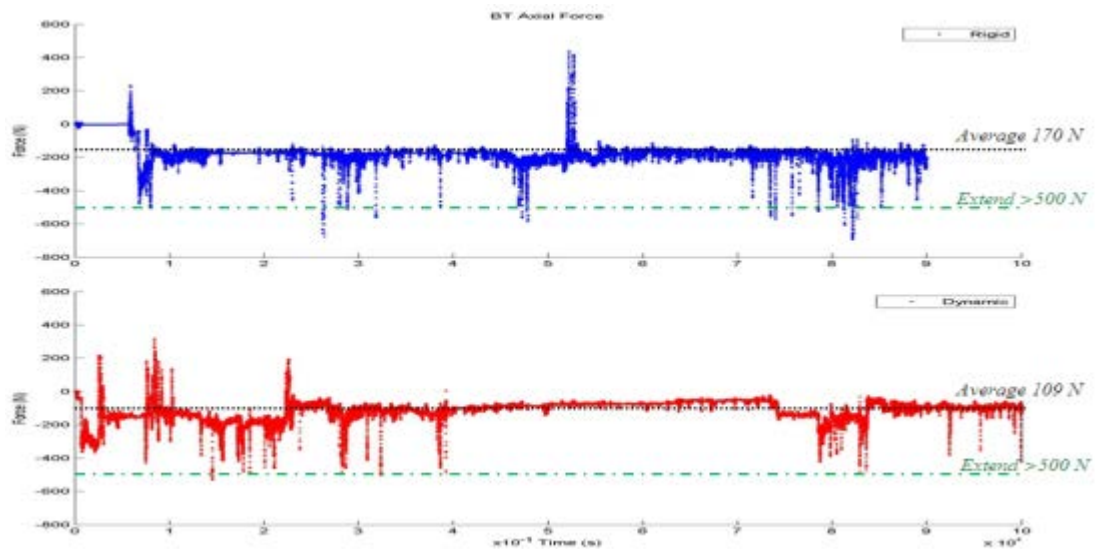
Force on back tube/ gas spring base	Average		Peak	
	Rigid	Dynamic	Rigid	Dynamic
Axial force (N)	-170	-109	-693	-530
Normalised force (N/BW)	0.67	0.43	2.72	2.08

Figure 6.24 Forces on the back tube (BT) and gas spring base (GB) and table of loading data which normalised by child weight

Figure 6.24 shows the comparison of force data obtained from the back tube (BT) on the rigid backrest seating system (blue line) and from the gas spring base (GB) of the dynamic backrest system (red line). Positive values of BT or GB represent a tension force and negative values denote a compression force on the component. On average the forces imparted were 170 N and 109 N on the rigid and dynamic systems, respectively. The peak force on the rigid system was 693 N whilst the force on the GB (dynamic component) peaked at 530 N.

The enlarged graphs in Figure 6.25 show an expanded view of one of the peak forces associated with a strong extensor spasm. The force was nearly to two times of his bodyweight: about 500 N on the rigid backrest system and 400 N on the dynamic backrest system. The frequency of extensions was similar in both the rigid and dynamic backrest systems, about five times per hour. In view of the duration of the spasm, each episode lasted about 7-8 seconds. Comparing data of both seating systems, it is apparent that, qualitatively, the dynamic seating systems did not reduce the frequency or duration of the extensor spasms.
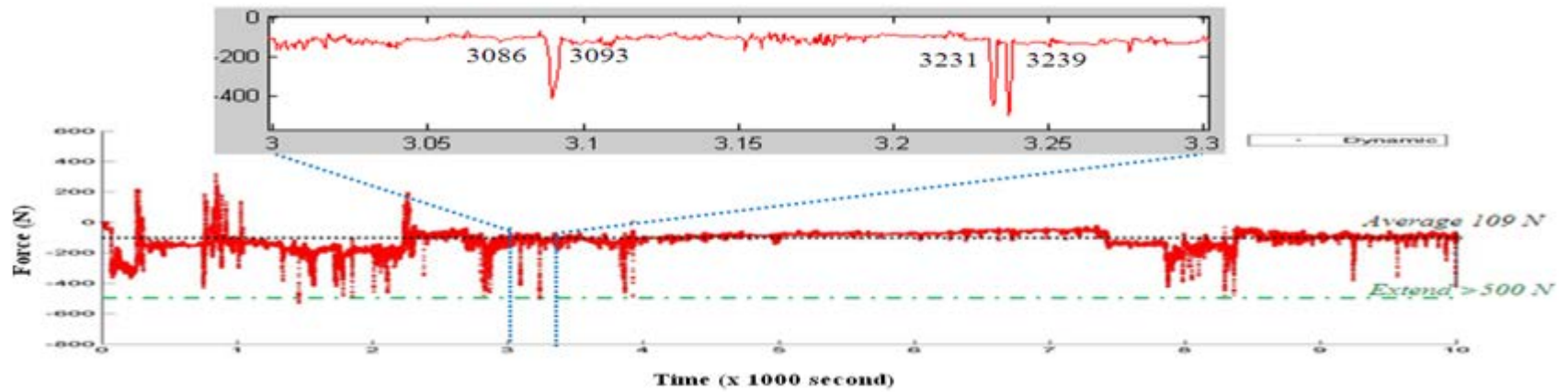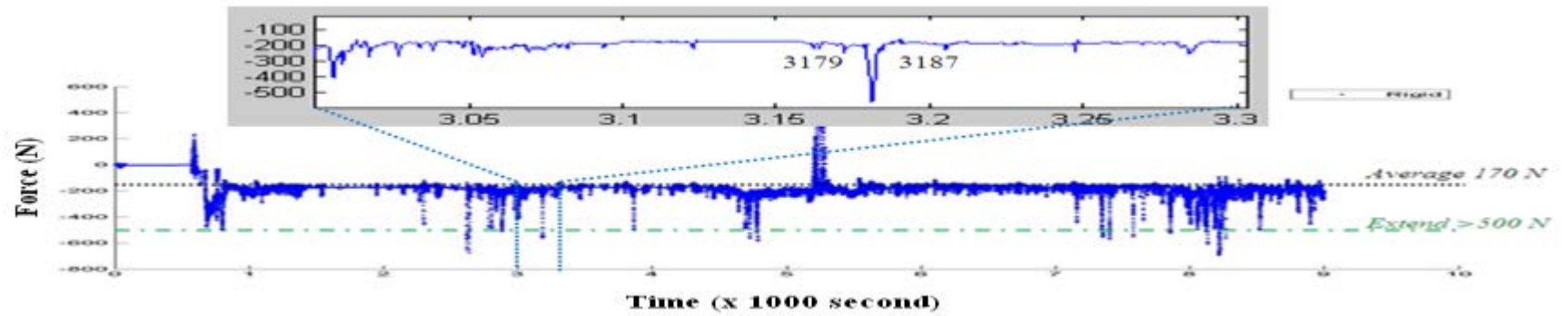
Figure 6.25 Expanding of sharp raised forces on BT

6.9   STRESS ANALYSIS OF COMPONENTS

This section illustrates the stresses on the chassis components as a result of using the stress analysis method detailed in chapter 3. The average and peak stress values of components when sitting on rigid and dynamic backrest seating and travelling on the bus are shown in Table 6.21.
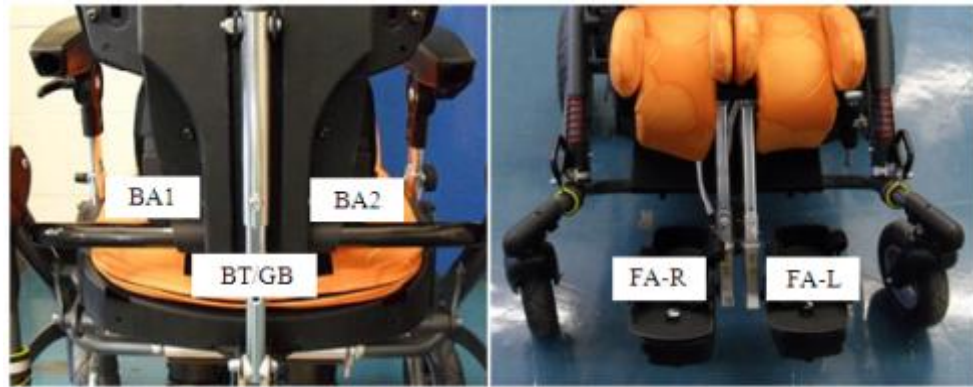
Figure 6.26 Critical components on the chair

Table 6.21 Average and peak stress on components

Component	Applied stress (MPa)					
	Average			**Peak**		
	Rigid	**Dynamic**	**Travelling**	**Rigid**	**Dynamic**	**Travelling**
BA1	75.11	73.57	110.17	223.33	203.89	283.90
BA2	21.88	32.34	22.37	80.02	90.57	53.12
BT/GB	0.87	1.02	0.89	2.75	2.73	2.94
FA-L	0.99	0.86	0.62	25	28	22
FA-R	1.84	0.97	1.15	60	46	49

The von Mises stresses on both sides of the BA were separately determined. Average stresses were less than the steel yield stress of 250 MPa, however peak stresses were high almost reaching the yield stress particularly on BA1. These peaks

occurred when the children extended their bodies, which averaged less than five times per hour. Moreover, this load is much lower that the fatigue limit of steel.

The S-N diagram in Figure 6.27, depicts the total number of repetitive loading cycles (N_f) at different stress amplitudes that steel and aluminium can experience before failure. It is clear by comparing the data tabulated in Table 6.21 that fatigue failure is unlikely to occur for the components, since the peak stresses in the steel are below the fatigue limit, and N_f for the aluminium footrests will be $> 10^{10}$.
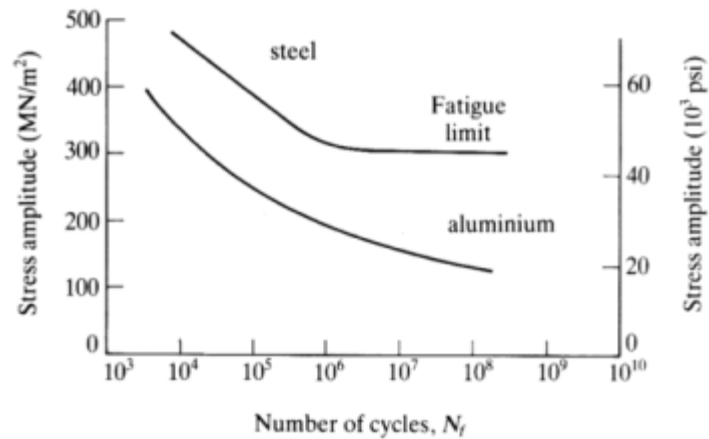
Figure 6.27 S-N curves for steel and aluminium (http://www.efunda.com)

Compared to the S-N curves, the tensile stresses on the backrest angle tube (BT) and gas spring base (GB), which are aluminium, were significantly smaller than on the BA. The stresses on the foot supports (FA-L and FA-R) were also insignificant when compared to the yield stress of aluminium, 276 MPa. However, these components were assembled with other parts which may be able to yield from the applied stress, especially in areas of stress concentrations.

6.10   DISCUSSION AND CONCLUSION

The difficulty of recruiting and working with this population should not be underestimated. Understandably the parents and children have not had an easy past few years and many were reluctant to volunteer. Moreover, obtaining ethical approval to work with such a population demanded thought and consideration over and above that which is required for a normal, healthy population. Population identification, recruitment, consent and testing all had their challenges to overcome. Recruitment of twelve participants for the main study, out of less than thirty potential participants is testament to the sensitivity of the recruiters WESTmarc and James Leckey Design Ltd.).

Initially, the investigation period was a year, from October 2010 - August 2011. Due to the research population being in a specific and small group, the recruitment process was time-consuming work. Furthermore difficulties were encountered in the management of the participants, their physiotherapists, teachers and researchers. Also most participants preferred that the study took place at their school or nursery school thus permission from those places were required, as well as the need to halt the test during school holidays. For these reasons, the investigation period needed to be asked for three extensions since 2010 until finished in 2012.

6.10.1 Project Participants

During the testing periods, participants were mostly in sitting positions and did not have much activity and movement on their chairs. Therefore results were not easily separated by participants' activity. The imparted forces and moments were therefore summarised using averages and peaks throughout a day.

Contrary to expectations, results from twelve children with CP did not find a significant difference between rigid and dynamic backrest systems. On average, the magnitudes of forces on backrest were 114 N and 129 N. The maximum forces were up to 650 N and 450 N on the rigid and dynamic systems respectively. These peak forces seemed to decrease on the dynamic system, however, these differences were not significant ($p = 0.76$), due to the large between-subject variability.

In terms of the normalised force on the Mygo seating systems, it is interesting to note that all twelve children had similar force, as a proportion of their bodyweight, on the backrest and footrest. In conclusion, the average force on the backrest was 0.6-0.7 BW, with 0.1-0.4 BW downward on each footrest. These can be used to approximate the applied forces by the weight of the children in future wheelchair designs. The peak forces were passed up to 3.5 BW or 650 N on the backrest and 2.5 BW or 450 N on the footrest during a strong extensor spasm, also useful for design purposes. This result also accords with the earlier observation, which showed that the peak force on the backrest was 1050 N, or about 3.5 BW, when testing with children with a mean age of 10.5 years (Brown et al., 2001).

Sitting balance is well described by measuring the COP, as it can inform as to the direction in which the body sways and is useful for positioning management. In this study, participants were well positioned (i.e. balanced) even when exerting extensor force. The horizontal COP was found at 0.06-0.10 m left side from the midline and vertical COP was 0.13 m above the seat. It seems possible that these results were due to the fact that most of participants had a right-sided dominance. Again, there was no significant difference of COP locus between the two seating systems. Further analysis of the COP showed that sitting on the dynamic system had a larger lateral swing than the rigid system, -0.1 m and 0.22 m from average point, respectively. The present findings seem to be consistent with another research which found the change of back angle in reclining did not result in a significant change in COP. But the largest effect on COP was observed during pelvis rotations when tilting the seat (van Geffen et al., 2008).

6.10.2 A case study

In contrast to earlier findings from 12 participants, a noticeable and consistent reduction in contact force was detected in the case of a boy who experienced severe extensor spasms. The child presented in the case study exhibited frequent extensor spasms during testing while most of the other participants did not. Results from this boy showed the forces and moments on the backrest were consistently decreased when using the dynamic backrest system. The results of this boy corroborate the findings of previous work that compared the force between rigid and dynamic

seating systems only when participants generated extensor spasms (Cimolin et al., 2009).

As discussed in section 4.6, there might be a considerable error with the Fy data: the axial force on back angle tube, BA, due to the effect of large crosstalk in calibration matrix. However, the data was still useful for comparative purposes, since no adjustment had been made between the two backrest systems, thus the difference in force can be estimated with a degree of confidence.

6.10.3 Gas spring selection

The dynamic mechanism enabled the backrest to adopt reclining positions providing more space and more range of motion in the chair when children extended their bodies. This motion was accompanied by a significant reduction in peak force and bending moment on the right footrest, which was the dominant side of most participants.

As mentioned in chapter 5, at the full stroke length the gas spring could be compressed up to maximum of 60 mm, equivalent to a recline of 20 degrees from original position. If the user requires more backrest recline, the gas spring can be shortened to provide a suitable position. The decrease of gas spring's stroke length reduces the travel range of backrest. If the user still exerted force on the backrest when the travel range of gas spring was ended, the dynamic backrest would behave like the rigid backrest system. This issue need to be taken into consideration when prescribing a dynamic backrest system, especially to those with strong extensor spasms who may benefit from a wide range reclining backrest.

When the gas spring is in the locked position, the stiffness of the gas spring plays an important role in providing the movement of the backrest after the threshold force had been reached. The evidence from this study showed the problem when an inappropriate size of gas spring was chosen. If a small sized gas spring was chosen for a child who had more weight or had strong extensor spasms, the backrest was easily reclined until the maximum travel length was achieved and the pressure in the spring was not sufficient to bring the child back to the upright position when extensor spasm had been stopped. Furthermore, an excessive range of backward

movement made the child uncomfortable and lead to unnecessary spasms. It is therefore recommended that to select the gas spring size for use in the dynamic backrest system one needs to determine the potential maximum force that will be applied on the backrest. Alternatively, an iterative process in which the most appropriate size of gas spring is finally determined through trial and error over a period of a day or two.

One unanticipated finding from working with this this sample of children was that most of them required some space at the back of the chair to put their enteral feeding pump backpack and personal belongings which weigh about 1-2 kg. The enteral feeding bag, which was typically hung from the backrest as the tube was not long enough to put under the seat, was found to interact and potentially affect the backrest angle and the positioning support when hanging on dynamic backrest system. Future designs may wish to consider this need and design an appropriate location away from dynamic components, attached to the rigid part of the chassis.

CHAPTER 7
LONGITUDINAL CASE STUDY OF THE FUNCTIONAL EFFECT OF A DYNAMIC COMPONENT

7.1   INTRODUCTION

The objective of the study was to understand the interaction of the Mygo dynamic backrest seating system with a user during daily living activities and to investigate the effect on the quality of movement over a long period of use. In particular, the smoothness of upper limb motion would be an indication of improve function.

The study protocol was approved by the University Ethics Committee – University of Strathclyde (UEC). The protocol involved monthly sessions of laboratory-based motion analysis together with a qualitative assessment of any quality of life or functional skill changes as assessed by asking the primary caregiver.

7.2   PARTICIPANT

A single participant was recruited from the population of children with CP who participated in our previous research (Chapter 6). Invitation letters were written to all potential participants; the pack included the participant information sheet (PIS) and consent form for the parent. The PIS had details of the inclusion and exclusion criteria for the participants, so that the parent could assess their child and confirmed that both inclusion and exclusion criteria were adhered to.

After all letters were sent to the prospective participants, difficulties were encountered in recruiting participants for the long term of the testing. Consequently, only one informed consent form was returned. The volunteering participant was a six years old girl who did not have any plans of undergoing surgery for the current condition within the period of the following six months.

7.3   STUDY WHEELCHAIR AND GAS SPRING

The participant used her own chair on which was attached a gas spring on the backrest tube enabling a dynamic system. Three sizes, 50, 100 and 150 N of gas springs (Bansbach, Germany) were considered to fit in the child's chair. In this case, considering the factors of her weight and her severity of extensor spasms, the 50 N gas spring was chosen to replace the rigid manual backrest adjustment tube.

7.4   TEST PROCEDURE

The child and parent were asked to attend the Biomechanics laboratory based testing every month throughout the six month study period in the Biomedical Engineering Department, University of Strathclyde, Glasgow. Monthly assessments were carried out on the first Friday of every month, according to the preference of the participant's parents. The monthly assessments consisted of two parts. Firstly a motion analysis assessment of participant's movement was conducted and secondly a qualitative assessment of using the dynamic backrest system by child's parents.

On the first day, after the gas spring was integrated into the backrest of the participant's chair, enabling the dynamic backrest system, the participant was transferred to it and minor adjustments were made, done by her parents. She had a few minutes to get familiar with the new backrest system before some motion capturing data were recorded.

7.4.1 Motion Analysis

- *Motion capture*

A twelve-camera Vicon MX system (Vicon – UK, 14 Minns Business Park, West Way, Oxford OX2 0JB, UK), using infrared cameras (six T40 and six T60), was used for kinematic data capturing at a frequency of 100 Hz. The marker trajectories were reconstructed and labelled in Vicon NEXUS (Version 1.8.2). Before capturing data from the Vicon system, the capture volume was calibrated with a five marker wand Figure 7.1. This calibration wand was waved within the intended area of the twelve cameras to ensure that all markers on the wand were captured by all cameras, and a static calibration determined the global coordinate system.

Figure 7.1 A five marker wand

The testing area in the Motion Analysis Laboratory was arranged to be a child friendly as possible with appropriate furniture and entertainment provided. Parents were asked to transfer the child into and out of the chair, and stay around during testing period.

- *Marker set*

Two 25 millimetre diameter retro-reflective spherical markers were attached to the wheelchair and three of 14 millimetre diameter markers were attached to the child, as can be seen in Figure 7.2. Hook and loop tape was fastened on to her wrists for the markers to be put on, and a hair band was used to put marker on her head. Furthermore the two other markers were attached to both sides of the wheelchair handle to create the medial-lateral direction of a local reference system; where the x direction is perpendicular to the frontal plane of the user, the y direction is perpendicular to the sagittal plane and the z direction is vertical. The markers on the wheelchair were defined to ensure that the motion of the chair was captured as the child's extensor spasm could cause the wheelchair to move about during an extensor spasm.

Figure 7.2 Three markers placed on the child to track the moving position of head and wrists, and two markers on the wheelchair for a local reference system

- *Testing task*

Unfortunately the volunteered child could not perform any voluntary movement, and so the movement was assessed as she sat still on her chair (Figure 7.3). The motion of her head and wrists was tracked when she was watching three videos (three tasks). The first video was 'Animal sounds', 2.25 minutes; the second video was a more interactive song, 'If you are happy and you know it', 2.20 minutes and the final video was a cartoon, 'Peppa Pig', 5 minutes. No voluntary movement was required while the test was in progress, which took about 10 minutes in total.

Figure 7.3 Laboratory set up: participant was sitting on the Mygo
seating system and parents was in the same room

This procedure was not the ideal test protocol. It was hoped that voluntary movement would be assessed when participant was encouraged to move to touch the signs or play with toys as shown in Figure 7.4, but this was not possible due to the severity of the individual's CP.

Figure 7.4 Colour marks on left and right hand side on the wheelchair table

- *Data analysis*

Once testing was completed, kinematic data were exported from Vicon Nexus as an ASCII file. Using MATLAB (version 7.12.0.635 R2011a) the kinematic data were uploaded, and a low pass filter using a 4th order Butterworth filter with a 6 Hz cut off frequency as recommended in the Biomechanics of human movement was used (Winter, 1979). All voluntary and involuntary movement was assumed to be belowe this frequency, and therefore the higher frequency experimental noise would be removed by this filter. The trajectories were then differentiated (Winter, 2009) using the MATLAB gradient function to give velocity, acceleration and jerk respectively.

To get the velocity, v at the r direction, can be differentiate with respect to time,

$$v = \frac{dr}{dt}$$
<div align="right">Equation (7.1)</div>

Similarly, the acceleration is,

$$a = \frac{dv}{dt} = \frac{d^2r}{dt^2}$$
<div align="right">Equation (7.2)</div>

Then the third derivative of r is the jerk,

$$j = \frac{da}{dt} = \frac{d^2v}{dt^2} = \frac{d^3r}{dt^3}$$
<div align="right">Equation (7.3)</div>

Where,

r is the position vector of the maker

t is the time (s)

v is the velocity (m/s)

a is the acceleration (m/s^2)

j is the jerk (m/s^3)

The jerk is the time rate of change of the acceleration (Sandin, 1990). It can be used to refer to an unsteadiness of movement.

7.4.2 Assessment of Using a Dynamic Backrest System

- *Parental Assessment*

During the child's motion analysis, the parents also were asked to complete an evaluation form to document their experience using the dynamic seating system. A one page assessment form was designed and made up of a mix of open and rated-response type questions which was completed in around five minutes. The areas which were investigated were the satisfaction levels with the way of using the dynamic backrest system compared with the rigid backrest system. Each question had 2 scores maximum: strongly agree = 2, agree = 1, neutral = 0, disagree = 1, strongly disagree = -2. At the end of form was an additional section which allowed parent to include further comments regarding any other problems, suggestions and improvements they would like to be made.

7.5   RESULTS

The volunteer used the Mygo wheelchair with a 95 degree backrest angle and a 20 degree tilt. Her left hand always was fastened with an armrest to restrict its involuntary movement, which left unrestricted could have inflicted self-harm.

7.5.1 Kinematic Data

Table 7.1 shows the average of the velocity, acceleration and jerk, which were calculated from the trajectories of the head, right and left wrists as explained in section 7.4.1.

Table 7.1 Average of the velocity, acceleration and jerk in each month

Mean	Task 1						Task 2						Task 3					
	1st	2nd	3rd	4th	5th	6th	1st	2nd	3rd	4th	5th	6th	1st	2nd	3rd	4th	5th	6th
Velocity (m/s)																		
Head	0.03	0.01	0.04	0.03	0.02	0.02	0.03	0.01	0.03	0.02	0.02	0.03	0.00	0.01	0.01	0.03	0.01	0.02
Right wrist	0.07	0.05	0.09	0.09	0.04	0.05	0.05	0.05	0.10	0.02	0.05	0.05	0.02	0.04	0.04	0.09	0.02	0.04
Left wrist	0.12	0.01	0.02	0.01	0.03	0.00	0.08	0.02	0.02	0.01	0.03	0.01	0.01	0.01	0.01	0.01	0.02	0.01
Acceleration (m/s$^{2)}$)																		
Head	0.17	0.06	0.21	0.21	0.11	0.10	0.16	0.07	0.16	0.18	0.11	0.16	0.02	0.06	0.06	0.18	0.07	0.11
Right wrist	0.38	0.28	0.50	0.50	0.21	0.19	0.29	0.26	0.54	0.49	0.24	0.28	0.10	0.22	0.22	0.50	0.10	0.17
Left wrist	0.49	0.06	0.01	0.06	0.16	0.02	0.44	0.09	0.09	0.05	0.15	0.07	0.04	0.07	0.05	0.08	0.10	0.07
Jerk (m/s^3)																		
Head	1.10	0.36	1.43	1.40	0.72	0.66	1.04	0.45	1.10	1.12	0.73	1.03	0.14	0.37	0.40	1.17	0.42	0.68
Right wrist	2.40	1.80	3.09	3.22	1.28	1.07	1.86	1.66	3.50	3.27	1.50	1.77	0.63	1.44	1.34	3.20	0.64	1.02
Left wrist	2.95	0.41	0.69	0.41	1.04	0.11	2.88	0.56	0.57	0.50	0.95	0.43	0.26	0.42	0.34	0.54	0.62	0.45
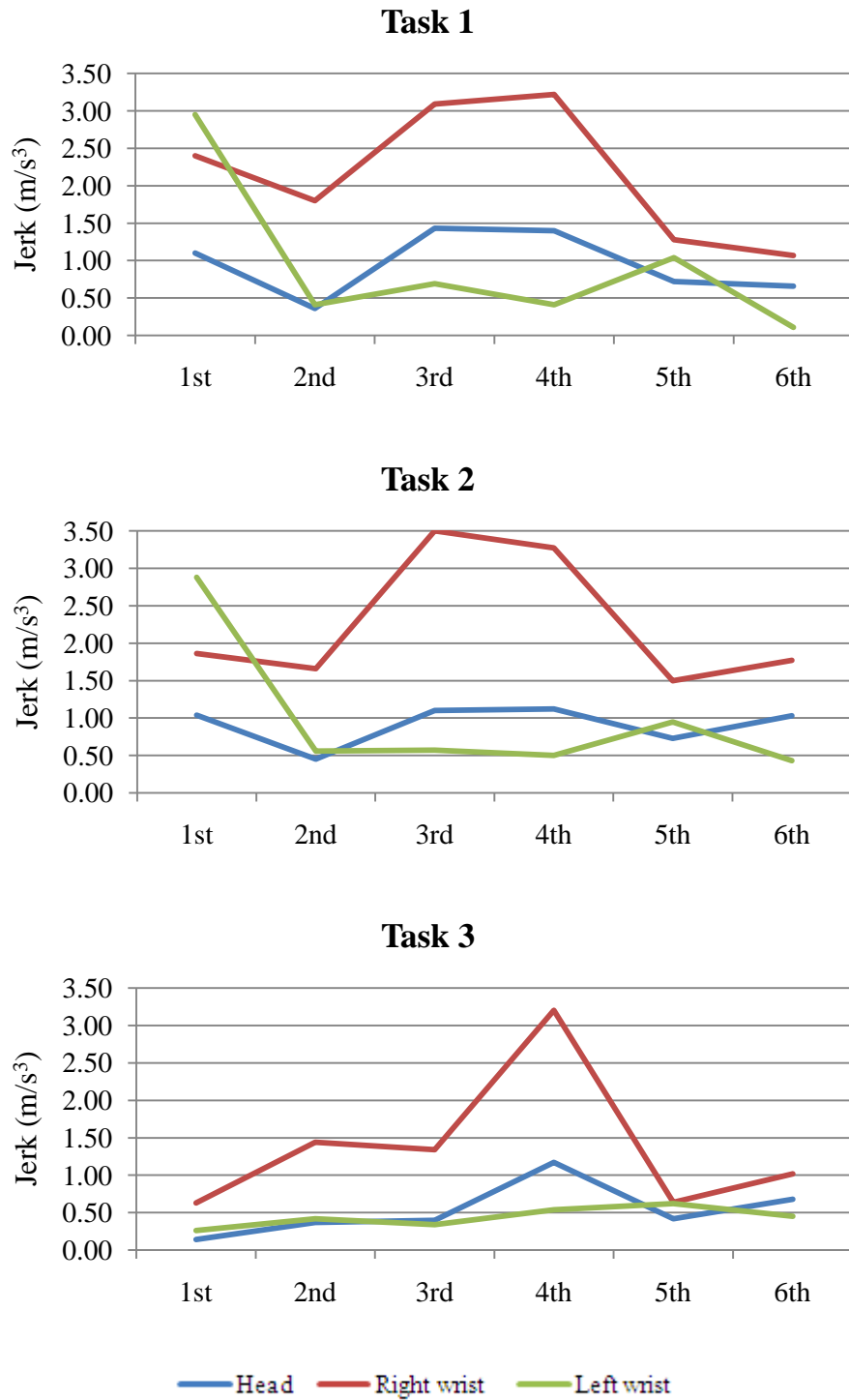
Figure 7.5 Jerk data of head, right and left wrist compared in each month

On the first test, the child was not comfortable with the new seating system and laboratory environment, and she presented with involuntary movements (athetosis). In tasks 1 and 2 her left hand was initially free but, based on her parents' suggestion that she might injure herself, the hand was restrained. Consequently the jerk in task 3 was obviously decreased from 2.95 and 2.88 m/s^3 to 0.26 m/s^3 during test in first month.

When comparing the three tasks, the participant was observed to have more steadiness of movement in the later tasks, and especially in the last task. There were several possible explanations for this result. For example, the participant may have been more relaxed and comfortable when sitting on the chair longer, familiarising to the laboratory environment, or that the cartoon got her attention more than the previous songs.

Figure 7.5 shows the results of the jerk within each task throughout the six months of testing. These results do not indicate whether the participant developed smoother movement or not. Any trends were unclear: jerk varied from month to month and from task to task depending on the reactions of the participant during the test session, for example, irritability and tiredness, both had effects on her movement and were uncontrolled variables.

The examples of trajectories of three markers on head, right and left wrists are presents in Figure 7.6 and Figure 7.7 in frontal and sagittal views, respectively.

In the frontal view (Figure 7.6), the participant had involuntary movements (athetosis) of her head and hands. Her left hand was fastened on the armrest when testing. Her right hand moved in range of 0.14 m, or -0.23 - -0.09 m along Y axis with a dominant frequency of 6 - 9 Hz. Her Head moved in the range of 0.10 m, between -0.07 – 0.03 m along Y axis, at 3-5 Hz. In the sagittal view (Figure 7.7), her right hand moved in range of 0.24 m, or 0.18 -0.42 m along Y axis whereas head moved in range of 0.20 m, between -0.06 – 0.15 m along Y axis.
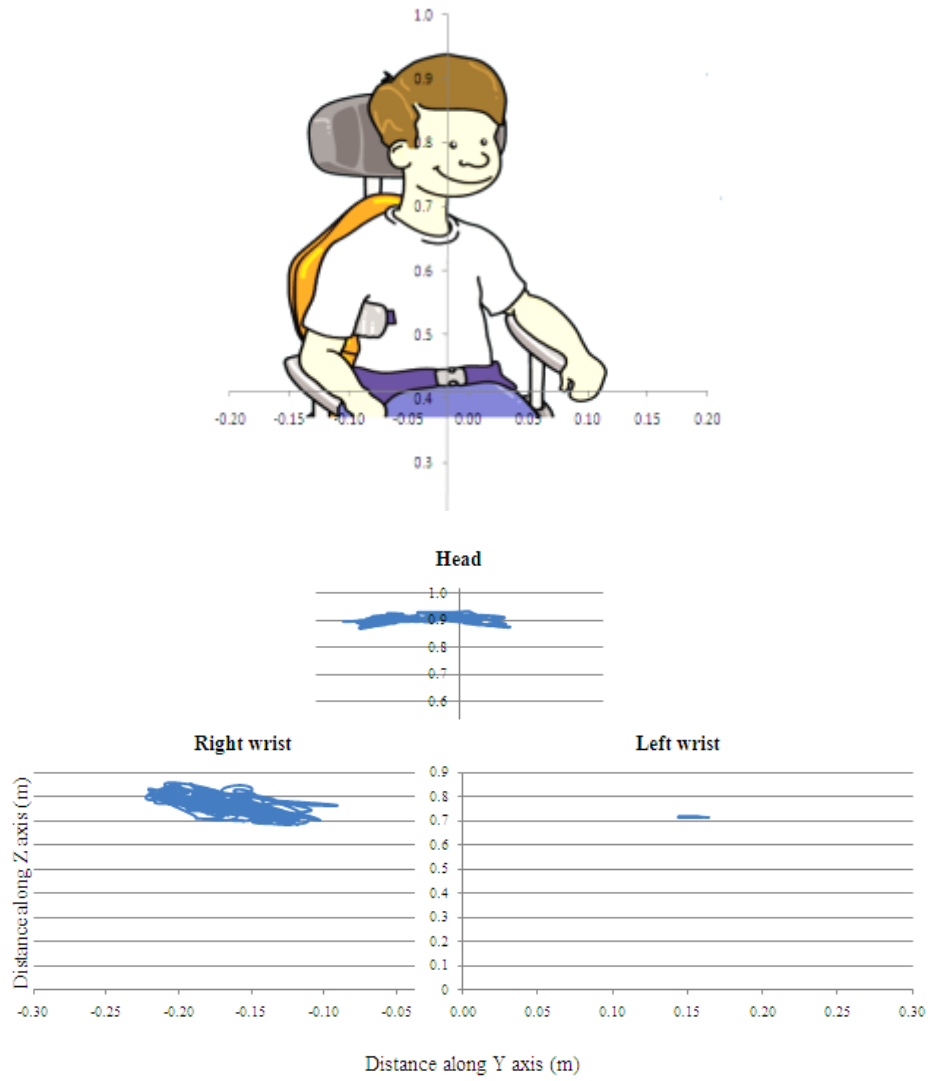
Figure 7.6 Trajectory of head, right and left wrist in the frontal view
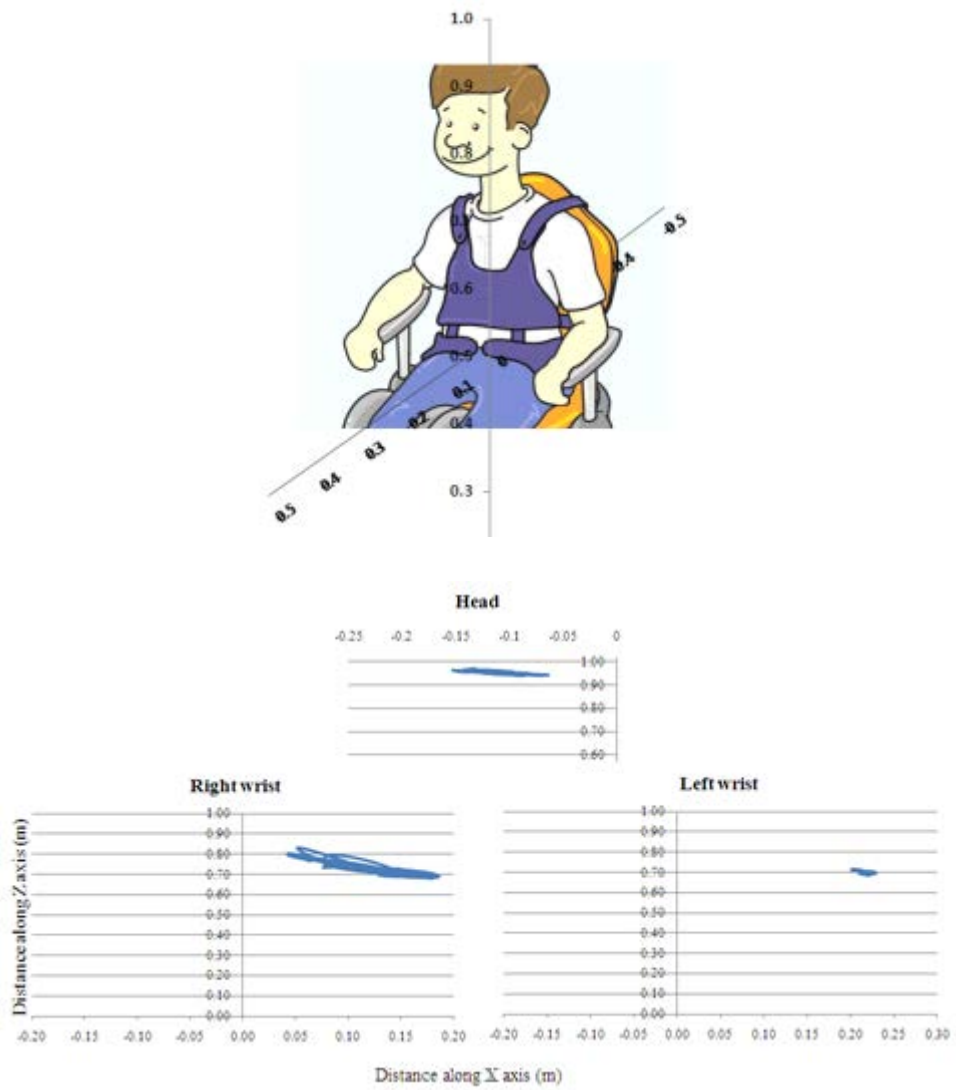
Figure 7.7 Trajectory of head, right and left wrist in the sagittal view

7.5.2 Parents' Assessment

To assess the effect of using the dynamic backrest seating system, a rated-response type questionnaire was used. It is apparent from this assessment that the scores increased with each month of testing.

Table 7.2 Assessment of the dynamic backrest system and comments from parent

Assessment	1st	2nd	3rd	4th	5th	6th
• **With the chair, it is easy to**						
Get my child into/out of the chair	0	0	1	1	1	1
Feed	0	0	1	1	1	1
Change	0	0	1	0	0	0
Get on/off transportation	0	0	1	1	1	1
Adjust the seat	1	-1	-1	1	1	1
Maintain the seat	0	0	1	1	1	1
Manage in general	1	0	1	1	1	1
• **The chair helps my child to**						
Maintain attention	0	0	0	1	1	0
Communicate	0	0	0	0	0	0
Feel secure	0	1	1	1	1	1
Look stable on the chair	0	1	1	1	1	1
Maintain skin condition	0	0	0	0	0	0
My child likes the chair	0	1	1	0	1	1
Sum	2	2	8	9	10	9

Other comments:

- *Locking mechanism was not working. Hence we and the school had a problem keeping the backrest in the desired position (2nd test).*
- *Difficulty in reclining position adjustment due to a problem with the tube. Hence the backrest would not stay upright (3nd test).*

7.6   DISCUSSION AND CONCLUSION

The major limit of the longitudinal study was the number of participants. Whilst we are very grateful for the family that did volunteer, only recruiting one participant for this longitudinal study makes interpretation difficult, especially when the participant was relatively docile compared to other population members. Indeed, the previous chapter demonstrated that the dynamic component may be more effective when combined with strong extensor spasms, and fortunately (for the girl) our volunteer did not exhibit these symptoms. This poor recruitment potentially implies that the population experience with the cross-sectional study was not wholly positive, as evidenced by their unenthusiastic to volunteer again. Some parents of potential participants who did not want to participate in this longitudinal study mentioned the reasons:

- It was difficult for them to travel to the Motion Analysis Laboratory, Biomedical Engineering Department, University of Strathclyde.
- The child had difficulty attending the study through six months.
- Their child might have operation or special treatment within the six months of investigation.

This study set out with the aim of assessing any change of movement in CP after using a dynamic backrest system for a long time. Unfortunately, our participant was not able to perform voluntary movement, and thus the testing tasks were only in sitting position without any prescribed function of the upper body. However, the kinematic methods adopted worked well and a similar methodology could be recommended for future work.

As mentioned that the volunteered child could not perform any voluntary movement, and so the movement was assessed as she sat still on her chair. This kinematic data were analysed to examine the smoothness of movement, by calculating jerk (Sandin, 1990). When differentiating three times, one must be aware that the signal to noise ratio decreases: the numerical differentiation amplifies small experimental errors. Therefore, the results could be indicative of differences in experimental error, perhaps due to different calibrations, between the test days. However, a 6Hz low pass filter was used to smooth out the data, which should be

highly sufficient to smooth out the random experimental errors emanating from the 100Hz motion analysis system, which one has to assume would be of the order of 100Hz. Therefore we have some confidence that the jerk calculations are indicative of the jerk experienced at the time of testing.

The test indicated that there were no changes in athetoid movement after a long period of using the dynamic backrest system. This was to be expected, since these athetoid movements were not strong enough to deform the gas spring to any great extent. Therefore any contact forces between the user and chair would not be different between a rigid and dynamic system for this child. Any changes that did occur would probably be more linked to maturation rather than any relationship with the chair.

Along with the motion analysis results, a survey was used to evaluate the long term effects of using the dynamic backrest system compared with the rigid system. The survey comprised thirteen questions. Each question contained a set of answer with a 2 score maximum. The results from these questionnaire showed an improvement over time when the family used the chair. However, when we finished the long term test with dynamic system, parent preferred to change the backrest back to the rigid system because the rigid back strut is easier to control the preferable angular position when compared to the dynamic backrest system. Thus, the results could be interpreted as the family knowing that an improvement was the intended outcome and a desirable, and therefore they provided the data, either consciously or subconsciously, to that effect.

CHAPTER 8
CONCLUSIONS AND
RECOMMENDATIONS

8.1 CONCLUSIONS AND FINDING

The sample recruited in this work did not show any significant differences in contact forces on the backrest between the rigid and dynamic systems. However, the users may have benefitted from the reclining nature of the dynamic backrest as can be seen by the forces on the right-sided (presumably the dominant side) footrest being reduced. Another important finding was that as the dynamic backrest was tilted back, participants were still well positioned in the midline of the seat.

The results have provided a useful and interesting set of data. Seat design should safely accommodate the maximum expected loads. As a result, the force exerted on a child's seat throughout daily activity due to their own weight, inertia and function are important parameters to be determined. Peak forces on the backrest during static sitting were 1BW; which increased to 2BW when the chair was bumped down stairs. The rigid system exhibited maximum peak forces of 2.5BW on the backrest in response to a strong extensor spasm, which reduced to a maximum of approximately 1.75BW for the dynamic system.

These data are supportive of the notion that a dynamic chair may be beneficial to occupants who exhibit strong extensor spasms; in as much as the reduction in contact force could (1) decrease the likelihood and extent of any pain and injury; (2) decrease the potential for muscle hypertrophy and (3) decrease the incident of chassis failures.

The potential benefit achievable in the reduction of the contact forces however may not result in clinical improvement. In the short term (a few hours of testing) the reduction of contact forces did not reduce the frequency and duration of a user's extensor spasm. Furthermore, dynamic seating had no long-term benefit to either child or caregivers in the long term for a child with no extensor spasms. Clearly, further short and long-term studies, focussing only on children with strong extensor spasms, are necessary to clarify the response of dynamic seating in such critical circumstances. Such studies will reduce the variability associated with the variety of symptoms exhibited by children with CP, and will identify the importance of, or lack of, dynamic components for contact force reduction.

8.2   RECOMMENDATION FOR FUTURE WORK

Although the study has achieved its objectives, some of the issues emerging from this study are worthy to be considered for future research, together with some recommendations about how these could be achieved.

- To verify our finding that a dynamic component lessens chassis forces, further investigation should be planned for a larger number of participants, with a focus on children who have strong extensor spasms. Both the short term differences should be determined, in addition to a longitudinal study addressing any long-term benefits on the biomechanics and neurophysiology of the users.

- This study only considered a dynamic backrest. There is potential for the whole chair to become more compliant and "active", utilising multiple dynamic components in the back, seat and footrests, allowing unrestricted hip, knee, ankle and spine extension. Such a chair may have significant potential benefits for users with severe extensor spasm.

- One may increase the population from which a sample is recruited by expanding the inclusion criteria. Future participants could be children who experience extensor spasms, no matter what the type of neurological conditions i.e. cerebral palsy, multiple sclerosis or spinal cord injury.

- Strain gauges were used directly on wheelchair components in this study. Whilst this provided a direct measure of chassis strain without need for separating the components, this methodology resulted in a difficulty with regards to component calibration. An alternative would be to attach the strain gauges to uniform pylons, which are then inserted in the chassis structure. This procedure has its own issues, and it is probably not until this method is tried will the advantages and disadvantages of the two alternatives will become apparent.

REFERENCES

AGARWAL, A. & VERMA, I. 2012. Cerebral palsy in children: An overview. *Journal of Clinical Orthopaedics and Trauma,* 3**,** 77-81.

AISSAOUI, R., BOUCHER, C., BOURBONNAIS, D., LACOSTE, M. & DANSEREAU, J. 2001. Effect of seat cushion on dynamic stability in sitting during a reaching task in wheelchair users with paraplegia. *Archives of Physical Medicine and Rehabilitation,* 82**,** 274-281.

ANNE FENETY, P., PUTNAM, C. & WALKER, J. M. 2000. In-chair movement: validity, reliability and implications for measuring sitting discomfort. *Applied Ergonomics,* 31**,** 383-393.

ASHWAL, S., RUSSMAN, B. S., BLASCO, P. A., MILLER, G., SANDLER, A., SHEVELL, M. & STEVENSON, R. 2004. Practice Parameter: Diagnostic assessment of the child with cerebral palsy. *Neurology,* 62**,** 851-863.

AULT, H. K., MARRYANNE, HELEN & BAR. Year. Design of a Dynamic Seating System for Clients with Extensor Spasms. *In:* RESNA, 20-24 June 1997 Pittsburgh. 187-189.

BANSBACH. 2012. *Lockable gas springs - Main type B - Details* [Online]. Available: http://www.bansbach.de/com/gasfedern/gasdruckfedern-blockierbar-bauart-b-details-2.html [Accessed 28 October 2012].

BAR, C. A. 1991. Evaluation of cushions using dynamic pressure measurement. *Prosthetics and Orthotics International,* 15**,** 232-240.

BARNABY, A. 1994. A survey og maginal wheelchair users. *Journal of Rehabilitation Research and Development,* 31**,** 297-302.

BARNES, M. R. 1998. Review: Management of spasticity. *Age and Ageing* 27**,** 239-245.

BECKWITH, T. G., LIENHARD, J. H. & MARANGONI, R. D. 1993. *Mechanical measurements,* Reading, Massachusetts, Addison-Wesley.

BENHAM, P. P. & CRAWFORD, R. J. 1987. *Mechanics of engineering materials,* London, United Kingdom, Longman Scientific & Technical.

BENHAM, P. P. & CRAWFORD, R. J. 1996. *Mechanics of engineering materials,* London, United Kingdom, Longman Scientific & Technical.

BONELLIE. 2007. *Antenatal and perinatal risk factors for cerebral palsy in Scotland* [Online]. Available: http://www2.napier.ac.uk/cprs//research/index.htm [Accessed 29 Jan 2010].

BOWKER, P. 1993. *Biomechanical basis of orthotic management*, Butterworth-Heinemann.

BRAMBLE, K. 2010. *mechanics of materials* [Online]. Available: http://www.engineersedge.com/column_buckling/column_ideal.htm [Accessed 2011].

BRIENZA, D. M. & KARG, P. E. 1998. Seat cushion optimization: A comparison of interface pressure and tissue stiffness characteristics for spinal cord injured and elderly patients. *Archives of Physical Medicine and Rehabilitation,* 79**,** 388-394.

BROWN, D., ZELWANGER, A. & BERTOCI, G. 2001. Quantification of Forces associated with Episodic full body extenxor spasticity in children. *RESNA***,** 358-60.

CANS, C., DE-LA-CRUZ, J. & MERMET, M.-A. 2008. Epidemiology of cerebral palsy. *Paediatrics and Child Health,* 18**,** 393-398.

CARLSON, M., LONSTEIN, J., BECK, K. O. & WILKIE, D. C. 1986. Seating for Children and Young Adults with Cerebral Palsy. *Clinical Prosthetics and Orthotics,* 10**,** 137-158.

CHALUPNIK, J. 1968. Stress concentrations in bolt-thread roots. *Experimental Mechanics,* 8**,** 398-404.

CIMOLIN, V., PICCININI, L., AVELLIS, M., CAZZANIGA, A., TURCONI, A., CRIVELLINI, M. & GALLI, M. 2009. 3D-Quantitative evaluation of a rigid seating system and dynamic seating system using 3D movement analysis in individuals with dystonic tetraparesis. *Disability and Rehabilitation: Assistive Technology,* 4**,** 422-428.

CLARK, J., MORROW, M. & MICHAEL, S. 2004. Wheelchair postural support for young people with progressive neuromuscular disorders *International Journal of Therapy and Rehabilitation,* 11**,** 365-373.

CLARK, M. 2006. Shear force initiatiative. *European pressure ulcer advisory panel,* 7.

COGHER, L., SAVAGE, E. & SMITH, M. 1992. *Management of Disability Series: Cerebral Palsy, The Child and Young Person*, Chapman & Hall Medical.

COOPER, D. & ANTONIUK, E. 2007. Dynamic Seating – A spectrum of applications. *23rd International Seating Symposium.* Florida, USA.

COOPER, D., DILABIO, M., BROUGHTON, G. & BROWN, D. 2001. Dynamic seating components for the reduction of spastic activity and enhancement of function. *17th International Seating Symposium.* Florida, USA.

CRAWFORD, S. A., STINSON, M. D., WALSH, D. M. & PORTER-ARMSTRONG, A. P. 2005. Impact of Sitting Time on Seat-Interface Pressure and on Pressure Mapping With Multiple Sclerosis Patients. *Archives of Physical Medicine and Rehabilitation,* 86**,** 1221-1225.

DAWLEY, J. & JULIAN, R. 2003. Purpose, Use And Fabrication Of A Custom Made Dynamic Backrest. *19th International Seating Symposium.* Florida, USA.

DING, D., LEISTER, E., COOPER, R. A., COOPER, R., KELLEHER, A., FITZGERALD, S. G., & & BONINGER, M. L. 2008. Usage of tilt-in-space, recline, and elevation seating functions in natural environment of wheelchair users. *Journal of Rehabilitation Research & Development,* 45**,** 973-984.

EVANS, M. A. & NELSON, W. B. Year. A Dynamic Solution to Seating Clients with Fluctuating Tone. *In:* RESNA, 7-12 June 1996 Salt lake City, Utah. 189-190.

FARRICIELLI, S. 2010. Kinetic Seating: From the Office to the Wheelchair. New Haven, Connecticut, USA: Yale Venture Challenge.

FROSSARD, L., BECK, J., DILLON, M. & EVANS, J. 2003. Development and Preliminary Testing of a Device for the Direct Measurement of Forces and Moments in the Prosthetic Limb of Transfemoral Amputees during Activities of Daily Living. *The American Academy of Orthotists & Prosthetists,* 15**,** 135-142.

GELBER, D. A. & JEFFERY, D. R. (eds.) 2002. *Clinical evaluation and management of spasticity,* Totowa, New Jersey: Humana Press

GERALIS, E. 1991. Children with Cerebral Palsy: a parents' guide. *What is Cerebral Palsy?* United States of America: Woodbine House, Inc.

GIL-AGUDO, A., DE LA PEÑA-GONZÁLEZ, A., DEL AMA-ESPINOSA, A., PÉREZ-RIZO, E., DÍAZ-DOMÍNGUEZ, E. & SÁNCHEZ-RAMOS, A. 2009. Comparative study of pressure distribution at the user-cushion interface with different cushions in a population with spinal cord injury. *Clinical Biomechanics,* 24**,** 558-563.

GREEN, E. M. & NELHAM, R. L. 1991. Development of sitting ability, assessment of children with a motor handicap and prescription of appropriate seating systems. *Prosthetics and Orthotics International,* 15**,** 203-216.

GRIEVE, D. W., MILLER, D. I., MIT, D. & PAUL, J. P. 1975. *Techniques for the analysis of human movement*, London : Lepus Books.

HAGBERG, B., HAGBERG, G., BECKUNG, E. & UVEBRANT, P. 2001. Changing panorama of cerebral palsy in Sweden. VIII. Prevalence and origin in the birth year period 1991-94. *Acta Paeditrica,* 90**,** 271-277.

HAHN, M. E., SIMKINS, S. L., GARDNER, J. K. & KAUSHIK, G. 2009. A Dynamic Seating System for Children with Cerebral Palsy. *Journal of Musculoskeletal Research,* 12**,** 21-30.

HAM, R., ALDERSEA, P. & PORTER, D. 1998. *Wheelchair users and postural seating a clinical approach,* New York, USA, Churchill Livingstone.

HBM 2009. CANHEAD Data Sheet. *Pin assignment CB1010.* Darmstadt, Germany: HOTTINGER BALDWIN MESSTECHNIK GmbH.

HENDERSON, J., PRICE, S., BRANDSTATER, M. & MANDAC, B. 1994. Efficacy of three measures to relieve pressure in seated persons with spinal cord injury. *Arch Phys Med Rehabil,* 75**,** 535-539.

HIROSE, H., AIKAWA, T. & NAKAI, K. 2008a. Measurement of the user's load on the PSDs for a long period of time. *24th International Seating Symposium.* Vancouver, BC Canada.

HIROSE, H., AIKAWA, T. & NAKAI, K. Year. Measurement of the User's Load on the PSDs for a Long Period of Time. *In:* 24th International Seating Symposium, 6-8 March 2008 2008b Westin Bayshore Resort & Marina 1601 Bayshore Drive, Vancouver, BC Canada. 279.

HIROSE, H. & KONAUASHIB, M. Year. A Long Time Interface Pressure Measurement on a Wheelchair and the Pressure Ulcer Risk in Nursing Home Wheelchair. *In:* 22nd International Seating Symposium, 2006 Westin Bayshore Resort & Marina 1601 Bayshore Drive, Vancouver, BC Canada. 240.

HOBSON, D. A. 1992. Comparative effects of posture on pressure and shear at the body-seat interface. *Journal Of Rehabilitation Research And Development,* 29**,** 21-31.

HOFFMANN, K. 2010. The equations given here for the Wheatstone bridge circuits. *The linearity error of the Wheatstone bridge circuits.* Darmstadt Germany

HOLMES, K. J., MICHAEL, S. M., THORPE, S. L. & SOLOMONIDIS, S. E. 2003. Management of scoliosis with special seating for the non-ambulant spastic cerebral palsy population--a biomechanical study. *Clinical Biomechanics,* 18**,** 480-487.

INSTRON 2009. ElectroPuls™ E10000 Test System. *System Reference Manual* MA, United States of America: Illinois Tool Works Inc. (ITW).

JACOBSSON, B. & HAGBERG, G. 2004. Antenatal risk factors for cerebral palsy. *Best Practice & Research Clinical Obstetrics & Gynaecology,* 18**,** 425-436.

JAN, Y.-K., JONES, M. A., RABADI, M. H., FOREMAN, R. D. & THIESSEN, A. 2010. Effect of Wheelchair Tilt-in-Space and Recline Angles on Skin Perfusion Over the Ischial Tuberosity in People With Spinal Cord Injury. *Archives of Physical Medicine and Rehabilitation,* 91**,** 1758-1764.

JUVINALL, R. C. & MARSHEK, K. M. 1991. *Fundamentals of machine component design*, New York : Wiley

KRÄGELOH-MANN, I. & CANS, C. 2009. Cerebral palsy update. *Brain and Development,* 31**,** 537-544.

KULAK, W. & SOBANIEC, W. 2003. Risk factors and prognosis of epilepsy in children with cerebral palsy in north-eastern Poland. *Brain and Development,* 25**,** 499-506.

LACOSTE, M., THERRIEN, M., CÔTÉ, J. N., SHRIER, I., LABELLE, H. & PRINCE, F. 2006. Assessment of Seated Postural Control in Children: Comparison of a Force Platform Versus a Pressure Mapping System. *Archives of Physical Medicine and Rehabilitation,* 87**,** 1623-1629.

LANCE, J. 1980. *Pathophysiology of spasticity and clinical experience with baclofen. In: Feldman RG, Young RR, Koella WP (eds),* Chicago.

LAUGHTON, B. 2004. Management of children with cerebral palsy. *CME,* 22**,** 434-438.

LECKEY 2010. The new 2010 Mygo. James Leckey design Co.,Ltd, Kilwee Business Park Dunmurry BT17 0HD Northern Ireland United Kingdom.

LETTS, R. 1991. *General principles of seating*, Boca Raton : CRC Press.

LIEBER, R. L. 1990. Hypothesis: Biarticular Muscles Transfer Moments Between Joints. *Developmental Medicine & Child Neurology,* 32**,** 456-458.

LUSARDI, M. M. & NIELSEN, C. C. 2007. *Orthotics and prosthetics in rehabilitation*, Saunders Elsevier.

MAGNISSALIS, E. A. 1992a. *Studies of prosthetic loading by means of pylon transducers* Ph.D, University of Strathclyde.

MAGNISSALIS, E. A. 1992b. *Studies of prosthetic loading by means of pylon transducers.* PhD, University of Strarhclyde.

MARIOLI, D., ROLLA, P. & TARONI, A. 1992. Strain gauge transducers: an evaluation of accuracy limits. *Measurement* 110.

MAYALL, J. K. & DESHARNAIS, G. 1995. *Positioning in a wheelchair : a guide for professional caregivers of the disabled adult* Thorofare, NJ

MCGINLEY, J. L., BAKER, R., WOLFE, R. & MORRIS, M. E. 2009. The reliability of three-dimensional kinematic gait measurments: A systematic review. *Gait & Posture,* 29**,** 360-369.

MEDICALADVISORYSECRETARIAT. 2005. Intrathecal baclofen pump for spasticity: an evidence-based analysis. *Ontario Health Technology Assessment Series* [Online], 5.

MERIAM, J. L. & KRAIGE, G. L. 1997. *Engineering mechanics: Statics,* Chichester, New York., Wiley.

MOTAVALLI, S. & AHMAD, F. 1993. Measurement of seating comfort. *Computers & Industrial Engineering,* 25**,** 419-422.

NEILSON, P. D. & MCCAUGHEY, J. 1982. Self-regulation of spasm and spasticity in cerebral palsy. *Journal of Neurology, Neurosurgery & Psychiatry,* 45**,** 320-330.

NWAOBI, O. 1987. Seating orientations and upper extremity function in children with cerebral palsy. *Phys Ther,* 67**,** 1209-12.

NWAOBI, O. M. 1986. EFFECTS OF BODY ORIENTATION IN SPACE ON TONIC MUSCLE ACTIVITY OF PATIENTS WITH CEREBRAL PALSY. *Developmental Medicine & Child Neurology,* 28**,** 41-44.

OATIS, C. A. 2004. *Kinesiology : the mechanics and pathomechanics of human movement* Philadelphia, Lippincott Williams & Wilkins

ORPWOOD, R. Year. A Compliant Seating System for a Child with Whole Body Extensor Spasms. *In:* RESNA '96 Annual Conference, 1996 Salt Palace Convention Center, Salt Lake City, Utah. 261-262.

PANTELIADIS, C. P. & STRASSBURG, H. M. 2004. *Cerebral palsy Principles and management,* Greece, Prof. Dr med. Christos P Panteliadis Thessalonoki.

PAPAVASILIOU, A. S. 2009. Management of motor problems in cerebral palsy: A critical update for the clinician. *European Journal of Paediatric Neurology,* 13**,** 387-396.

PARKINSON, M. B., CHAFFIN, D. B. & REED, M. P. Year. Maintaining balance in seated reaches. *In:* International Conference of Rehabilitation Engineering and Assistive Technology Society of North America, 2002 Hyatt Regency Mineapolis Hotel Minneapolis, MN, USA. 224.

PHAROAH 1998. epidemiology of cerebral palsy in England and Scotland. *Archieves of Disease in Chailhood,* 79**,** F21-F25.

PICCININI, L., CIMOLIN, V., AVELLIS, M., CAZZANIGA, A., TURCONI, A. C., MARCELLO CRIVELLINI2 & GALLI, M. 2009. 3D-Quantitative evaluation of a rigid seating system and dynamic seating system using 3D movement analysis in individuals with dystonic tetraparesis. *Disability & Rehabilitation: Assistive Technology*

POLLIACK, A. A. & SCHEINBERG, S. 2006. A New Technology for Reducing Shear and Friction Forces on the Skin: Implications for Blister Care in the Wilderness Setting. *Wilderness and Environmental Medicine,* 17**,** 109-119.

PRATT, D. J., BOWKER, P., WARDLAW, D. & MCLAUCHLAN, J. 1979. Load measurement in orthopaedics using strain gauges. *Journal of Biomedical Engineering,* 1**,** 287-296.

PRESTON, L. A. & HECHT, J. S. 1999. *Spasticity management: rehabilitation strategies,* Maryland USA, American Occupational Therapy Association.

REID, M., ELLIOTT, B. & ALDERSON, J. 2007. Shoulder joint kinetics of the elite wheelchair tennis serve. *British Journal of Sports Medicine,* 41**,** 739-744.

ROSENBAUM, P. 2006. Classification of abnormal neurological outcome. *Early Human Development,* 82**,** 167-171.

ROSENBAUM, P., PANETH, N., LEVITON, A., GOLDSTEIN, M. & BAX, M. 2007. A report: the definition and classification of cerebral palsy April 2006. *Developmental Medicine & Child Neurology,* 49**,** 8-14.

SALIHU, H. M. 2008. Epidemiology of stillbirth and fetal central nervous system injury. *Semin Perinatol,* 32**,** 232-8.

SANDIN, T. R. 1990. The jerk. *The Physics Teacher,* 28**,** 36-40.

SANTANGELO, M. & O'REILLY, K. 1999. Long term rehab increasing independence. *Rehab Management: The Interdisciplinary Journal of Rehabilitation,* 12**,** 60-65.

SCHERZER, A. L. 2001. *Early diagnosis and interventional therapy in cerebral palsy : an interdisciplinary age-focused approach* New York, New York : M. Dekker

SCIBERRAS C, S. N. 1999. Cerebral palsy in Malta 1981 to 1990. *Developmental Medicine & Child Neurology,* 41**,** 501-508.

SCPE 2000. Surveillance of cerebral palsy in Europe: a collaboration of cerebral palsy surveys and registers. *Developmental Medicine & Child Neurology,* 42**,** 816-824.

SHARMA, P., SHARMA, U. & KABRA, A. 1999. Cerebral Palsy - Clinical Profile and Predisposing Factors *Indian Pediatrics* 36**,** 1038-1042.

SHEVELL, M. I., MAJNEMER, A. & MORIN, I. 2003. Etiologic yield of cerebral palsy: a contemporary case series. *Pediatric Neurology,* 28**,** 352-359.

SIMON, D. & FOULDS, R. Year. Developing a quantitative measure of muscle spasticity. *In:* Bioengineering Conference, 2004. Proceedings of the IEEE 30th Annual Northeast, 17-18 April 2004 2004. 196-197.

SIMPSON, R. C., LOPRESTI, E. F. & COOPER, R. A. 2008. How many people would benefit from a smart wheelchair? *Journal of Rehabilitation Research & Development,* 45**,** 53-72.

STALL, R. 2013. *Caregiver Handbook part 4* [Online]. AARP real possibilities. Available: http://www.acsu.buffalo.edu/~drstall/hndbk4.html#Part4G [Accessed 2013].

STOCKTON, L. & RITHALIA, S. 2009. Pressure-reducing cushions: Perceptions of comfort from the wheelchair users' perspective using interface pressure, temperature and humidity measurements. *Journal of Tissue Viability,* 18**,** 28-35.

TAM, E. W., MAK, A. F., LAM, W. N., EVANS, J. H. & CHOW, Y. Y. 2003. Pelvic movement and interface pressure distribution during manual wheelchair propulsion. *Archives of Physical Medicine and Rehabilitation,* 84**,** 1466-1472.

TREFLER, E., HOBSON, D. A., TAYLOR, S. J., MONAHAN, L. C., SHAW, C. G. & ZIMBLEMAN, C. 1993. *SEATING AND MOBILITY: For Persons with Physical Disabilities*, San Antonio: Therapy Skill Builders.

TREFLER, E. & SCHMELER, M. 2001. Seating for Postural Control. *In:* BRUBAKER, C. E. & BRIENZA, D. M. (eds.) *A State of the Science Conference on Seating Issues for Persons with Disabilities.* Orlando, Florida.

TREW, M. & EVERETT, T. 2001. *Human movement: an introductory text*, Churchill Livingstone.

VAN GEFFEN, P., REENALDA, J., VELTINK, P. H. & KOOPMAN, B. F. J. M. 2008. Effects of sagittal postural adjustments on seat reaction load. *Journal of Biomechanics,* 41**,** 2237-2245.

WERNER, D. 2009. Disabled Village Children: A guide for community health workers, rehabilitation workers, and families.: Hesperian Health Guides.

WILLIAM, D. & CALLISTER 2007. *Materials science and engineering: an introduction,* Hoboken, NY, John Wiley & Sons, Inc.

WINTER, D. A. 1979. *Biomechanics of human movement*, New York : Wiley

WINTER, D. A. 2009. *Biomechanics and motor control of human movement* New Jersey, John Wiley & Sons Inc.

WISSEL, J., MÜLLER, J., DRESSNANDT, J., HEINEN, F., NAUMANN, M., TOPKA, H. & POEWE, W. 2000. Management of Spasticity Associated Pain with Botulinum Toxin A. *Journal of Pain and Symptom Management,* 20**,** 44-49.

WOOK, H. S., PATRANGENARU, V., SINGHOSE, W. & SPRIGLE, S. 2006. Identification of human-generated forces on wheelchairs during total-body extensor thrusts. *Clinical Biomechanics,* 21**,** 790-798.

WRIGHT C, C. J., PORTER-ARMSTRONG A. 2010. Establishing Best Practice in Seating Assessment for Children with Physical Disabilities using Qualitative Methodologies. *Disability and Rehabilitation: Assistive Technology* 5**,** 34-47.

YANG, T.-F., CHAN, R.-C., WONG, T.-T., BAIR, W.-N., KAO, C.-C., CHUANG, T.-Y. & HSU, T.-C. 1996. Quantitative Measurement of Improvement in Sitting Balance in Children With Spastic Cerebral Palsy After Selective Posterior Rhizotomy1. *American Journal of Physical Medicine & Rehabilitation,* 75**,** 348-352.

YOUNG, W. C. & BUDYNAS, R. G. 2002. *Roark's formulas for stress and strain*, McGraw-Hill, New York

ZACHARKOW, D. 1984. *wheelchair Posture and Pressure Sores,* Illinois, USA, Charles C Thomas Publisher.

ZAHEDI, M. S., SPENCE, W. D., SOLOMONIDIS, S. E. & PAUL, J. P. 1987. Repeatability of kinetic and kinematic measurements in gait studies of the lower limb amputee. *Prosthetics and Orthotics International,* 11**,** 55-64.

APPENDICES

APPENDIX A
MAXIMUM LOAD
CALCULATION

Strain gauges were arranged on the metal framework of the wheelchair, the backrest angle tube assembly (BA), backrest angle tube (BT) on the rigid backrest system or gas spring base (GB) of the dynamic backrest. To achieve calibration of force transducers, all those components were calibrated at a wide range of loads in tension, compression and torsion by using the Instron testing machine and the custom designed rig. The maximum loads of each specimen were calculated from the material properties. They were in the material elastic limit and regarded as safety factor, thus material yield was not reached, as this would damage the material structure and the strain gauges.

Using the yield strength, σ_y to find the maximum force that can put on the component before the deformation will occurs.
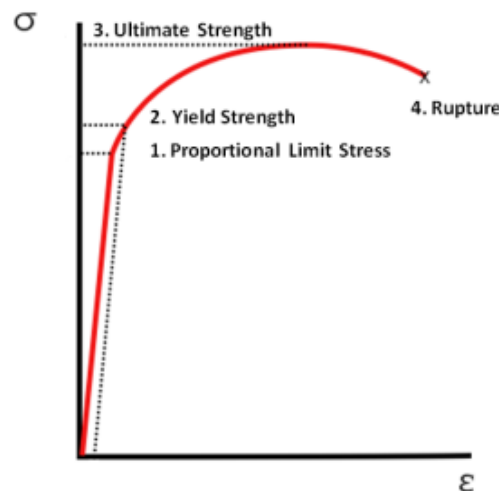
Figure A.1 Stress vs. Strain (http://creativecommons.org)

1) Area and Second Moment of Area

Tube

The area of force in tension or compression:

$$A = \frac{\pi}{4}(D^2_0 - D^2_i)$$

The second moment of area in bending:

$$I = \frac{\pi}{64}(D^4_0 - D^4_i)$$

The second moment of area in torsion:

$$J = \frac{\pi}{32}(D^4_0 - D^4_i)$$

A is the area (m^2)

I is the second moment of area, in bending, about X or Z axis (m^4)

J is the second moment of area, in torsion, about Y axis (m^4)

Do is the outer dimension of the material (m)

Di is the inner dimension of the material (m)

Trapezoid

The area of force in tension or compression:

$$A = \frac{(B+b)\,H}{2}$$

The second moment of area in bending:

$$I = \frac{H^3\,(b^2 + 4bB + B^2)}{36\,(b + B)}$$

B is the length of base, longer (m)

b is the length of top (m)

H is the height (m)

Table A.1 Material property and geometry dimension

Part	Cross section	Material	Modullus of Elastic (GPa)	Stress Yield Point (MPa)	Shear Yield Point (MPa)	Do (mm)	Di (mm)	r (mm)	l (mm)	A (mm²)	I (mm⁴)	J (mm⁴)
BA		Mild Steel	200	250	145	22.2	18.2	11.1	420.0	126.9	6533.7	13067.4
BT		Al 6061-T6	69	95	52.25	22.2	19.2	11.1	160.0	97.6	5272.3	10544.5
GB		Al 6061-T6	69	95	52.25	20.0	8.0	10.0	50.0	263.8	N/A	N/A
FA		Al 6061-T6	69	95	52.25	25.0	21.0	12.5	190.0	199.5	$Ix = 14767$ $Iz = 21578$	N/A

Outer (mm)

B	b	H
25	19.5	22.7

Inner (mm)

B	b	H
21	15.5	20.7

Reference: *Machine design Theory and Practice .A.D.Deutschman, W.A Michels & C.E. Wilson. MacMillan Publishing 1975. Machinery's Handbook 27th ed*

2) **Axial force** *(F)*

- Buckling force

$$F_{buckling} = \frac{\pi^2 EI}{KL^2}$$

E is Modulus of Elasticity (GPa)

I is the second moment of area, in bending (m^4)

L is length of material (m)

K is Effective length constant

Table A.2 Effective length constant

End Fixings	Theoretical K value	Practical K value
pinned frictionless ends	1	1
fixed ends	0.5	0.65
fixed - pinned and guided	0.7	0.8
fixed - free	2	2.1

Note: In practice, the effective length constant is increased by a factor approximately 10-20% (Bramble, 2010)

- Axial force

$$F = \sigma_y A$$

F is the axial force (N)

σ_y *is the yield stress (N/m^2)*

A is the cross section area (m^2)

3) **Bending moment** *(M)*

$$M = \frac{\sigma_y I}{y}$$

σ_y *is Yield Strength (MPa)*

I is the second moment of area (m^4)

y is the radius of material (m)

$$M = F \times distance$$

4) Torsion Moment (*T*)

$$T = \frac{\tau J}{r}$$

T is the torque (Nm)

r is the outer radius of the shaft (m)

τ is the maximum shear stress at the outer surface (Pa)

J is the moment of inertia about Y axis (m^4)

5) Example Calculation for BA

- Area and Second Moment of Area

The area of force:

$$A = 126.86 \text{ mm}^2$$

The second moment of area:

$$I = 6533.72 \text{ mm}^4$$

The area torsion in twist:

$$J = 13067.44 \text{ mm}^4$$

- Buckling force

$$F_{buckling} = \frac{3.14^2 \times 200 \; GPa \; \times 6533.72 \; mm^4}{(0.65 \times 0.42)^2 \; m^2}$$

$$F_{buckling} = 172.86 \; kN$$

- Axial force (*F*)

$$Fmax = 250 \; MPa \; \times 126.86 \text{ mm}^2$$

$$Fmax = 31715 \; N$$

Give the safety factor, 5; $Fmax = \frac{31715}{5} \; N$

$$\boldsymbol{Fmax = 6.34 \; kN}$$

- Bending moment (M)

$$M = \frac{250\ MPa \times 6533.72\ mm^4}{11.1\ mm}$$

$$M = 148.5\ Nm$$

$$M = F \times distance$$

For 3 points bending,

$$M = \frac{F}{2} \times distance$$

$$F = \frac{2M}{distance}$$

$$F = \frac{2 \times 148.5\ Nm}{0.14\ m}$$

$$F = 2.2\ kN$$

Give the safety factor, 5

$$\boldsymbol{F(bending)max = 425\ N}$$

- Torsion Moment (T)

$$T = \frac{145\ MPa\ 13067.44\ mm^4}{11.1\ mm}$$

$$T = 170.7\ Nm$$

Give the safety factor, 5

$$\boldsymbol{T\ max = 35\ Nm}$$

APPENDIX B
MATLAB CODES

- ***Strain converted to forces and moments***

```matlab
%upload excel data sheet
name='Rigid_XX';

gas_spring_stiffness=10.74;
%gas spring length m
gas_spring_length=0.275;
data_upload=strcat(name,'.XLSX');


%strain gauge conversion matrix
 %strain gauge for BA1
 matrix{1,1}=[10.6228852100000,0.383533240000,-0.695946643000000,...
     -0.195791738000000,0.0775954900000000,0.0316851950000000;...
     2.45516959600,-40.2873266300,4.54596429500,1.37746659400000,...
     -3.147858316,-0.7699465310;1.7061768660000,1.02331149900000,...
     -10.0731209800000,-0.0275346930000000,-0.277714163000000,...
     -0.392154977000000;-0.144334002000000,-0.0868512350000000,...
     0.819565470000000,0.108127538000000,-0.0222894040000000,...
     0.0365911500000000;0.00300967800000000,0.0170773040000000,...
     -0.0184250570000000,-0.00509756900000000,-0.178485381000000,...
     -0.000546315000000000;0.910529183000000,0.0637346720000000,...
     -0.0377928560000000,-0.0134198350000000,-0.0376480720000000,...
     -0.103254480000000;];


%strain gauge for BA2
 matrix{2,1}=[-11.9802756900000,1.01612960800,-0.185564237000000,...
     0.344322253000000,-0.481603302000000,-0.559635053000000;...
     -10.8984442600000,-35.0276156100000,-17.0382743500000,...
     4.68441446900000,-5.28998097400000,-3.72657265900000;...
     3.99237217100000,-0.581578409000000,12.0663641100000,...
     -0.527767080000000,0.554312142000000,0.849505427000000;...
     0.681227952000000,-0.243379515000000,1.23740777900000,...
     -0.213612101000000,0.168342529000000,0.188485335000000;...
     0.0709025920000000,-0.00432802500000000,0.0369115590000000,...
     -0.0123854140000000,-0.166477249000000,0.0147057580000000;...
     1.34968066500000,-0.266505904000000,0.460064669000000,...
     -0.116809268000000,0.156599828000000,0.264676813000000;];


 %strain gauge for BT of rigid
 name1=strrep(name,'_','');
 if norm(findstr('id',name1))~=0
 matrix{5,1}=[-10.1154634600000,-0.0601514950000000;...
     -0.00110987800000000,0.0511900360000000;];
 elseif norm(findstr('yn',name1))~=0
 matrix{5,1}=-29.532;
```

```matlab
    end

 %determining the number of rows in data
[R,C]=size(num);

for r=1:R
    %convert all the strain gauge outputs
    BA1(r,:)=matrix{1,1}*num(r,1:6)';
    BA2(r,:)=matrix{2,1}*num(r,7:12)';
    FL(r,:)=matrix{3,1}*num(r,13:15)';
    FR(r,:)=matrix{4,1}*num(r,16:18)';
    BT(r,:)=matrix{5,1}*num(r,19:20)';

    %Fx direction sum of shear forces measured at strain gauges
calibration
    %matrix already changed direction
    Fx(r,:)=BA1(r,1)+BA2(r,1);
    %Fy unbalanced force in y direction, the Fy in postion one sign
is
    %changed to that of the global coordinate system
    Fy(r,:)=(-BA1(r,2)+BA2(r,2));
    %Fz direction sum of shear forces measured at strain gauges
    Fz(r,:)=BA1(r,3)+BA2(r,3);
    %Mx
    %needs to be completed
    %My if the two signs are the same direction i.e torque if
positive
    %or negative with respect to the global coordinate system, the
total is
    %the average.if the signs are opposite the external torque
measured at
    %either end is opposite and total is the sum of the torques.
    if BA1(r,5)>0 && BA2(r,5)>0 || BA1(r,5)<0 && BA2(r,5)<0
        My(r,:)=(BA1(r,5)+BA2(r,5))/2;
    elseif BA1(r,5)<0 && BA2(r,5)>0 || BA1(r,5)>0 && BA2(r,5)<0
        My(r,:)=BA1(r,5)+BA2(r,5);
    end
end

%average force and moments
for n=1:2
BA(1,n+18)=mean(BT(:,n));
end
for n=1:3
BA(1,n+12)=mean(FL(:,n));
BA(1,n+15)=mean(FR(:,n));
end
for n=1:6
%first row average
BA(1,n)=mean(BA1(:,n));
BA(1,n+6)=mean(BA2(:,n));
end
%second row peak
for n=1:6
    if abs(max(BA1(:,n)))>abs(min(BA1(:,n)))
    BA(2,n)=max(BA1(:,n));
    elseif abs(max(BA1(:,n)))<abs(min(BA1(:,n)))
    BA(2,n)=min(BA1(:,n));
```

```matlab
        end
    if abs(max(BA2(:,n)))>abs(min(BA2(:,n)))
    BA(2,n+6)=max(BA2(:,n));
    elseif abs(max(BA2(:,n)))<abs(min(BA2(:,n)))
    BA(2,n+6)=min(BA2(:,n));
    end
end
for n= 1:2
    if abs(max(BT(:,n)))>abs(min(BT(:,n)))
    BA(2,n+18)=max(BT(:,n));
    elseif abs(max(BT(:,n)))<abs(min(BT(:,n)))
    BA(2,n+18)=min(BT(:,n));
    end
end

for n=1:3
    if abs(max(FR(:,n)))>abs(min(FR(:,n)))
    BA(2,n+15)=max(FR(:,n));
    elseif abs(max(FR(:,n)))<abs(min(FR(:,n)))
    BA(2,n+15)=min(FR(:,n));
    end
end

for n=1:3
    if abs(max(FL(:,n)))>abs(min(FL(:,n)))
    BA(2,n+12)=max(FL(:,n));
    elseif abs(max(FL(:,n)))<abs(min(FL(:,n)))
    BA(2,n+12)=min(FL(:,n));
    end
end

%backrest force
%FBx
%BT is positive as sign is in opposite direction with global
coordinate
%system
FBx=-Fx+BT(:,1)*sind(theta);
%FBz
FBz=-Fz+BT(:,1)*cosd(theta);
%magnitude of backrest force
for r=1:R
    FB(r,:)=(FBx(r,:)^2+FBz(r,:)^2)^0.5;
end

%height of COP up chair
%the approximate distance the backrest strut applies forces on
backrest
%from origin in meters
drx=0.09;
drz=0.18;

%in the situation where the backrest force is being applied on the
backrest
%either component of the force will be negative. otherwise a pulling
force
%will be applied to the backrest.
for r=1:R
    if FBx(r,:)<0 || FBz(r,:)<0
```

```matlab
    dB(r,3)=(-My(r,:)-drz*BT(r,1)*sind(theta)-
drx*BT(r,1)*cosd(theta))/FB(r,:);
    elseif FBx(r,:)>0 || FBz(r,:)>0
    dB(r,3)=(-My(r,:)-drz*BT(r,1)*sind(theta)-
drx*BT(r,1)*cosd(theta))/-FB(r,:);
    end
end
 %shear force of backrest is equal to the sum of the y force in the
opposite
%direction
    FBy=-Fy;


%the two Mz moments are summed to find unbalanced Mz moment
    Mz=BA1(:,6)+BA2(:,6);


%the two Mx moments are summed to find unbalanced Mz moment
    Mx=BA1(:,4)+BA2(:,4);


%the x and z distance of the cop measured with respect to the global
%coordinate system
    x=dB(:,3).*sind(theta);
    z=dB(:,3).*cosd(theta);


%the moment Mz is a result of Fx and Fy, the moment arm x is know
but not
%y, which can now be sloved

    y=(-Mz-FBy.*x)./FBx;
%y is the same as db(:,2) as it is not projected

    dB(:,2)=y;


%plotting COP
plot(dB(:,2),dB(:,3),'.')
xlabel('COP along y direction relative to global coordinates')
ylabel('COP along z direction relative to global coordinates')
title('Backrest Centre of pressure')


%saving figures
%This sets the units of the current  figure (gcf = get current
figure) on paper  to centimeters.
xSize = 29.7; ySize = 21;


%These are my size variables, width of 30 and a height of 21
xLeft = (29.7-xSize)/2; yTop = (21-ySize)/2;


%Additional coordinates to center  the figure on A4-paper
set(gcf,'PaperPosition',[xLeft yTop xSize ySize])
%saveas(gcf,name,'fig');
saveas(gcf,strcat(name,sheet{1,s}),'jpg');


if abs(max(FcR))>abs(min(FcR))
    Foot(2,2)=max(FcR);
    elseif abs(max(FcR))<abs(min(FcR))
    Foot(2,2)=min(FcR);
end
%average and peak force on Backrest
```

```matlab
Back(1,1)=mean(FB);

if abs(max(FB))>abs(min(FB))
    Back(2,1)=max(FB);
    elseif abs(max(FB))<abs(min(FB))
    Back(2,1)=min(FB);
end
  %sum average and peak
 sum(1,1)=mean(Fx);
 if abs(max(Fx))>abs(min(Fx))
    sum(2,1)=max(Fx);
    elseif abs(max(Fx))<abs(min(Fx))
    sum(2,1)=min(Fx);
 end
 sum(3,1)=mean(Fy);
 if abs(max(Fy))>abs(min(Fy))
    sum(4,1)=max(Fy);
    elseif abs(max(Fy))<abs(min(Fy))
    sum(4,1)=min(Fy);
 end
 sum(5,1)=mean(Fz);
 if abs(max(Fz))>abs(min(Fz))
    sum(6,1)=max(Fz);
    elseif abs(max(Fz))<abs(min(Fz))
    sum(6,1)=min(Fz);
 end
 sum(7,1)=mean(Mx);
 if abs(max(Mx))>abs(min(Mx))
    sum(8,1)=max(Mx);
    elseif abs(max(Mx))<abs(min(Mx))
    sum(8,1)=min(Mx);
 end
 sum(9,1)=mean(My);
  if abs(max(My))>abs(min(My))
    sum(10,1)=max(My);
    elseif abs(max(My))<abs(min(My))
    sum(10,1)=min(My);
 end
 sum(11,1)=mean(Mz);
 if abs(max(Mz))>abs(min(Mz))
    sum(12,1)=max(Mz);
    elseif abs(max(Mz))<abs(min(Mz))
    sum(12,1)=min(Mz);
 end
 sum(14,1)=mean(BT(:,1));
 if abs(max(BT(:,1)))>abs(min(BT(:,1)))
    sum(15,1)=max(BT(:,1));
    elseif abs(max(BT(:,1)))<abs(min(BT(:,1)))
    sum(15,1)=min(BT(:,1));
 end
 sum(16,1)=mean(BT(:,2));
 if abs(max(BT(:,2)))>abs(min(BT(:,2)))
    sum(17,1)=max(BT(:,2));
    elseif abs(max(BT(:,2)))<abs(min(BT(:,2)))
    sum(17,1)=min(BT(:,2));
  end
 sum(18,1)=mean(FB);
 if abs(max(FB))>abs(min(FB))
    sum(19,1)=max(FB);
```

```matlab
    elseif abs(max(FB))<abs(min(FB))
    sum(19,1)=min(FB);
 end
 sum(21,1)=mean(FL(:,1));
if abs(max(FL(:,1)))>abs(min(FL(:,1)))
    sum(22,1)=max(FL(:,1));
    elseif abs(max(FL(:,1)))<abs(min(FL(:,1)))
    sum(22,1)=min(FL(:,1));
end
    sum(23,1)=mean(FL(:,2));
if abs(max(FL(:,2)))>abs(min(FL(:,2)))
    sum(24,1)=max(FL(:,2));
    elseif abs(max(FL(:,2)))<abs(min(FL(:,2)))
    sum(24,1)=min(FL(:,2));
end
    sum(25,1)=mean(FL(:,3));
if abs(max(FL(:,3)))>abs(min(FL(:,3)))
    sum(26,1)=max(FL(:,3));
    elseif abs(max(FL(:,3)))<abs(min(FL(:,3)))
    sum(26,1)=min(FL(:,3));
end
    sum(27,1)=mean(FcL);
if abs(max(FcL))>abs(min(FcL))
    sum(28,1)=max(FcL);
    elseif abs(max(FcL))<abs(min(FcL))
    sum(28,1)=min(FcL);
end
    sum(30,1)=mean(FR(:,1));
if abs(max(FR(:,1)))>abs(min(FR(:,1)))
    sum(31,1)=max(FR(:,1));
    elseif abs(max(FR(:,1)))<abs(min(FR(:,1)))
    sum(31,1)=min(FR(:,1));
end
    sum(32,1)=mean(FR(:,2));
if abs(max(FR(:,2)))>abs(min(FR(:,2)))
    sum(33,1)=max(FR(:,2));
    elseif abs(max(FR(:,2)))<abs(min(FR(:,2)))
    sum(33,1)=min(FR(:,2));
end
    sum(34,1)=mean(FR(:,3));
if abs(max(FR(:,3)))>abs(min(FR(:,3)))
    sum(35,1)=max(FR(:,3));
    elseif abs(max(FR(:,3)))<abs(min(FR(:,3)))
    sum(35,1)=min(FR(:,3));
end
    sum(36,1)=mean(FcR);
if abs(max(FcR))>abs(min(FcR))
    sum(37,1)=max(FcR);
    elseif abs(max(FcR))<abs(min(FcR))
    sum(37,1)=min(FcR);
end
```

- *Stress analysis on material (BA)*

```matlab
%y distance from neutral axis
y=11.1/10^3;
%r radius same as y
r=y;
%I moment of inertia
I=6533.71828/10^12;
% J rotational moment of inertia
J=13067.43656/10^12;
%cross sectional area
A=126.856/10^6;

%capital S normal stress small s shear
%SIDE BA1
%position A
Sy=(-BA1(:,4)*y)/I+BA1(:,2)/A;
Sx=0;
syx=(BA1(:,5)*r)/J+BA1(:,1)/A;
sxy=syx;
for n=1:length(Sy)
%stress tensor
point_A{n,:}=[Sx,sxy(n,:);syx(n,:),Sy(n,:)];
%principal stress or eigenvalues
[V D]=eig(point_A{n,:});
%von misses J2 flow
AJ2_BA1(n,:)=(1/2^0.5)*((D(1,1)-D(2,2))^2+D(1,1)^2+D(2,2)^2)^0.5;
end
clear Sy Sx syx sxy
%position B
Sy=(-BA1(:,6)*y)/I+BA1(:,2)/A;
Sz=0;
syz=(BA1(:,5)*r)/J+BA1(:,3)/A;
szy=syz;
 for n=1:length(Sy)
%stress tensor
point_B{n,:}=[Sy(n,:),syz(n,:);szy(n,:),Sz];
%principal stress or eigenvalues
[V D]=eig(point_B{n,:});
%von misses J2 flow
BJ2_BA1(n,:)=(1/2^0.5)*((D(1,1)-D(2,2))^2+D(1,1)^2+D(2,2)^2)^0.5;
end
clear Sy Sz syz szy
%position C
Sy=(-BA1(:,1)*y)/I+BA1(:,2)/A;
Sx=0;
syx=(BA1(:,5)*r)/J+BA1(:,1)/A;
sxy=syx;
for n=1:length(Sy)
%stress tensor
point_C{n,:}=[Sx,sxy(n,:);syx(n,:),Sy(n,:)];
%principal stress or eigenvalues
[V D]=eig(point_C{n,:});
%von misses J2 flow
CJ2_BA1(n,:)=(1/2^0.5)*((D(1,1)-D(2,2))^2+D(1,1)^2+D(2,2)^2)^0.5;
end
clear Sy Sx syx sxy
%--------------------SIDE BA2
```

```matlab
%position A
Sy=(-BA2(:,4)*y)/I+BA2(:,2)/A;
Sx=0;
syx=(BA2(:,5)*r)/J+BA2(:,1)/A;
sxy=syx;
for n=1:length(Sy)
%stress tensor
point_A{n,:}=[Sx,sxy(n,:);syx(n,:),Sy(n,:)];
%principal stress or eigenvalues
[V D]=eig(point_A{n,:});
%von misses J2 flow
AJ2_BA2(n,:)=(1/2^0.5)*((D(1,1)-D(2,2))^2+D(1,1)^2+D(2,2)^2)^0.5;
end
clear Sy Sx syx sxy
%position B
Sy=(-BA2(:,6)*y)/I+BA2(:,2)/A;
Sz=0;
syz=(BA2(:,5)*r)/J+BA2(:,3)/A;
szy=syz;
for n=1:length(Sy)
%stress tensor
point_B{n,:}=[Sy(n,:),syz(n,:);szy(n,:),Sz];
%principal stress or eigenvalues
[V D]=eig(point_B{n,:});
%von misses J2 flow
BJ2_BA2(n,:)=(1/2^0.5)*((D(1,1)-D(2,2))^2+D(1,1)^2+D(2,2)^2)^0.5;
end
clear Sy Sz syz szy
%position C
Sy=(-BA2(:,1)*y)/I+BA2(:,2)/A;
Sx=0;
syx=(BA2(:,5)*r)/J+BA2(:,1)/A;
sxy=syx;
for n=1:length(Sy)
%stress tensor
point_C{n,:}=[Sx,sxy(n,:);syx(n,:),Sy(n,:)];
%principal stress or eigenvalues
[V D]=eig(point_C{n,:});
%von misses J2 flow
CJ2_BA2(n,:)=(1/2^0.5)*((D(1,1)-D(2,2))^2+D(1,1)^2+D(2,2)^2)^0.5;
end
clear Sy Sx syx sxy
%mean first column max second column
stress_BA1(1,1)=mean(AJ2_BA1);
stress_BA1(1,2)=max(AJ2_BA1);
stress_BA1(2,1)=mean(BJ2_BA1);
stress_BA1(2,2)=max(BJ2_BA1);
stress_BA1(3,1)=mean(CJ2_BA1);
stress_BA1(3,2)=max(CJ2_BA1);

stress_BA2(1,1)=mean(AJ2_BA2);
stress_BA2(1,2)=max(AJ2_BA2);
stress_BA2(2,1)=mean(BJ2_BA2);
stress_BA2(2,2)=max(BJ2_BA2);
stress_BA2(3,1)=mean(CJ2_BA2);
stress_BA2(3,2)=max(CJ2_BA2);
```

- *Kinematic analysis*

```matlab
%load the ASCII data
NAME='XX';
 [num, txt, raw] =xlsread(strcat(NAME,'.CSV'));

%sort data out
varibles={'Trajectories'};
[R,C]=size(txt);
for v=1:length(varibles)
for c=1:C
for r=1:R
if findstr(varibles{1,v},txt{r,c})~=0
countr=r;
countc=c;
end
end
end
end

[R1,C1]=size(raw);cell=0;
for n=countr+5:R1
    if isnumeric(raw{n,1})==1
        cell=cell+1;
        frame(cell,:)=raw{n,1};
    end

    if isnumeric(raw{n,1})==0, break
    end
end

frame(isnan(frame))=[];
time=0.01*frame;
column_length=length(time);

varibles={'chairright','chairleft','rightwrist','leftwrist','head'};
for v=1:length(varibles)
for c=1:C
for r=1:R
if findstr(varibles{1,v},txt{r,c})>0
countr=r;
countc=c;
eval(['data' '= num(countr+2:countr+1+column_length,
countc:countc+2);']);
data(isnan(data))=0;
%convert to m
ndata= 0.001.*data;
marker=ndata;
cutoff=5;
order=6;
nyquist_frequency=200;
%   first the data is checked to ensure there are no gaps then it is
%   filtered by a butterwroth filter
    [r,c]=size(marker);
    %the time length the data should be extrapolated to
    time=(1:r)';
for m=1:c
```

```matlab
    %time is the artifical base that is created if the data needs
    %interpolated
    for n=1:r
        if marker(n,m)==0
            time1(n,:)=0;
        end
        if marker(n,m)~=0
            time1(n,:)=n;
        end
    end
end
    %removing all the zeros from the artfical time
    time1(all(time1,2)==0,:)=[];
    %removing all the zeros from the marker data first marker1 is
the data
    %to be splined
    marker1=marker;
    marker1(all(marker1,2)==0,:)=[];
for m=1:3
    %extrapolation of the data
    datann(:,m)= interp1(time1,marker1(:,m),time,'spline','extrap');
    %filtering data with selected order butterworth
    Wn=cutoff/nyquist_frequency;
    [b,a]=butter(order,Wn,'low');
    % filtfilt used to reverse filter the data
    nnndata(:,m)=filtfilt(b,a,datann(:,m));
  end
name = genvarname([varibles{1,v}]);
eval([name '= nnndata;']);
%saving to dynamic folder
trajectories.(name) = eval(name);
end
end
end
end
%local wheelchair system
y=trajectories.chairleft-trajectories.chairright;
%origin
O=(trajectories.chairleft+trajectories.chairright)./2;
clear R
for n=1:length(y)
z(n,:)=[0,0,1];
x(n,:)=cross(y(n,:),z(n,:));
y(n,:)=cross(z(n,:),x(n,:));

x(n,:)=x(n,:)/norm(x(n,:));
y(n,:)=y(n,:)/norm(y(n,:));
z(n,:)=z(n,:)/norm(z(n,:));

R{n,:}=[x(n,:)',y(n,:)',z(n,:)'];

local.rightwrist(n,:)=R{n,:}'*(trajectories.rightwrist(n,:)-
O(n,:))';
local.leftwrist(n,:)=R{n,:}'*(trajectories.leftwrist(n,:)-O(n,:))';
local.head(n,:)=R{n,:}'*(trajectories.head(n,:)-O(n,:))';

end
```

```matlab
clearvars -except trajectories NAME local R
%ordered x,y and z components then magnitude
% Prieto analysis
sz = size(local.head,1);
for i = 1:3
    temp_mean = mean(local.head(:,i),1);
    mean_local_head(1:sz,i) = temp_mean;
    temp_mean = mean(local.leftwrist(:,i),1);
    mean_local_leftwrist(1:sz,i) = temp_mean;
    temp_mean = mean(local.rightwrist(:,i),1);
    mean_local_rightwrist(1:sz,i) = temp_mean;
        central_local_head = local.head - mean_local_head;
    central_local_leftwrist = local.leftwrist -
mean_local_leftwrist;
    central_local_rightwrist = local.rightwrist -
mean_local_rightwrist;
        RD.head = sqrt(sum(central_local_head.^2,2));
    RD.leftwrist = sqrt(sum(central_local_leftwrist.^2,2));
    RD.rightwrist = sqrt(sum(central_local_rightwrist.^2,2));

    MD.head = mean(RD.head,1);
    MD.leftwrist = mean(RD.leftwrist,1);
    MD.rightwrist = mean(RD.rightwrist,1);

    for j = 1:sz-1
        temp_totex_head(j) = sqrt((local.head(j+1,1)-
local.head(j,1))^2 + ...
            (local.head(j+1,2)-local.head(j,2))^2 + ...
            (local.head(j+1,3)-local.head(j,3))^2);
        temp_totex_leftwrist(j) = sqrt((local.leftwrist(j+1,1)-
local.leftwrist(j,1))^2 + ...
            (local.leftwrist(j+1,2)-local.leftwrist(j,2))^2 + ...
            (local.leftwrist(j+1,3)-local.leftwrist(j,3))^2);
        temp_totex_rightwrist(j) = sqrt((local.rightwrist(j+1,1)-
local.rightwrist(j,1))^2 + ...
            (local.rightwrist(j+1,2)-local.rightwrist(j,2))^2 + ...
            (local.rightwrist(j+1,3)-local.rightwrist(j,3))^2);
        TOTEX.head(j) = sum(temp_totex_head(1:j));
        TOTEX.leftwrist(j) = sum(temp_totex_leftwrist(1:j));
        TOTEX.rightwrist(j) = sum(temp_totex_rightwrist(1:j));
    end;

    T = 0.01:0.01:(sz-1)*0.01;
    MVELO.head = TOTEX.head./T;

end;


%velocity
for n=1:3
velocity.head_global(:,n)=gradient(trajectories.head(:,n),0.01);
velocity.rightwrist_global(:,n)=gradient(trajectories.rightwrist(:,n
),0.01);
velocity.leftwrist_global(:,n)=gradient(trajectories.leftwrist(:,n),
0.01);
velocity.head(:,n)=gradient(local.head(:,n),0.01);
velocity.rightwrist(:,n)=gradient(local.rightwrist(:,n),0.01);
velocity.leftwrist(:,n)=gradient(local.leftwrist(:,n),0.01);
end
```

```matlab
for n=1:length(local.head)
    velocity.head(n,4)=norm(velocity.head(n,:));
    velocity.rightwrist(n,4)=norm(velocity.rightwrist(n,:));
    velocity.leftwrist(n,4)=norm(velocity.leftwrist(n,:));
    velocity.head_global(n,4)=norm(velocity.head_global(n,:));

velocity.rightwrist_global(n,4)=norm(velocity.rightwrist_global(n,:)
);
velocity.leftwrist_global(n,4)=norm(velocity.leftwrist_global(n,:));
end

%acceleration
for n=1:3
acceleration.head_global(:,n)=gradient(velocity.head_global(:,n),0.0
1);
acceleration.rightwrist_global(:,n)=gradient(velocity.rightwrist_glo
bal(:,n),0.01);
acceleration.leftwrist_global(:,n)=gradient(velocity.leftwrist_globa
l(:,n),0.01);
acceleration.head(:,n)=gradient(velocity.head(:,n),0.01);
acceleration.rightwrist(:,n)=gradient(velocity.rightwrist(:,n),0.01)
;
acceleration.leftwrist(:,n)=gradient(velocity.leftwrist(:,n),0.01);
end
for n=1:length(acceleration.head)
    acceleration.head(n,4)=norm(acceleration.head(n,:));
    acceleration.rightwrist(n,4)=norm(acceleration.rightwrist(n,:));
    acceleration.leftwrist(n,4)=norm(acceleration.leftwrist(n,:));

acceleration.head_global(n,4)=norm(acceleration.head_global(n,:));
acceleration.rightwrist_global(n,4)=norm(acceleration.rightwrist_glo
bal(n,:));
acceleration.leftwrist_global(n,4)=norm(acceleration.leftwrist_globa
l(n,:));
end

%jerk
for n=1:3
jerk.head_global(:,n)=gradient(acceleration.head_global(:,n),0.01);
jerk.rightwrist_global(:,n)=gradient(acceleration.rightwrist_global(
:,n),0.01);
jerk.leftwrist_global(:,n)=gradient(acceleration.leftwrist_global(:,
n),0.01);
jerk.head(:,n)=gradient(acceleration.head(:,n),0.01);
jerk.rightwrist(:,n)=gradient(acceleration.rightwrist(:,n),0.01);
jerk.leftwrist(:,n)=gradient(acceleration.leftwrist(:,n),0.01);
end
for n=1:length(jerk.head)
    jerk.head(n,4)=norm(jerk.head(n,:));
    jerk.rightwrist(n,4)=norm(jerk.rightwrist(n,:));
    jerk.leftwrist(n,4)=norm(jerk.leftwrist(n,:));
    jerk.head_global(n,4)=norm(jerk.head_global(n,:));
    jerk.rightwrist_global(n,4)=norm(jerk.rightwrist_global(n,:));
    jerk.leftwrist_global(n,4)=norm(jerk.leftwrist_global(n,:));
end

save(NAME)
```

APPENDIX C
SAMPLE DATA AND
CALCULATION METHOD

This section shows the sample calculation of BA from the raw strain data to the resultant of force and COP.

- *Sample raw data*

Rigid Backrest system
Sample raw data of BA (um/m) from 119006 samples, testing period 198 minutes

Line	Fx1	Fy1	Fz1	Mx1	My1	Mz1	Fx2	Fy2	Fz2	Mx2	My2	Mz2
1	5.98	0.95	6.19	-50.51	-0.06	98.88	-5.31	-0.19	-4.04	-27.97	-1.39	104.7
2	5.89	0.91	5.84	-48.39	-0.06	98.19	-5.20	-0.19	-3.96	-27.65	-1.35	102.8
3	5.94	0.91	5.72	-47.64	-0.05	98.45	-5.24	-0.20	-3.98	-27.85	-1.34	102.5
4	6.02	0.91	5.69	-47.39	-0.05	98.56	-5.26	-0.19	-3.88	-27.37	-1.29	102.3
5	5.94	0.88	5.43	-45.89	-0.05	97.96	-5.20	-0.19	-3.82	-27.00	-1.25	100.9
6	5.83	0.87	5.16	-44.18	-0.05	97.32	-5.14	-0.19	-3.80	-26.97	-1.22	99.82
7	5.85	0.87	5.10	-43.70	-0.05	97.29	-5.19	-0.19	-3.80	-27.04	-1.21	99.87
8	5.90	0.86	5.09	-43.55	-0.04	97.51	-5.31	-0.20	-3.71	-26.62	-1.18	99.92
9	5.82	0.85	5.15	-43.84	-0.04	96.44	-5.24	-0.10	-3.15	-23.72	-1.05	98.67
10	5.68	0.84	5.25	-44.08	-0.04	94.25	-5.07	0.04	-2.42	-19.91	-0.88	96.81

Dynamic Backrest system

Sample raw data of BA (um/m) from 116409 samples, testing period 194 minutes

Line	Fx1	Fy1	Fz1	Mx1	My1	Mz1	Fx2	Fy2	Fz2	Mx2	My2	Mz2
1	4.85	1.40	2.09	-15.57	-0.14	80.11	-4.61	-0.27	-5.95	-36.75	-1.65	76.89
2	4.51	1.39	2.34	-16.74	-0.13	74.60	-4.36	-0.03	-5.02	-32.14	-1.38	73.61
3	4.22	1.37	2.53	-17.56	-0.12	70.14	-4.24	0.14	-4.38	-29.09	-1.17	70.27
4	3.99	1.34	2.54	-17.39	-0.09	66.54	-4.17	0.26	-3.96	-27.22	-1.01	66.98
5	3.84	1.31	2.42	-16.63	-0.09	64.50	-4.12	0.29	-3.78	-26.42	-0.92	64.89
6	3.68	1.28	2.24	-15.44	-0.10	62.67	-4.07	0.31	-3.66	-25.98	-0.84	63.02
7	3.55	1.27	2.12	-14.67	-0.10	61.44	-4.05	0.35	-3.59	-25.61	-0.80	62.11
8	3.41	1.25	2.07	-14.28	-0.10	60.21	-4.01	0.39	-3.44	-24.82	-0.76	61.38
9	3.31	1.23	2.04	-13.99	-0.10	59.28	-3.98	0.42	-3.31	-24.21	-0.73	60.69
10	3.20	1.22	1.97	-13.51	-0.12	58.36	-3.98	0.44	-3.23	-23.81	-0.71	59.85

- *Coefficient matrices*

Raw data of both rigid and dynamic systems were converted to force and moment by using the same coefficient matrix which was explained in section XX before.

Force [F]	Coeficient matrices [M]						Signal [S]
BA1							
Fx1	10.62	2.46	1.71	-0.14	0	0.91	SFx1
Fy1	0.38	-40.29	1.02	-0.09	0.02	0.06	SFy1
Fz1	-0.7	4.55	-10.07	0.82	-0.02	-0.04	SFz1
Mx1	-0.2	1.38	-0.03	0.11	-0.01	-0.01	SMx1
My1	0.08	-3.15	-0.28	-0.02	-0.18	-0.04	SMy1
Mz1	0.03	-0.77	-0.39	0.04	0	-0.1	SMz1
BA2							
Fx2	-11.98	-10.9	3.99	0.68	0.07	1.35	SFx2
Fy2	1.02	-35.03	-0.58	-0.24	0	-0.27	SFy2
Fz2	-0.19	-17.04	12.07	1.24	0.04	0.46	SFz2
Mx2	0.34	4.68	-0.53	-0.21	-0.01	-0.12	SMx2
My2	-0.48	-5.29	0.55	0.17	-0.17	0.16	SMy2
Mz2	-0.56	-3.73	0.85	0.19	0.01	0.26	SMz2

BA

In each line, forces and moments ([F] : F_x F_y F_z M_x M_y M_z) on both sides of BA were calculated by matrix multiplication as following:

From Equation (0.1)   *[F] = [M] [S]*

$F_x = M_{11} . SFx + M_{12} . SFy + M_{13} . SFz + M_{14} . SMx + M_{15} . SMy + M_{16} . SM_Z$

$F_y = M_{21} . SFx + M_{22} . SFy + M_{23} . SFz + M_{24} . SMx + M_{25} . SMy + M_{26} . SM_Z$

$F_z = M_{31} . SFx + M_{32} . SFy + M_{33} . SFz + M_{34} . SMx + M_{35} . SMy + M_{36} . SM_Z$

$Mx = M_{41} . SFx + M_{42} . SFy + M_{43} . SFz + M_{44} . SMx + M_{45} . SMy + M_{46} . SM_Z$

$My = M_{51} . SFx + M_{52} . SFy + M_{53} . SFz + M_{54} . SMx + M_{55} . SMy + M_{56} . SM_Z$

$Mz = M_{61} . SFx + M_{62} . SFy + M_{63} . SFz + M_{64} . SMx + M_{65} . SMy + M_{66} . SM_Z$

These calculations were performed by MATLAB. Average and peak forces of each channel were computed.

- *Forces and moments*

BA
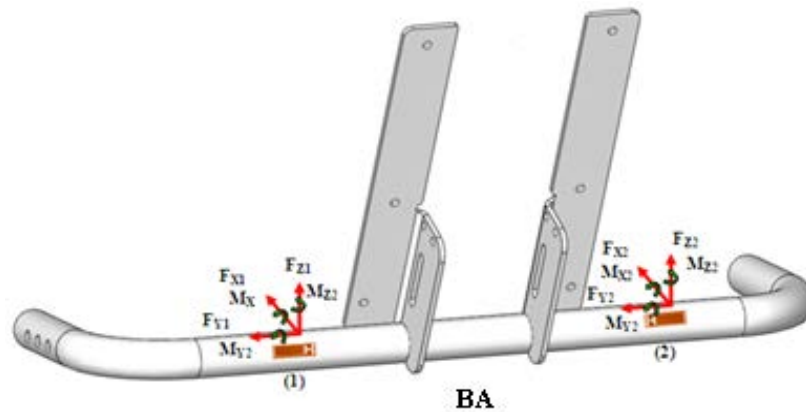
Rigid Backrest system

Forces and moments on BA (N, Nm)

Line	Fx1	Fy1	Fz1	Mx1	My1	Mz1	Fx2	Fy2	Fz2	Mx2	My2	Mz2
1	72.59	-140.86	-88.54	2.28	0.13	-4.26	-3.35	-380.23	33.05	16.90	1.59	21.78
2	71.44	-137.82	-84.97	2.22	0.13	-4.29	-3.52	-374.81	32.78	16.66	1.56	21.44
3	71.91	-137.37	-83.80	2.20	0.13	-4.27	-2.98	-373.43	32.20	16.60	1.56	21.32
4	72.75	-136.95	-83.41	2.20	0.13	-4.21	-2.46	-372.46	32.87	16.57	1.54	21.23
5	71.69	-134.69	-80.84	2.14	0.12	-4.24	-2.40	-367.43	32.59	16.36	1.52	20.95
6	70.41	-132.80	-78.07	2.10	0.12	-4.28	-2.46	-364.35	32.05	16.21	1.50	20.74
7	70.54	-132.30	-77.46	2.10	0.12	-4.27	-1.95	-364.52	31.99	16.21	1.50	20.70
8	71.03	-131.84	-77.32	2.10	0.11	-4.25	-0.44	-362.96	32.47	16.17	1.48	20.55
9	70.23	-130.96	-77.70	2.10	0.12	-4.21	0.41	-358.74	36.84	16.04	1.43	20.22
10	68.58	-129.21	-78.11	2.10	0.11	-4.12	0.62	-354.35	42.75	15.89	1.37	19.84

Dynamic Backrest system

Forces and moments on BA (N, Nm)

Line	Fx1	Fy1	Fz1	Mx1	My1	Mz1	Fx2	Fy2	Fz2	Mx2	My2	Mz2
1	56.21	-117.83	-42.24	2.14	0.06	-3.63	1.20	-288.99	-6.21	11.63	1.31	15.50
2	52.41	-114.36	-43.25	2.07	0.06	-3.37	1.57	-283.40	0.78	11.33	1.22	14.83
3	49.26	-111.29	-43.90	2.02	0.06	-3.17	3.00	-276.01	4.53	10.92	1.12	14.04
4	46.60	-107.70	-43.00	1.95	0.06	-3.01	4.58	-267.83	6.09	10.46	1.05	13.23
5	44.88	-104.76	-41.31	1.88	0.05	-2.95	5.39	-261.75	6.39	10.17	1.00	12.74
6	43.02	-101.46	-39.05	1.82	0.05	-2.91	5.96	-256.43	6.22	9.91	0.96	12.32
7	41.48	-99.81	-37.69	1.78	0.05	-2.92	6.31	-254.22	6.15	9.76	0.94	12.10
8	39.99	-98.35	-36.98	1.76	0.05	-2.91	6.52	-252.49	7.10	9.66	0.92	11.93
9	38.81	-96.79	-36.50	1.75	0.05	-2.92	6.80	-250.54	7.80	9.57	0.91	11.77
10	37.62	-95.59	-35.61	1.72	0.05	-2.92	7.36	-248.10	7.95	9.44	0.89	11.54

- *Summation of BA1 and BA2*

BA
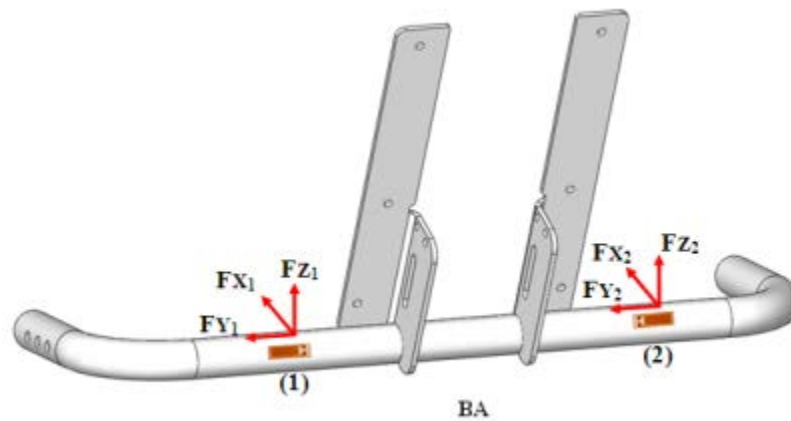
Due to BA had 2 sets of strain gauges namely BA1 and BA2 on the left and right side as shown in figure above. Summations of forces are following:
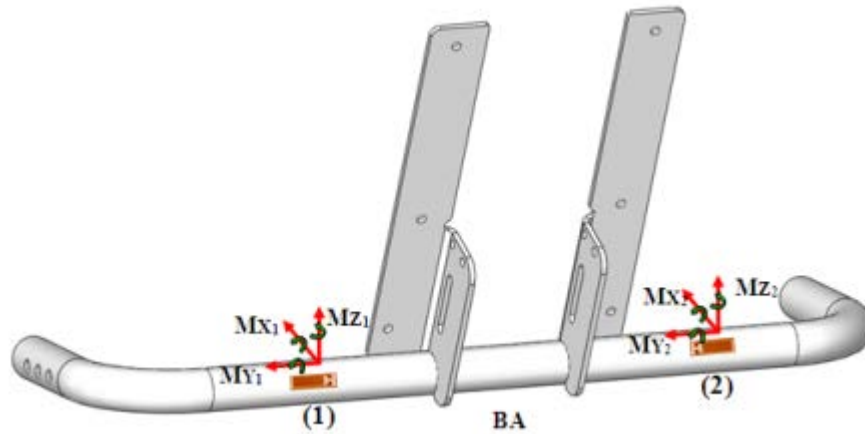
$$Fx = Fx_1 + Fx_2$$

$$Fy = Fy_1 + Fy_2$$

$$Fz = Fz_1 + Fz_2$$

Fx and Fz direction sum of shear forces measured at strain gauges

Fy unbalanced force in y direction, the Fy in position one sign is changed to that of the global coordinate system

The two Mx moments are summed to find unbalanced Mx moment.

$$Mx = Mx_1 + Mx_2$$

My has two conditions if the two signs are the same direction i.e. torque is positive or negative with respect to the global coordinate system, the total is the average of them.

$$My = (My_1 + My_2) / 2$$

If the signs are opposite the external torque measured at either end is opposite and total is the sum of the torques.

$$My = My_1 + My_2$$

The two Mz moments are summed to find unbalanced Mz moment.

$$Mz = Mz_1 + Mz_2$$

APPENDIX D
ETHICAL APPROVALS

Study Title: ***Stress Analysis of Seating Systems for Children with Special Needs***

REC Reference Number: ***10/S1001/41***

NHS R&D offices Reference Number: ***GN10CO288***

Documents:

- Research Protocol
- Information sheet for parent
- Information sheet for child
- Information sheet for school
- Parent consent form
- Child assent form

(Details are available on CD)

Study Title: *Stress Analysis of a Dynamic Seating System for Children with Special Needs*

REC Reference Number: *11/AL/0367*

NHS R&D offices Reference Number: *GN11CO368*

Documents:

- Research Protocol
- Information sheet for parent
- Information sheet for child
- Information sheet for school
- Parent consent form
- Child assent form

(Details are available on CD)

Study Title: **_Effect of a dynamic backrest seating system on a child with CP_**

UEC Reference Number: **_UEC1012/48_**

Documents:

- Research Protocol
- Information sheet for parent
- Parent consent form
- Parent assessment of new backrest
- Information sheet for physiotherapist
- Physiotherapist consent form
- Alignment assessment

(Details are available on CD)